https://www.mdc-berlin.de/de/veroeffentlichungstypen/clinical-journal-club

Als gemeinsame Einrichtung von MDC und Charité fördert das Experimental and Clinical Research Center die Zusammenarbeit zwischen Grundlagenwissenschaftlern und klinischen Forschern. Hier werden neue Ansätze für Diagnose, Prävention und Therapie von Herz-Kreislauf- und Stoffwechselerkrankungen, Krebs sowie neurologischen Erkrankungen entwickelt und zeitnah am Patienten eingesetzt. Sie sind eingeladen, uns beizutreten. Bewerben Sie sich!

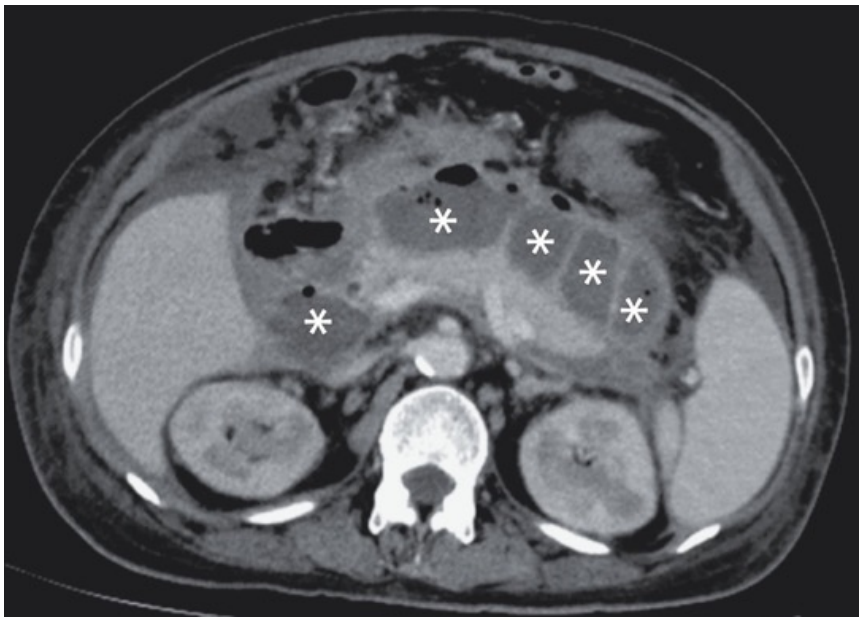

A 65-year-old woman with a recent history of acute necrotizing pancreatitis presented with a 5-day history of abdominal pain and fevers. Physical examination was notable for tenderness in the upper abdomen. Computed tomography of the abdomen is shown. What is the diagnosis?

Cystic pancreatic neoplasm

Intra-abdominal abscesses

Pancreatic pseudocyst

Solid pancreatic tumor

Walled-off pancreatic necrosis

A diagnosis of walled-off pancreatic necrosis was made on the basis of the CT of the abdomen showing a large, well-circumscribed fluid collection containing gas and septations in the pancreatic region and extending into the retroperitoneal spaces on both sides. This is a late complication of acute necrotizing pancreatitis and is defined by formation of an encapsulated collection of necrotic tissue and fluid. Stepped-up management includes antimicrobial agents, percutaneous drainage, and then endoscopic drainage.

CT looks quite the same

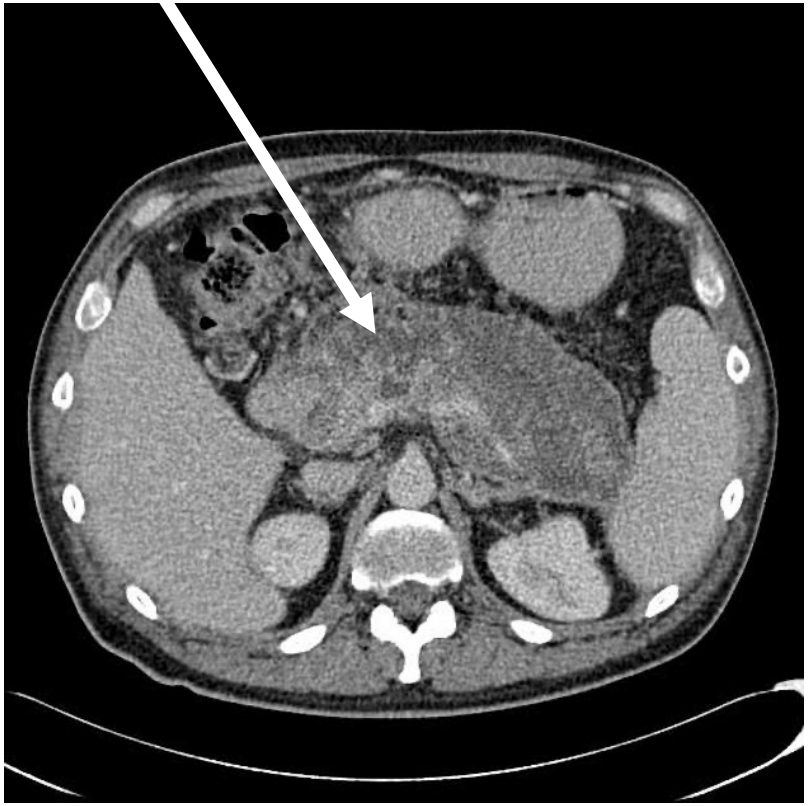

Walled-off pancreatic necrosis **(WOPN - abgekapselte Pankreasnekrose)** is a late, severe complication of acute necrotizing pancreatitis, characterized by a well-defined fibrous capsule enclosing liquefied and solid necrotic tissues. It typically develops four or more weeks after the initial pancreatic injury. Treatment is generally necessary for symptomatic patients or infected cases, with EUS-guided endoscopic drainage being the preferred intervention over traditional surgery.

A Note from the Editors

In 2026, the *New England Journal of Medicine* will publish every Thursday except for March 19, May 21, August 27, and December 24.

INTERACTIVE MEDICAL CASE

A Feverish Pace

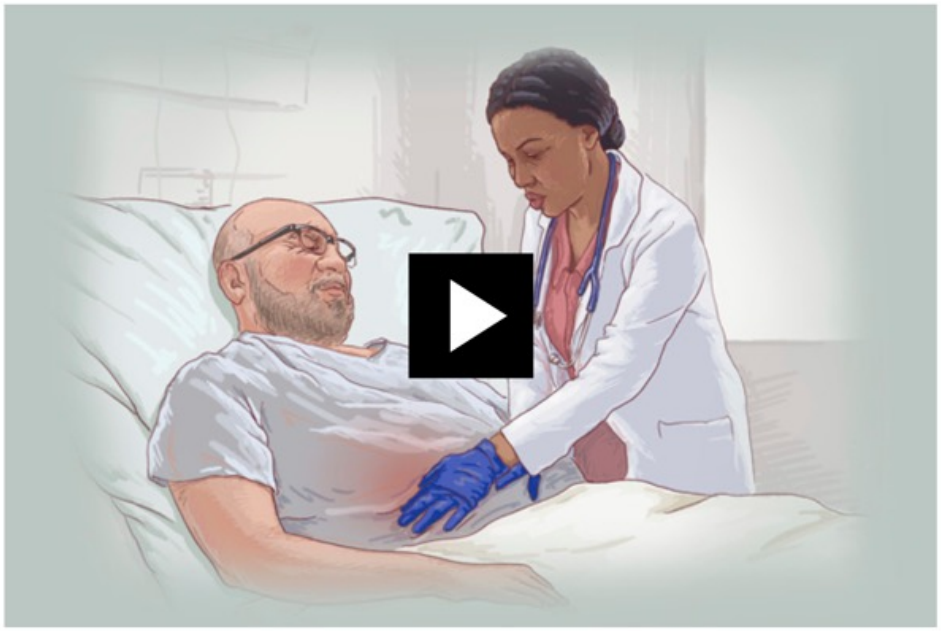

A 52-year-old man presented to his primary care clinic with a 3-week history of fevers, drenching night sweats, fatigue, myalgias, and dyspnea on exertion. . . .

Patient bitte ausziehen und flach legen

Case Presentation

A 52-year-old man presented to his primary care clinic with a 3-week history of fevers, drenching night sweats, fatigue, myalgias, and dyspnea on exertion.

He reported poor appetite and a weight loss of 6.8 kg that had occurred during the previous 3 weeks.

Two weeks before the onset of symptoms, he had traveled to Colorado for a family event. He had not gone hiking during his trip, and he reported not having had close contact with birds, wildlife, or exotic animals. He had no pets and had no history of international travel.

Patient History

Medical History

Overweight
Subclinical hypothyroidism
Hypertriglyceridemia
Gout
Alopecia
Vitamin D deficiency

Medications

Icosapent ethyl, 2 g twice daily
Allopurinol, 200 mg daily
Minoxidil, 5 mg daily
Cholecalciferol, 2000 units daily

Allergies

No known drug allergies

Social History

Reports rare alcohol consumption
Reports no use of tobacco or illicit drugs
Works as a software engineer

Family History

Mother with hypertension
Father with hypertension, coronary artery disease, and prostate cancer
Brother with hypothyroidism and gout
Maternal grandmother with brain cancer
Paternal grandmother with brain cancer

Die Untersuchungshaltung ist falsch
Oder der Patient hat Situs inversus
Oder der Ärztin ist Linkshändig
Kein Wunder, dass die Milz “nicht tastbar“ war

Physical Examination

Vital signs

Temperature, 37.8°C

Heart rate, 102 beats per minute

Blood pressure, 111/69 mm Hg

Respiratory rate, 16 breaths per minute

Oxygen saturation, 96% while the patient was breathing ambient air

Body-mass index, 26.0

General appearance

Sitting comfortably

Head, eyes, ears, nose, and throat

Anicteric sclerae

No conjunctival erythema

No cervical or supraclavicular lymphadenopathy

Heart

Tachycardia with a regular rhythm

Grade 2/6 systolic murmur at the left sternal border

Lungs

No increased work of breathing

Clear on auscultation

Abdomen

Normal bowel sounds

Tenderness on palpation in the right upper quadrant

Negative Murphy's sign

No rebound or guarding

Hepatomegaly without palpable splenomegaly

Arms and legs

Normal pulses

No edema of the legs or feet

No axillary or inguinal lymphadenopathy

Nervous system

No neurologic abnormalities

Die meisten schauen nur auf das „hoch“ oder „niedrig“

Laboratory Evaluation

Variable	Result	Normal Range	Flag
Sodium (mmol/liter)	134	136–142	Low
Potassium (mmol/liter)	4.2	3.5–5.0	–
Chloride (mmol/liter)	96	98–108	Low
Bicarbonate (mmol/liter)	26	22–32	–
Urea nitrogen (mg/dl)	12	9–25	–
Creatinine (mg/dl)	0.89	0.70–1.30	–
Glucose (mg/dl)	106	70–140	–
Estimated glomerular filtration rate (ml/min/1.73 m^2)	103	>60	–
Alanine aminotransferase (U/liter)	115	10–50	High
Aspartate aminotransferase (U/liter)	117	10–50	High
Alkaline phosphatase (U/liter)	663	40–130	High
Total protein (g/dl)	6.7	6.0–8.0	–
Albumin (g/dl)	3.6	3.5–5.2	–
Total bilirubin (mg/dl)	1.5	0.0–1.0	High
Direct bilirubin (mg/dl)	0.8	0.0–0.3	High
Lactate dehydrogenase (U/liter)	593	140–280	High
White-cell count (per mm^3)	6200	4000–10,000	–
Differential count (%)			
Neutrophils	71.4	48.0–76.0	–
Lymphocytes	13.9	18.0–41.0	Low
Monocytes	13.6	4.0–11.0	High
Eosinophils	0.3	0.0–5.0	–
Basophils	0.6	0.0–1.5	–
Immature granulocytes	0.2	0.0–0.9	–
Hematocrit (%)	35.9	36.0–48.0	Low
Hemoglobin (g/dl)	12.2	11.5–16.4	–
Platelet count (per mm^3)	339,000	150,000–450,000	–
SARS-CoV-2 RNA on PCR testing*	Not detected	Not detected	–
Influenza A virus RNA on PCR testing*	Not detected	Not detected	–
Influenza B virus RNA on PCR testing*	Not detected	Not detected	–
Respiratory syncytial virus RNA on PCR testing*	Not detected	Not detected	–
Erythrocyte sedimentation rate (mm/hr)	35	0–20	High
C-reactive protein (mg/liter)	125.3	0.0–10.0	High

Hyponatriämie, Leber-Enzyme, Anämie und Entzündungszeichen

Imaging Studies

Given the patient's constitutional symptoms, right upper quadrant tenderness with palpable hepatomegaly, and elevations in aminotransferases, bilirubin, and lactate dehydrogenase, computed tomography (CT) of the abdomen and pelvis was performed with contrast enhancement. Imaging revealed multiple hyperattenuating lesions in the liver and spleen (yellow dots). There was no lymphadenopathy.

CT of the Abdomen and Pelvis

Imaging Studies

Given the patient's constitutional symptoms, right upper quadrant tenderness with palpable hepatomegaly, and elevations in aminotransferases, bilirubin, and lactate dehydrogenase, computed tomography (CT) of the abdomen and pelvis was performed with contrast enhancement. Imaging revealed multiple hyperattenuating lesions in the liver and spleen (yellow dots). There was no lymphadenopathy.

CT of the Abdomen and Pelvis

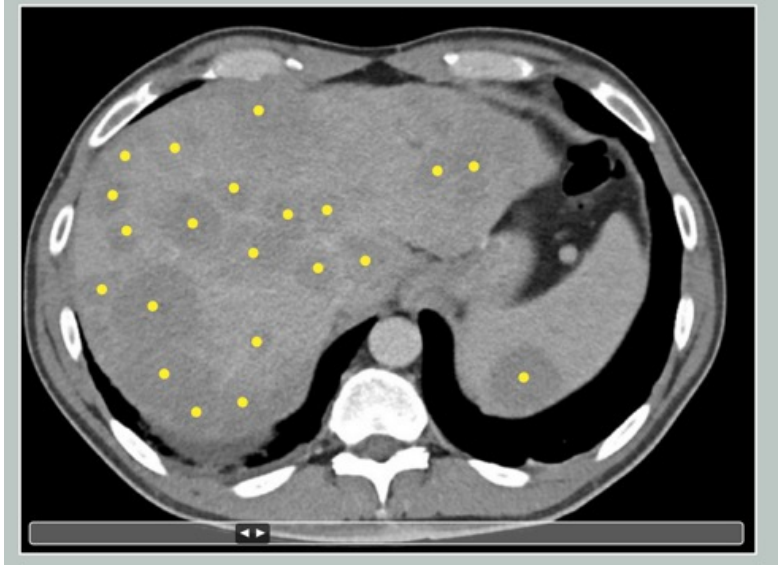

What Would You Do?

At this time, which of the following management strategies are most appropriate for this patient?

Select any number of the listed strategies to see whether they are appropriate choices and to learn about probable outcomes. You will be able to return to the list of choices to review the probable consequences of each choice.

Percentages listed with each management option represent reader responses. The percentages do not add up to 100 because multiple options can be selected.

- ☐ **A** Obtain blood cultures
- ☐ **B** Refer the patient for fine-needle aspiration of one of the liver lesions
- ☐ **C** Refer the patient for a core biopsy of one of the liver lesions
- ☐ **D** Initiate treatment with broad-spectrum antibiotic therapy

Submit

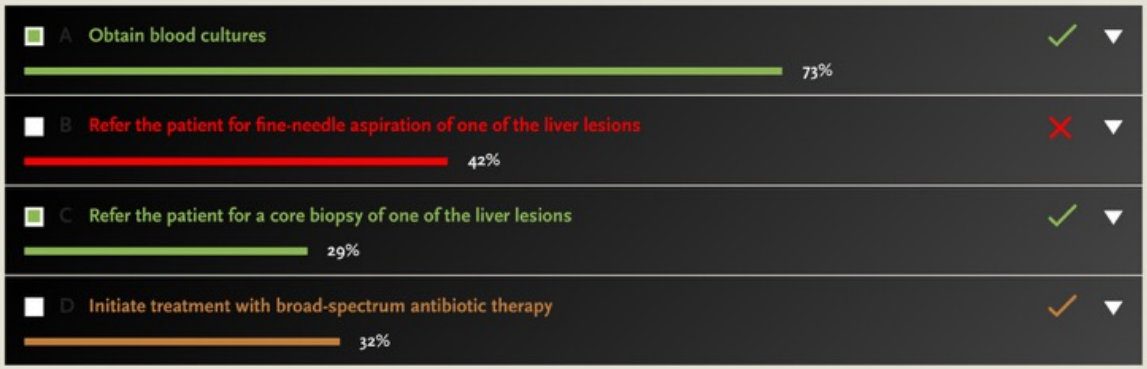

Microbiologic Analyses

A broad workup for infectious pathogens that can cause liver injury or constitutional symptoms in the context of liver and spleen lesions was undertaken.

Variable	Result	Normal Range	Flag
Blood cultures (×2)	Negative	Negative	–
Hepatitis A IgG	Nonreactive	Nonreactive	–
Hepatitis A IgM	Nonreactive	Nonreactive	–
Hepatitis B core antibody, IgM	Nonreactive	Nonreactive	–
Hepatitis B surface antibody	Nonreactive	Nonreactive	–
Hepatitis B surface antigen	Nonreactive	Nonreactive	–
Hepatitis C antibody	Not detected	Not detected	–
Hepatitis C RNA	Not detected	Not detected	–
Cytomegalovirus DNA (serum)	Not detected	Not detected	–
Epstein–Barr virus DNA (serum)	Not detected	Not detected	–
HIV type 1 and type 2 antibodies and HIV type 1 p24 antigen	Nonreactive	Nonreactive	–
Treponemal antibody, IgG	Negative	Negative	–
Cryptococcus urinary antigen	Negative	Negative	–
T-SPOT test for tuberculosis	Negative	Negative	–
Bartonella DNA	Negative	Negative	–
Brucella antibody	<1:20	<1:20	–
Coccidioides antigen	Not detected	Not detected	–
Histoplasma or blastomyces urinary antigen	Not detected	Not detected	–

Further Diagnostic Evaluation

Given the patient's constitutional symptoms, multiple hyperattenuating lesions in the liver and spleen, and negative infectious workup, the primary concern was metastatic disease from an unknown primary cancer. A core biopsy of one of the liver lesions under imaging guidance was planned.

While waiting for the liver lesion biopsy, positron emission tomography (PET)–CT was undertaken to evaluate for a possible primary cancer and, if present, the extent of malignant disease. PET-CT images from the skull base to the mid-thighs showed multiple ^{18}F-fluorodeoxyglucose (FDG)–avid liver lesions, with foci of uptake in the bone marrow.

PET-CT

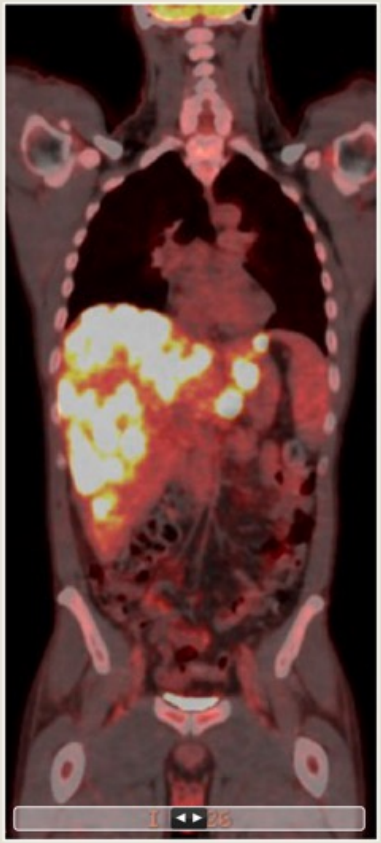

PET-CT

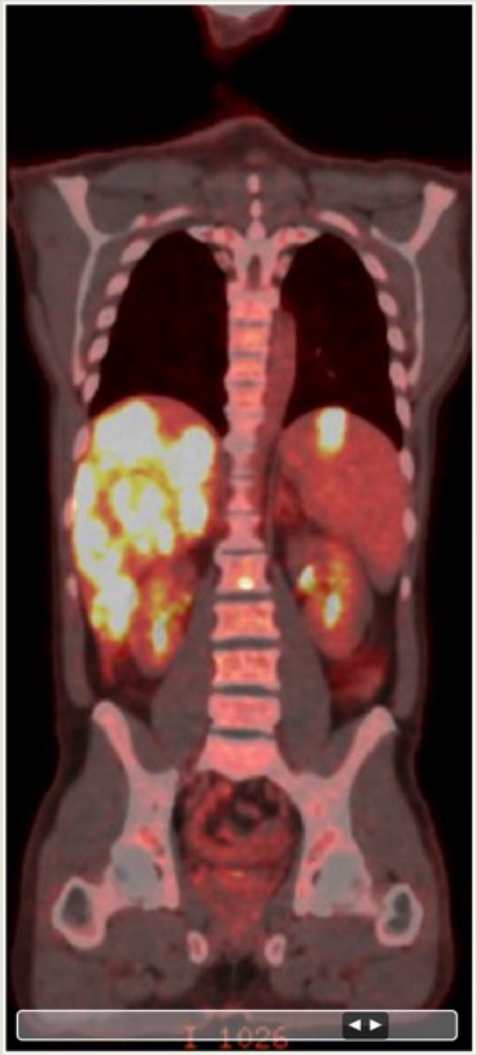

Bcl-2 (B-cell lymphoma 2) ist ein Protein, das den programmierten Zelltod (Apoptose) reguliert, indem es als zentraler Anti-Apoptose-Faktor wirkt. Es verhindert die Freisetzung von Cytochrom c aus den Mitochondrien, was Zellen vor dem Tod schützt. Eine Überexpression durch Gendefekte (z.B. t(14;18)) kann zu Tumoren führen.

Morphologic and Immunohistochemical Features of Diffuse Large B-Cell Lymphoma (DLBCL)

Click each type of stain listed below to see the histologic and immunophenotypic findings from the core liver biopsy.

The results of the core biopsy were consistent with DLBCL, a diagnosis that requires the presence of a diffuse population of large atypical mature B cells and the ruling out of Burkitt's lymphoma and other large B-cell lymphomas. This is accomplished by both review of morphologic features on hematoxylin and eosinophil staining and assessment for diagnostic patterns of protein expression (immunophenotype) on immunohistochemical staining, as well as the use of fluorescence in situ hybridization (FISH). In this case, the expression of BCL2, the absence of CD10 expression, and the absence of diffuse MYC expression on immunohistochemical staining ruled out Burkitt's lymphoma. The absence of CD10 expression also ruled out high-grade follicular lymphoma. The absence of a detectable MYC rearrangement by FISH (not shown) rules out a higher-grade subclassification of DLBCL defined by concurrent MYC and BCL2 rearrangements. Lastly, expression of BCL6 and MUM1, in addition to the absence of CD10 expression, supported subtyping of this DLBCL (with the use of the Hans algorithm) as the nongerminal center B-cell subtype.

Flow Cytometric Evidence of a Large B-Cell Lymphoma

Flow cytometry was performed on a portion of the biopsy because it may provide further supportive evidence of a large B-cell lymphoma. It detected a B-cell population monotypic of kappa light-chain expression, with no lambda expression, indicating monoclonality and supporting a neoplastic B-cell process. Further analysis revealed that the monotypic B cells coexpressed CD38 and lacked CD5 expression. This population also demonstrated a large cell size, correlating with the histologic finding of diffuse large B cells. These findings are typical for a flow cytometric profile of DLBCL. However, a definitive diagnosis of DLBCL requires histologic evaluation.

Hematoxylin and Eosin

CD20

CD3

CD10

BCL6

BCL2

MUM1

c-MYC

Ki-67

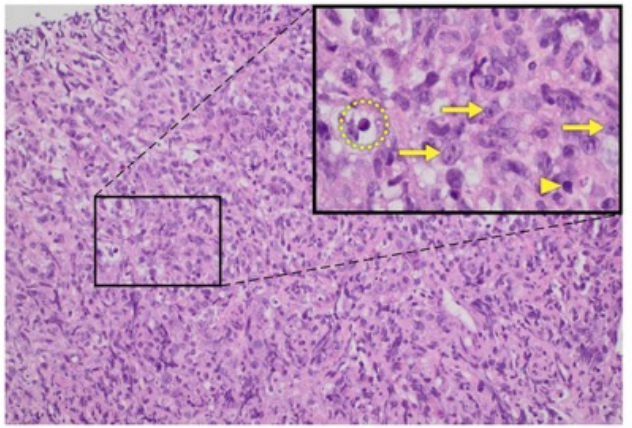

Low-power magnification (×200) of tissue stained with hematoxylin and eosin shows sheets of large, atypical lymphocytes with minimal residual liver parenchyma. Higher magnification (×1000; inset) reveals a relatively polymorphous infiltration of atypical lymphocytes (arrows). These cells are large compared to a small lymphocyte (arrowhead), exhibit scant-to-moderate amounts of eosinophilic to vesicular cytoplasm, and avoid irregular nuclear contours, vesicular chromatin, and prominent nucleoli. Frequent apoptotic bodies are also seen (dotted circle).

Das H im CHOP-Schema steht für **Hydroxydaunorubicin**, besser bekannt als **Doxorubicin** (auch Adriamycin). Es ist ein anthrazyklin-Antibiotikum, das als essenzieller Bestandteil der Chemotherapie gegen Lymphome wirkt, indem es die DNA der Krebszellen durch Interkalation schädigt und die Topoisomerase II hemmt. Typisch ist eine Rotfärbung des Urins. Daher „CHOP“

CD10 (Cluster of Differentiation 10), auch bekannt als **Neprilysin** oder **CALLA** (Common Acute Lymphoblastic Leukemia Antigen), ist eine zinkabhängige Zelloberflächen-Metalloendopeptidase. Es spielt eine entscheidende Rolle in der Pathologie als diagnostischer Marker für bestimmte B-Zell-Lymphome (z.B. follikuläres Lymphom, Burkitt-Lymphom) und verschiedene Karzinome (z.B. Nierenzellkarzinom).

Diffuse Large B-Cell Lymphoma (DLBCL) LEARNING MODULE

Click each of the tabs below for information about diffuse large B-cell lymphoma.

Epidemiology

DLBCL is the most common subtype of lymphoma.

It is a highly heterogeneous disease with marked pathologic, genetic, clinical, and prognostic variability among patients.

The annual age-standardized incidence is approximately 7.2 cases per 100,000 persons in the United States.

There is a male predominance, as in other non-Hodgkin's lymphomas.

Manifestations

Patients typically present with a rapidly enlarging mass, most commonly a lymph node in the neck or abdomen.

Occasionally, the primary mass may arise outside the lymph nodes; common extranodal sites include the gastrointestinal tract, skin and soft tissues, bone, and the genitourinary tract but can involve any organ.

Masses can destroy bone (causing spinal cord compression) or compress the great vessels (causing superior vena cava syndrome), airways (causing airway compromise), or viscera (causing obstruction).

Approximately one third of patients have B symptoms (e.g., fevers, drenching night sweats, and weight loss of more than 10% of body weight over a period of 6 months).

Patients with aggressive disease may present with tumor lysis syndrome.

BCL6 (B-cell lymphoma 6) ist ein essenzieller Transkriptionsfaktor, der als Hauptregulator die Bildung von Keimzentren in Lymphknoten und die Reifung von B-Zellen steuert. Als Onkogen ist eine Dysregulation von BCL6, oft durch Translokationen, ein treibender Faktor bei der Entstehung von B-Zell-Lymphomen, insbesondere dem diffusen großzelligen B-Zell-Lymphom (DLBCL)

Molekulare Prognose

Diagnosis and Molecular Prognostication

DLBCL is diagnosed after a biopsy of a lymph node or other involved tissue.

Several analyses are performed on the biopsy specimen to define the DLBCL subtype and inform prognostication.

- Histologic analysis assesses the morphology of the tumor cells and lymph-node architecture.
- Flow cytometry immunophenotyping confirms that involved cells are clonal B cells.
- Cytogenetic analysis with the use of karyotype or fluorescence in situ hybridization (FISH) identifies chromosomal abnormalities.
- Molecular studies assess gene mutations and epigenetic changes.

DLBCL is classified into one of two subtypes according to the B cell of origin: germinal center B-cell (GCB) or non-GCB.

- The Hans algorithm can be used by pathologists to classify DLBCL as GCB or non-GCB.
- The GCB subtype is associated with a better prognosis.

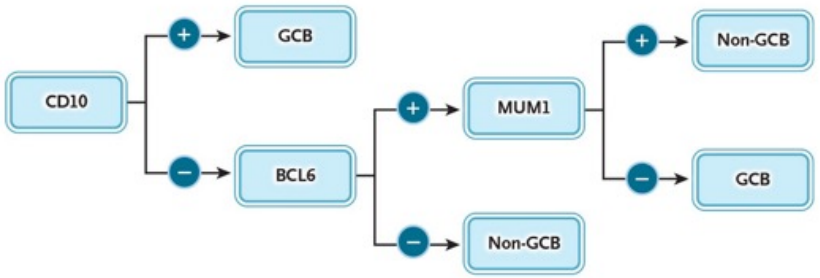

CD10 denotes cluster of differentiation 10, GCB germinal center B-cell, BCL6 B-cell lymphoma 6, and MUM1 multiple myeloma oncogene 1.

Multiple Myeloma Oncogene-1 (MUM1), auch als Interferon Regulatory Factor 4 (IRF4) bekannt, ist ein Transkriptionsfaktor, der in Keimzentrum-B-Zellen, aktivierten T-Zellen und Plasmazellen exprimiert wird. Er ist entscheidend für die B- und T-Zell-Differenzierung und dient als wichtiger diagnostischer Marker in der Hämatopathologie zur Klassifizierung von Lymphomen (z.B. DLBCL, Hodgkin-Lymphom)

Tumorstaging (Stadienbestimmung) ist die onkologische Diagnostik zur Feststellung der Ausbreitung eines Tumors. Es bestimmt Größe, Lymphknotenbefall und Metastasierung mittels TNM-Klassifikation, um die Prognose zu beurteilen und die Therapie zu planen.

Staging and Prognosis

Whole-body positron emission tomography–computed tomography (PET-CT) with ^{18}F-fluorodeoxyglucose is used to stage DLBCL. Bone marrow biopsy may be considered in select patients with a negative finding for bone or bone marrow involvement on PET-CT. Bone marrow biopsy is not necessary if PET-CT demonstrates bone or marrow involvement.

Stage	Involvement	Extranodal Status
Limited		
I	One node or one group of adjacent nodes	One extralymphatic site without nodal involvement
II	Two or more nodal regions on the same side of the diaphragm	Stage I or II by nodal involvement with limited contiguous extranodal involvement
Advanced		
III	Nodes on both sides of the diaphragm	Not applicable
IV	Additional noncontiguous extralymphatic organs with or without nodes	Not applicable

The tonsils, Waldeyer's ring, and the spleen are considered to be nodal tissue.

Klinische Prognose nach Skala

The International Prognostic Index (IPI) is used to estimate the likelihood of cure with standard therapy for specific groups of patients.

The IPI assigns 1 point to each of the following factors, which are correlated with poor progression-free and overall survival:

- Patient >60 years of age at diagnosis
- Disease stage III or IV
- Serum lactate dehydrogenase level above the upper limit of the normal range
- Eastern Cooperative Oncology Group performance-status score of 2–4 (i.e., performance status ranging from inability to carry out work activities to complete disability)
- More than one extranodal site of disease

The IPI groups patients into four risk categories:

- An IPI score of 0 or 1 indicates low risk, with an estimated overall survival of 88% at 5 years
- An IPI score of 2 indicates low-intermediate risk, with an estimated overall survival of 76% at 5 years
- An IPI score of 3 indicates high-intermediate risk, with an estimated overall survival of 67% at 5 years
- An IPI score of 4 or 5 indicates high risk, with an estimated overall survival of 54% at 5 years

Treatment

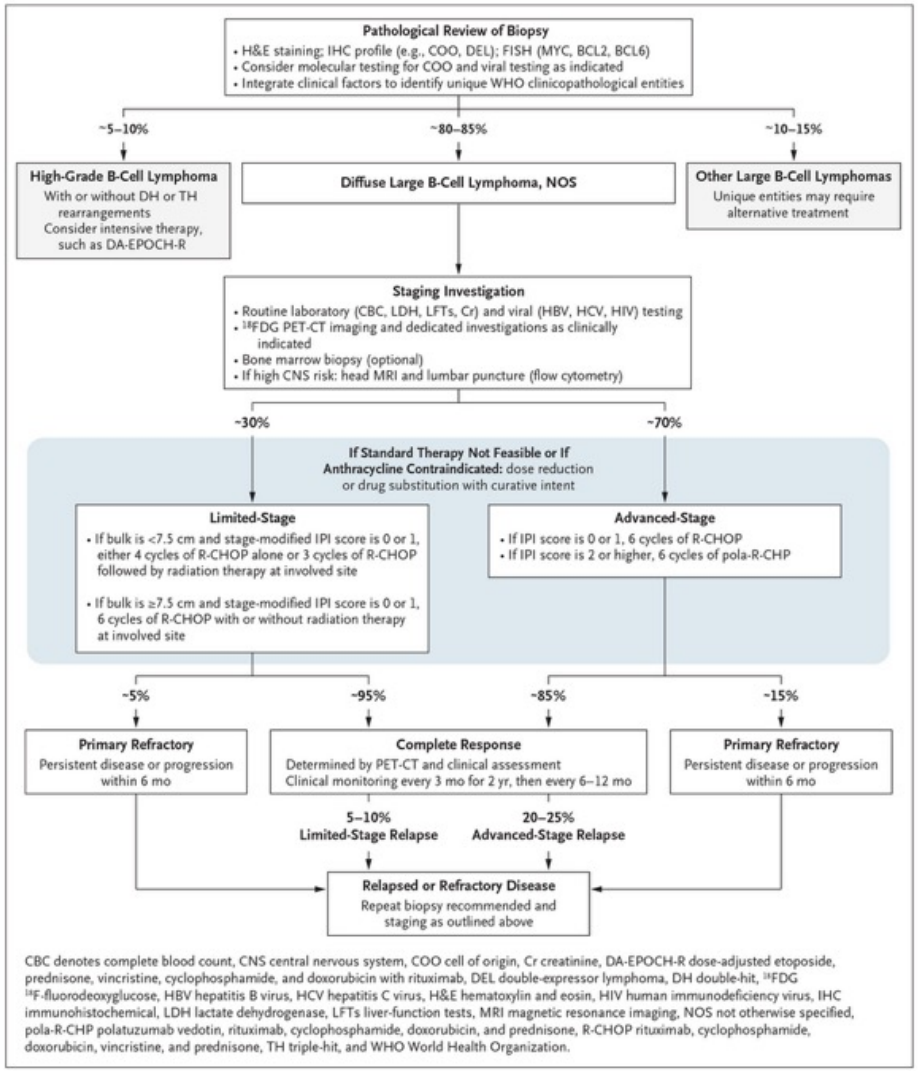

CBC denotes complete blood count, CNS central nervous system, COO cell of origin, Cr creatinine, DA-EPOCH-R dose-adjusted etoposide, prednisone, vincristine, cyclophosphamide, and doxorubicin with rituximab, DEL double-expressor lymphoma, DH double-hit, ^{18}FDG ^{18}F-fluorodeoxyglucose, HBV hepatitis B virus, HCV hepatitis C virus, H&E hematoxylin and eosin, HIV human immunodeficiency virus, IHC immunohistochemical, LDH lactate dehydrogenase, LFTs liver-function tests, MRI magnetic resonance imaging, NOS not otherwise specified, pola-R-CHP polatuzumab vedotin, rituximab, cyclophosphamide, doxorubicin, and prednisone, R-CHOP rituximab, cyclophosphamide, doxorubicin, vincristine, and prednisone, TH triple-hit, and WHO World Health Organization.

Management and Outcome

The patient was diagnosed with advanced (stage IV) DLBCL. He was treated with polatuzumab vedotin, an antibody-drug conjugate that targets CD79B, in combination with rituximab, cyclophosphamide, doxorubicin, and prednisone (pola-R-CHP) administered every 21 days, followed by 2 cycles of rituximab monotherapy administered every 21 days. In a randomized trial, progression-free survival with pola-R-CHP was superior to that with rituximab, cyclophosphamide, doxorubicin, vincristine, and prednisone (R-CHOP) in patients with DLBCL who had intermediate- to high-risk disease.

PET-CT

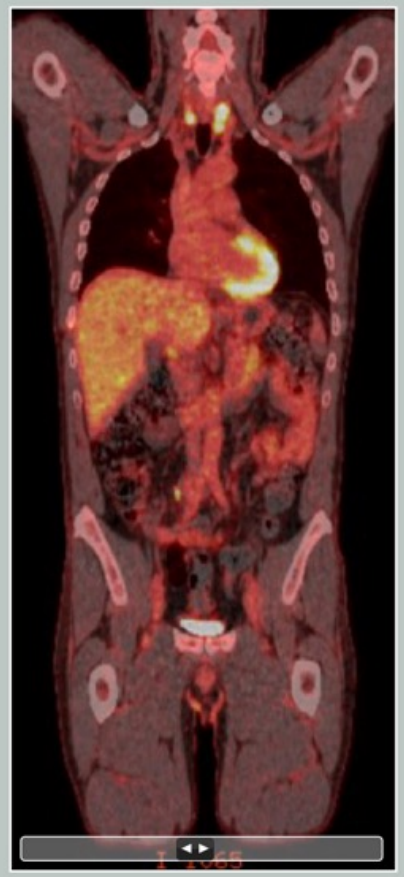

Polatuzumab-Vedotin (Handelsname Polivy®) ist ein Antikörper-Wirkstoff-Konjugat zur Behandlung aggressiver B-Zell-Lymphome (DLBCL). Es bindet spezifisch an CD79b auf der Oberfläche von B-Zellen und setzt dort das Zytostatikum MMAE frei. Der Wirkstoff ist sowohl in der Erstlinie (mit R-CHP) als auch bei rezidiviertem/refraktärem DLBCL (mit Bendamustin+Rituximab) zugelassen.

Monomethyl-Auristatin E (MMAE oder Vedotin) ist ein hochwirksames, synthetisches Zytostatikum, das als "Payload" in Antikörper-Wirkstoff-Konjugaten (ADCs) eingesetzt wird. Es hemmt die Zellteilung (Antimitotikum), indem es die Mikrotubuli-Polymerisation blockiert, was zum Zelltod (Apoptose) führt. Aufgrund seiner extremen Toxizität wird es nur gekoppelt an Antikörper verwendet.

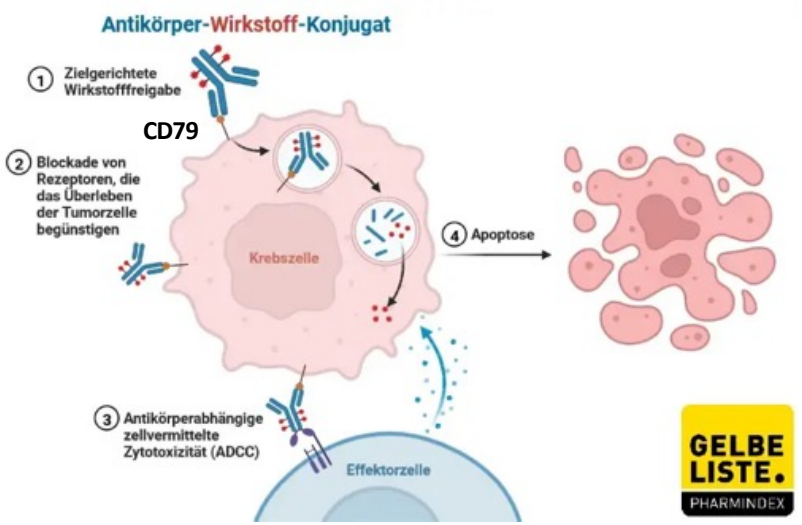

Monomethyl-Auristatin E (MMAE) und Vincristin sind beides hochwirksame Zytostatika, die als **Spindelgifte** wirken, indem sie die Mikrotubuli-Funktion stören und so die Zellteilung (Mitose) hemmen. Der wesentliche Unterschied liegt in ihrer Herkunft, Anwendung und Wirkweise im Körper:

Pola-R-CHP

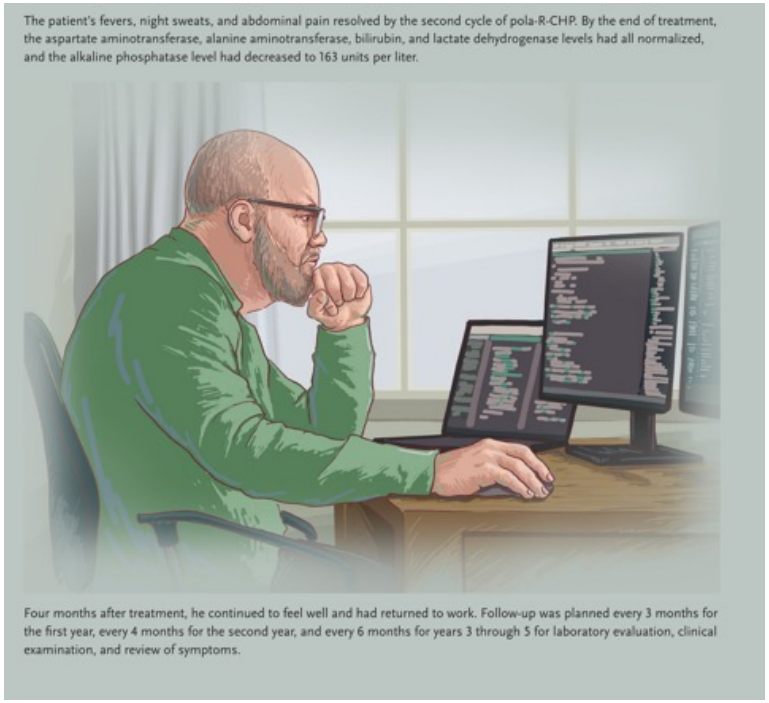

The patient's fevers, night sweats, and abdominal pain resolved by the second cycle of pola-R-CHP. By the end of treatment, the aspartate aminotransferase, alanine aminotransferase, bilirubin, and lactate dehydrogenase levels had all normalized, and the alkaline phosphatase level had decreased to 163 units per liter.

Four months after treatment, he continued to feel well and had returned to work. Follow-up was planned every 3 months for the first year, every 4 months for the second year, and every 6 months for years 3 through 5 for laboratory evaluation, clinical examination, and review of symptoms.

Pola-R-CHP ist ein moderner Behandlungsstandard für das diffuse großzellige B-Zell-Lymphom (DLBCL). Es kombiniert Polatuzumab Vedotin mit R-CHP, wobei Vincristin durch das Antikörper-Wirkstoff-Konjugat ersetzt wird. Die Kombination bietet im Vergleich zu R-CHOP ein besseres progressionsfreies Überleben (PFS) und ist der neue Standard in der Erstlinie.

Oncovin ist ein Handelsname für Vincristin

Teaching Points

- Lymphoma can manifest without lymphadenopathy and should be considered in patients with lesions in the liver or spleen (or both).
- Infectious causes of B symptoms (e.g., weight loss, night sweats, and fevers) with liver and spleen lesions include subacute bacterial endocarditis with systemic embolization, extrapulmonary tuberculosis, secondary syphilis, bacillary peliosis hepatis (e.g., from bartonella species), chronic brucellosis, and histoplasmosis, among others. A careful exposure and travel history should be obtained for patients with these findings.
- DLBCL is a highly heterogeneous disease entity with pathologic, genetic, clinical, and prognostic variability among patients. Broadly, the disease can be split into two overarching subtypes according to the B cell of origin (germinal center B cell or non-germinal center B cell).
- Pola-R-CHP is the preferred treatment for patients with advanced DLBCL who are at intermediate-to-high risk for death according to the International Prognostic Index. Treatment with pola-R-CHP is associated with a greater progression-free survival and event-free survival benefit than with R-CHOP.

INTERACTIVE MEDICAL CASE

Tick Tock

A 34-year-old man presented to the hospital with exercise intolerance, night sweats, and bradycardia. . . .

Case Presentation

A 34-year-old man presented to the hospital with exercise intolerance, night sweats, and bradycardia.

Two weeks before the current presentation, he saw his primary care physician for evaluation of myalgias and night sweats that had been present for 1 week. His symptoms had developed while he was on vacation along the Massachusetts coast and were initially accompanied by fevers that resolved within a few days. The patient's son also had a febrile illness during that time that had since resolved. His symptoms were attributed to a suspected viral illness.

On the day of presentation, the patient initially went to urgent care with persistent night sweats and new exercise intolerance. He was sent to the emergency department after he was found to have bradycardia, with a heart rate of 36 beats per minute.

On evaluation in the emergency department, the patient reported no fevers, chills, chest pain, dyspnea, palpitations, or lightheadedness. He said he did not have any sick contacts apart from his son.

Patient History

Medical History

Gastroesophageal reflux disease

Obesity

Recurrent ear infections in childhood

Medications

Omeprazole, 20 mg daily as needed for heartburn

Allergies

Amoxicillin (rash)

Social History

Drinks alcohol socially

Reports no history of tobacco or electronic cigarette use

Reports no history of illicit drug use

Lives an active lifestyle and is currently training for a marathon

Married with three children

Works in health care in Massachusetts

Family History

Paternal grandfather with atrial fibrillation and colon cancer, diagnosed at 62 years of age

Maternal uncle with prostate cancer, diagnosed in his 60s

Halsvenen, Halsvenenpulse und Füllungsdruck?
Herzaktion regelmäßig?

Physical Examination

Vital signs

Temperature, 36.7°C

Heart rate, 56 beats per minute

Blood pressure, 142/80 mm Hg

Respiratory rate, 18 breaths per minute

Oxygen saturation, 99% while the patient was breathing ambient air

General appearance

Well-appearing

Neck

Trachea at midline

No thyromegaly

No cervical lymphadenopathy

Heart

Bradycardia with an irregular rhythm

No murmurs, rubs, or gallops

Jugular venous pulsation not visualized

Lungs

Clear on auscultation

No wheezes, rhonchi, or rales

Abdomen

Soft, nondistended, and nontender on palpation

Normoactive bowel sounds

Arms and legs

Warm and well-perfused

No edema

Skin

No rashes or lesions

Nervous system

Grossly normal motor function

Awake, alert, and able to answer questions

No Brudzinski or Kernig signs

Dromotropie bezeichnet die Beeinflussung der **Geschwindigkeit der Erregungsleitung** im Herzen, insbesondere am AV-Knoten.

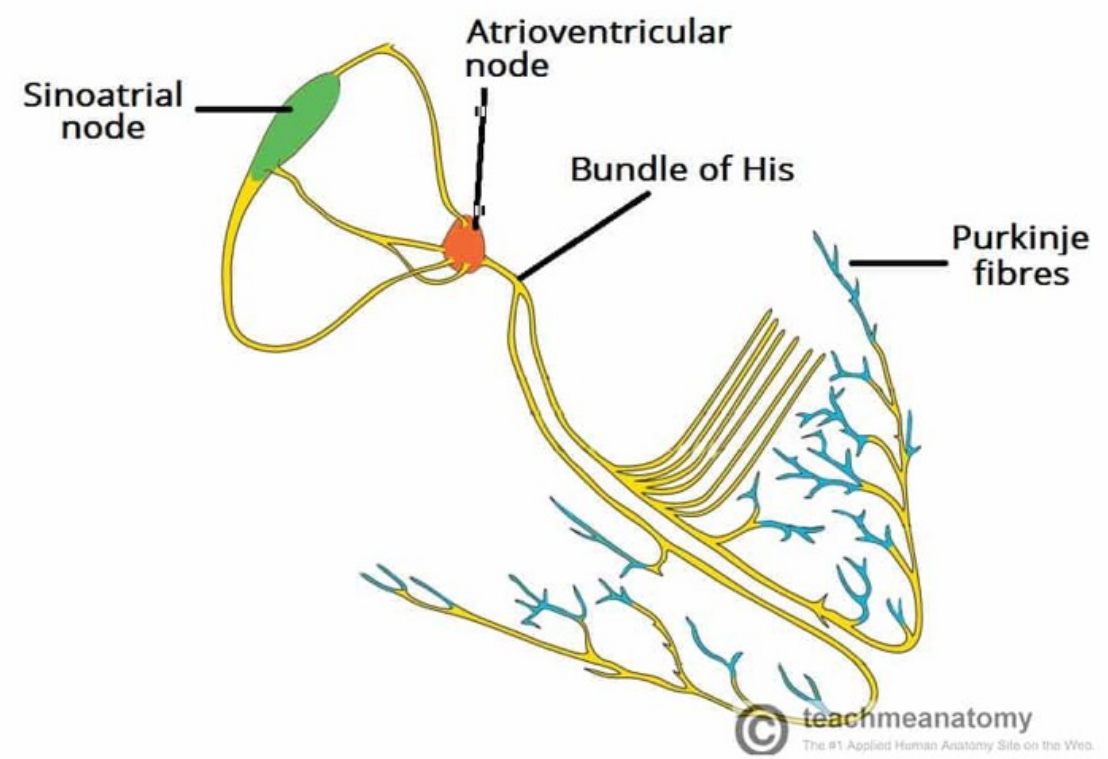

Electrocardiogram (ECG)

ECG on presentation was notable for Mobitz type I second-degree atrioventricular (AV) block as well as right bundle-branch block (RBBB). No previous ECGs were available for comparison.

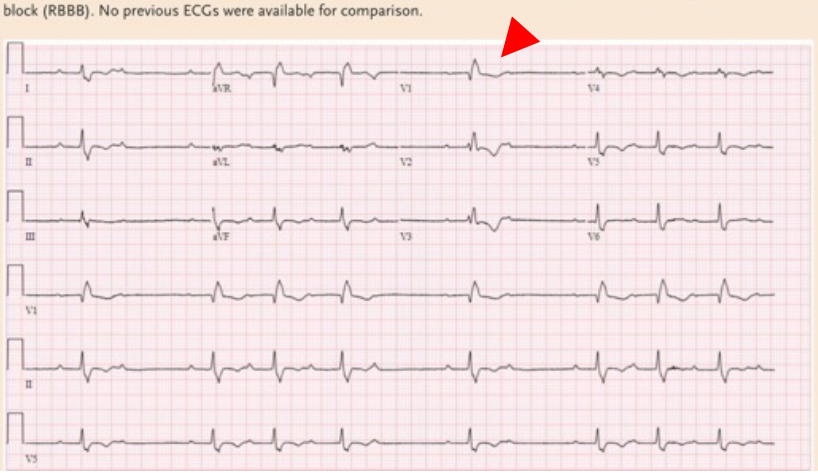

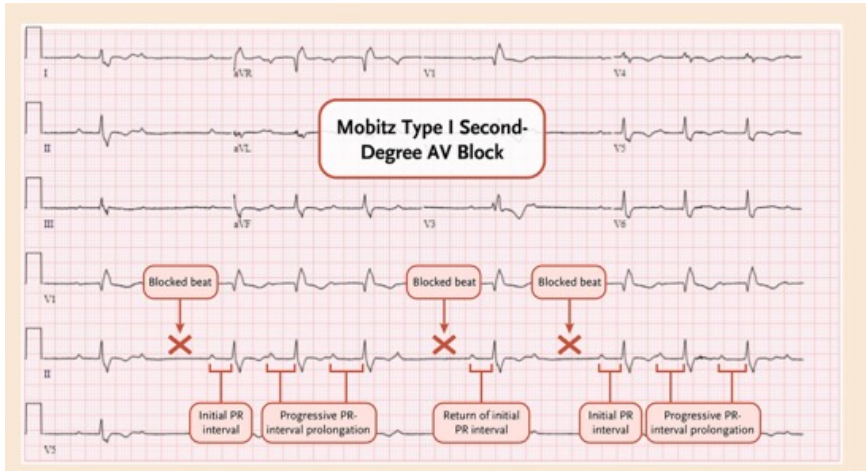

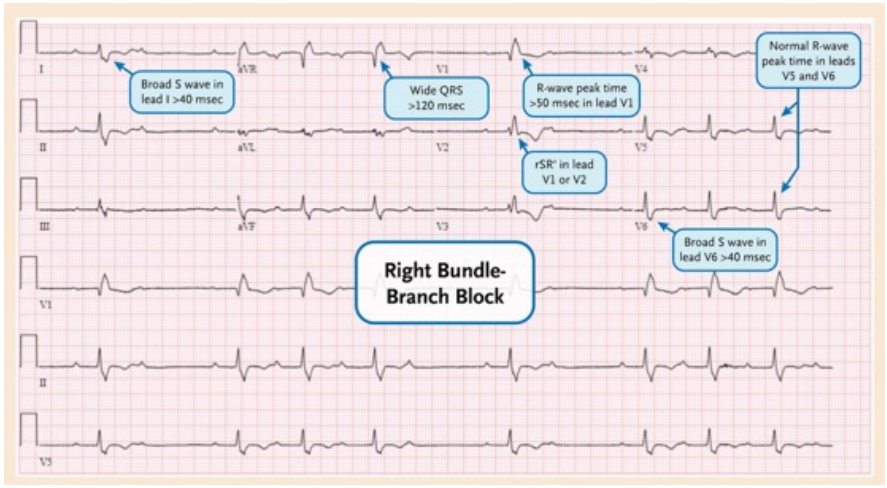

Terminale Vektor geht nach rechts und vorne
QRS>1,4 msek = RBBB

Karel Frederik Wenckebach (1864–1940) und Woldemar Mobitz (1889–1951) waren bedeutende Kardiologen, die Anfang des 20. Jahrhunderts grundlegende Formen des AV-Blocks (Herzrhythmusstörungen) beschrieben. Wenckebach identifizierte 1899 die progressive PQ-Zeit-Verlängerung (Typ I), während Mobitz 1924 diese und den Typ II klassifizierte.

- **Karel Frederik Wenckebach:** Niederländischer Internist, beschrieb die zunehmende Verlängerung des PR-Intervalls (PQ-Zeit), bis ein Schlag ausfällt (Wenckebach-Periodik).
- **Woldemar Mobitz:** Deutscher Internist, unterteilte den AV-Block 2. Grades in:
  - **Mobitz Typ I (Wenckebach):** PQ-Zeit wird länger, dann Ausfall; oft AV-Knoten-Ebene, meist harmlose Prognose.
  - **Mobitz Typ II:** PQ-Zeit konstant, dann plötzlicher Ausfall; oft unterhalb des AV-Knotens, ernste Prognose, meist Schrittmacher nötig.

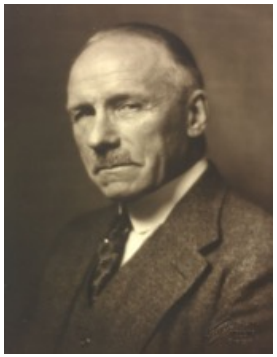

Karl Frederik Wenckebach
1964-1940

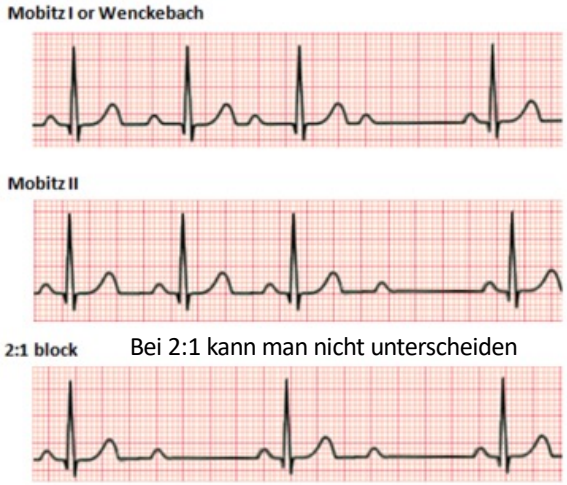

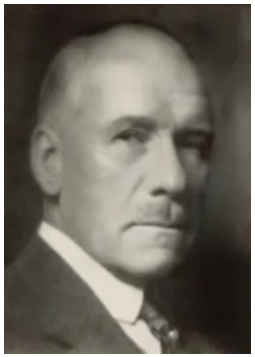

Woldemar Mobitz
1889-1951

AV-Block I. Grades

Hierbei ist die Erregungsleitung verzögert, und es kommt zu einer verspätet einsetzenden Kontraktion der Herzkammern. Diese Störung ist an einer Verlängerung der PQ-Zeit (über 200 ms) im EKG oder an einer Verkürzung des Abstandes zwischen der bei der Füllung der linken Herzkammer entstehenden E- und A-Welle im Echo erkennbar. Sie bleibt subjektiv unbemerkt und bedarf meist keiner Behandlung.

AV-Block II. Grades

Die Erregungsleitung und damit die Kammeraktion fällt teilweise aus. Dabei gibt es mehrere Möglichkeiten:

Die PQ-Zeit wird immer länger. Schließlich wird sie so lang, dass eine Vorhoferregung gar nicht mehr übergeleitet wird und eine einzelne Kammerkontraktion ausfällt. Die darauf folgende Vorhoferregung wird wieder normal übergeleitet. Dann beginnt die PQ-Zeit-Verlängerung wieder von neuem (*Wenckebachperiodik*). Die wissenschaftliche Definition eines Wenckebach-Blockes besagt, dass eine P-Welle nicht übergeleitet wird und die PQ-Zeit der P-Welle vor dem Ausfall länger ist als die PQ-Zeit der P-Welle nach dem Ausfall.

PQ-Abstand wird immer länger

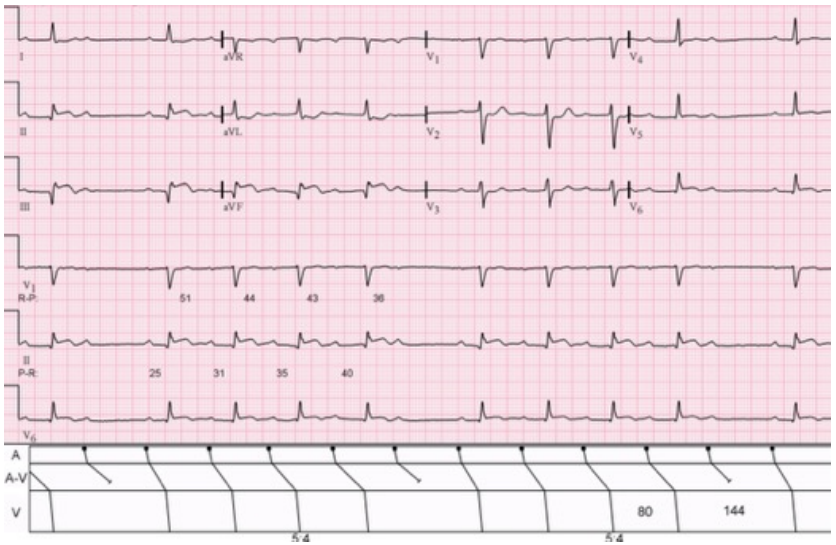

Mobitz Typ I (Wenckebach Perioden)

Plötzliches und unerwartetes Ausbleiben einer Kammeraktion auf eine Vorhoferregung, ohne dass das PQ-Intervall zuvor verlängert gewesen sein muss. Diese meist im His-Bündel (also unterhalb des AV-Knotens) lokalisierte Blockform wird als *Mobitz-Block* bezeichnet. Diese Blockform entsteht häufiger aufgrund von strukturellen Schädigungen des Herzens, daher ist die Prognose im Vergleich zum Wenckebach-Block ungünstiger, da die Gefahr besteht, dass der Rhythmus in einen totalen AV-Block übergeht.

Bei einem 2:1 Block wird regelmäßig nur jede 2. Vorhofaktion auf die Kammer übertragen werden. Bei höhergradigen AV-Blockierungen besteht ein 3:1 oder ein noch höheres Blockverhältnis.
Im englischen Sprachraum wird der Wenckebach-Block auch als *Mobitz Type I*, der Mobitz-Block als *Mobitz Type II* oder *Hay* bezeichnet. Die 2:1-Blöcke als „fixed-ratio-block“ und alle höhergradigen regelmäßigen Blockbilder als „high-grade AV-Block II“

PQ-Abstand bleibt immer gleich

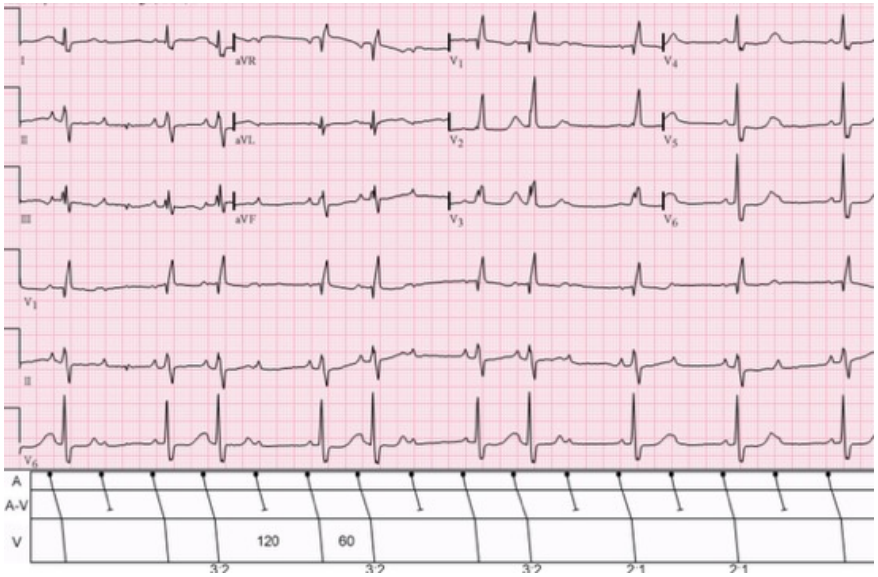

AV-Block II. Grades, zunächst Typ Mobitz (II) mit 3:2-Überleitung, dann 2:1-Block

Wenn P-Wellen und QRS-Komplexe im EKG **unabhängig voneinander** sind, handelt es sich um eine vollständige Trennung der Vorhof- und Kammeraktivität, was als **AV-Block III. Grades** (kompletter Herzblock) diagnostiziert wird.

AV-Block III Grades

Vollständiger Ausfall der Erregungsleitung zwischen Vorhof und Kammer (AV-Dissoziation). Die Kammer bleibt stehen oder schlägt in einem langsamen (bradykarden) Ersatzrhythmus asynchron zu den Vorhöfen weiter, der durch den als sekundärer Schrittmacher bezeichneten AV-Knoten (mit ca. 40–50 Impulsen pro Minute) oder die tertiären Schrittmacher (His-Bündel, Tawaraschenkel und Purkinje-Fasern mit einer Frequenz von ca. 20–30 Impulsen pro Minute) erzeugt wird. Ein AV-Block III. Grades kann mit normalen QRS-Komplexen (AV-Ersatzrhythmus) oder verbreiterten QRS-Komplexen (Kammerersatzrhythmus) auftreten.

Ein AV-Block III. Grades ist eine typische Indikation zur Implantation eines Herzschrittmachers.

Hals-Venen sind eindeutig

Laboratory Evaluation

The results of laboratory testing are shown below.

Variable[a]	Result	Normal Range	Flag
Sodium (mmol/liter)	140	136–142	–
Potassium (mmol/liter)	4.5	3.5–5.0	–
Chloride (mmol/liter)	102	98–108	–
Bicarbonate (mmol/liter)	25	23–32	–
Urea nitrogen (mg/dl)	20	9–25	–
Creatinine (mg/dl)	0.76	0.70–1.30	–
Estimated glomerular filtration rate (ml/min/1.73 m^2)	>120	>60	–
Glucose (mg/dl)	101	70–100	High
High-sensitivity troponin T (ng/liter)	<6	0–14	–
Thyrotropin (μIU/ml)	1.81	0.50–5.70	–
White-cell count (per mm^3)	6040	4000–10,000	–
Neutrophils (%)	64.2	48.0–76.0	–
Hematocrit (%)	41.3	36.0–48.0	–
Hemoglobin (g/dl)	13.8	11.5–16.4	–
Platelet count (per mm^3)	237,000	150,000–450,000	–
Prothrombin time (sec)	13.2	12.0–14.4	–
SARS-CoV-2 RNA on PCR testing	Not detected	Not detected	–
RSV on PCR testing	Negative	Negative	–
Influenza A virus on PCR testing	Negative	Negative	–
Influenza B virus on PCR testing	Negative	Negative	–

Chest Radiography

A posterior–anterior plain radiograph of the chest obtained on presentation showed a widened cardiac silhouette and no abnormalities in the lung fields.

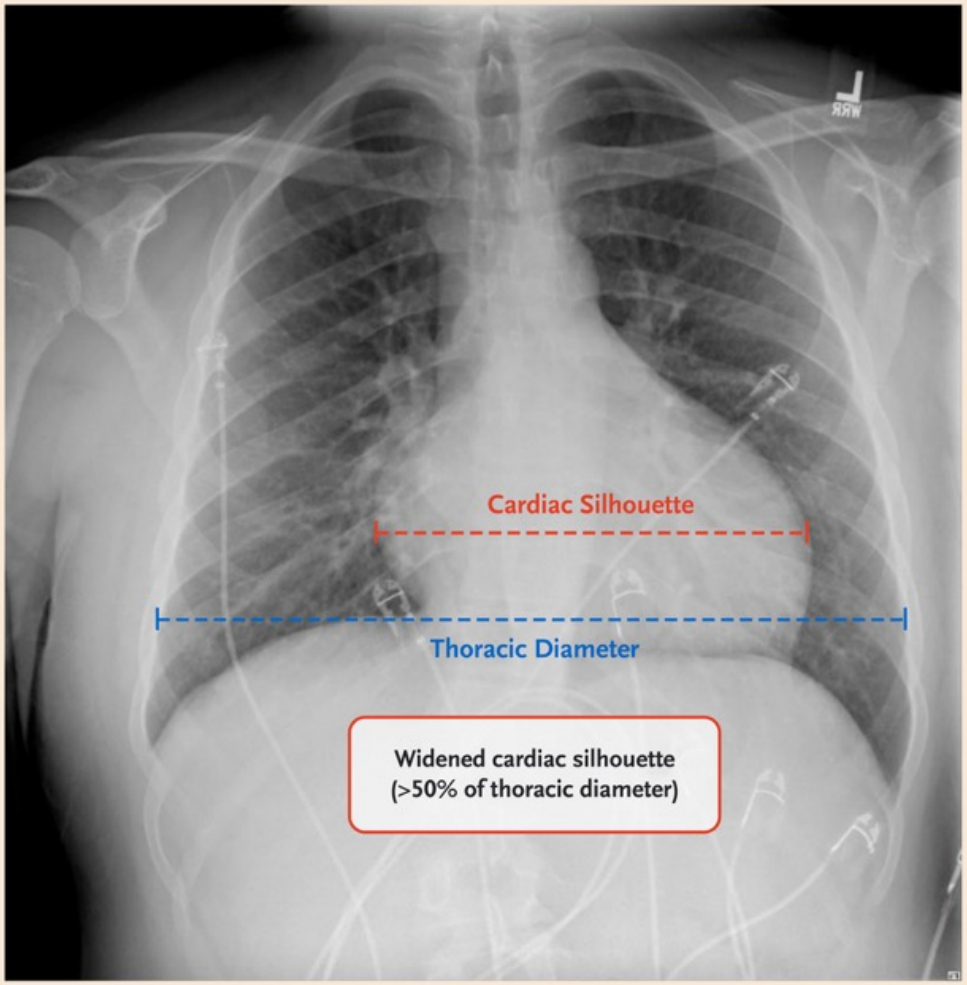

Kann man diesen Patienten nicht in die Röntgenabteilung schicken?

What Would You Do?

Which one of the following strategies is appropriate at this time?

Select a strategy to see whether it is an appropriate choice and to learn about the probable outcome. You will be able to return to the list of choices to review the probable consequences of each choice.

- A Admit the patient to the hospital for placement of a permanent pacemaker
- B Discharge the patient with a referral for outpatient cardiology follow-up
- C Admit the patient to the hospital for continuous ECG monitoring and additional testing
- D Immediately administer atropine
- E Admit the patient to the hospital for coronary angiography

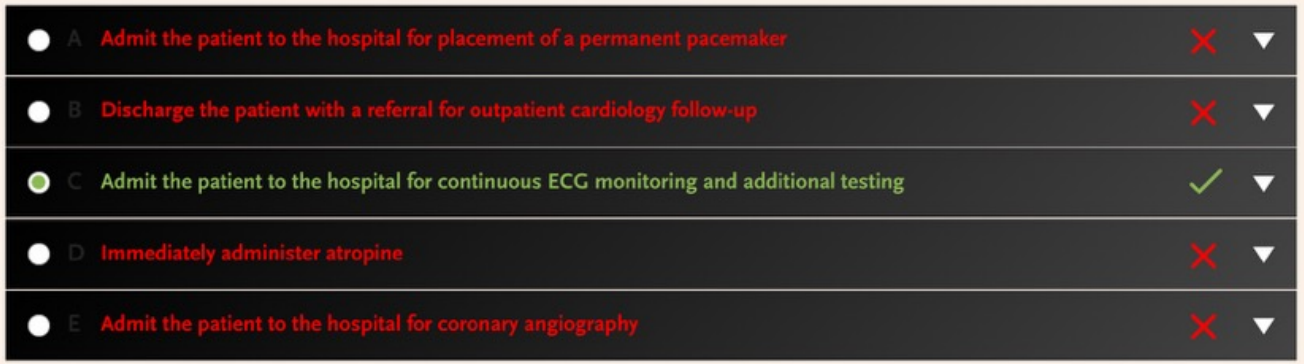

Atrioventricular (AV) Block

LEARNING MODULE

Classification

Select an AV block type to see the definition, the location of the block, and the ECG findings.

- (●) First-degree AV block
- ( ) Mobitz type I second-degree AV block
- ( ) Mobitz type II second-degree AV block
- ( ) Third-degree AV block (complete heart block)

Defined by a prolonged PR interval of >200 milliseconds without loss of atrioventricular conduction (i.e., every P wave is followed by a QRS complex). It represents delayed AV conduction rather than a true "block."

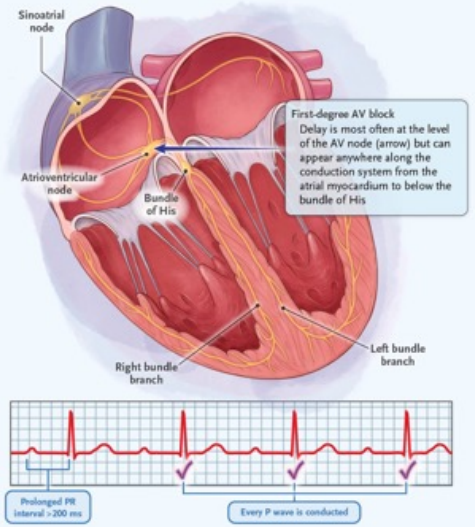

Causes

- Autonomic (increased vagal tone)
  - Carotid sinus hypersensitivity
  - Situational (vasovagal) syncope
- Cardiomyopathy (any cause)
- Congenital or inherited
  - Congenital heart disease
  - Myotonic dystrophy
  - Kearns–Sayre syndrome
- Degenerative fibrosis
- Drug-related
  - Beta-blockers
  - Calcium channel blockers
  - Digoxin
  - Other antiarrhythmic agents
- Infectious
  - Chagas' disease (trypanosomiasis)
  - Diphtheria
  - Infectious endocarditis and perivalvular abscess
  - Lyme disease
  - Rheumatic fever
  - Toxoplasmosis
  - Viral myocarditis
- Infiltrative
  - Amyloidosis
  - Hemochromatosis
  - Lymphoma
  - Other cancers
  - Sarcoidosis
- Ischemic
  - Coronary artery disease
  - Coronary vasospasm
  - Myocardial infarction
- Metabolic
  - Electrolyte abnormalities
  - Thyroid disorders
- Rheumatologic or inflammatory
  - Dermatomyositis
  - Rheumatoid arthritis
  - Scleroderma
  - Systemic lupus erythematosus
- Traumatic
  - Open-heart surgeries
  - Radiofrequency ablation
  - Septal procedures
  - Transcatheter-valve procedures

Früher sahen wir dies täglich

Symptoms

First-degree AV block and Mobitz type I second-degree AV block are most often asymptomatic. They can even be a normal finding in patients with high vagal tone, such as trained athletes. Mobitz type II second-degree AV block and third-degree AV block are more likely to produce symptoms due to bradycardia. Symptoms range from mild fatigue to syncope and even cardiac arrest in extreme cases.

Symptoms of AV block include:

- Fatigue
- Exercise intolerance
- Dizziness
- Presyncope
- Syncope
- Chest pain
- Dyspnea
- Cardiac arrest

Management

Management

Initial Management

Asymptomatic patients who are incidentally found to have first-degree AV block or Mobitz type I second-degree AV block typically do not require any treatment or additional workup. Patients with suspected symptomatic bradycardia and all patients with Mobitz type II second-degree AV block or third-degree AV block warrant hospitalization for monitoring, evaluation, and management.

After initial stabilization, the evaluation of patients admitted for AV block should include investigation for possible reversible causes; these include ischemia, infections (e.g., Lyme carditis), and medications (e.g., digoxin, beta blockers).

Long-Term Management

The mainstay of management for patients with Mobitz type II second-degree AV block or third-degree AV block without a reversible cause is placement of a permanent pacemaker owing to the risk of bradycardia associated with hemodynamic instability. In patients with suspected symptomatic bradycardia due to first-degree AV block or Mobitz type I second-degree AV block, additional investigation is generally warranted to establish the relationship between the patient's symptoms and bradycardia before preceding with placement of a permanent pacemaker.

Further Laboratory Evaluation

The patient was admitted to the hospital for continuous ECG monitoring and additional workup. Given that Lyme disease is endemic in Massachusetts, where the patient lives, and can cause heart block, further diagnostic studies were obtained. In addition to modified two-tiered serologic testing for Lyme disease (combined IgG–IgM screening immunoassay followed by separate immunoassays for IgG and IgM for confirmation), the patient was screened for babesiosis and anaplasmosis because these diseases are transmitted in the northeastern United States by the same species of tick, *Ixodes scapularis*.

Variable	Result	Normal Range	Flag
Lyme antibody screen	Positive	Negative	Abnormal
Lyme IgG	Positive	Negative	Abnormal
Lyme IgM	Positive	Negative	Abnormal
Thin blood parasite smear	No parasites seen	No parasites seen	–
Thick blood parasite smear	No parasites seen	No parasites seen	–
Babesia on PCR testing	No parasites seen	No parasites seen	–
Anaplasma on PCR testing	No parasites seen	No parasites seen	–
Ehrlichia on PCR testing	No parasites seen	No parasites seen	–

What Would You Do Next?

The patient's clinical presentation and positive serologic tests for Lyme disease were consistent with the diagnosis of Lyme carditis.

Which one of the following strategies represents a preferred treatment for this patient? Select a strategy to see whether it is an appropriate choice for treatment and to learn about the probable outcome. You will be able to return to the list of choices to review the probable consequences of each choice.

- ○ **A** Administer a 21-day course of oral doxycycline
- ○ **B** Administer a 21-day course of intravenous ceftriaxone
- ○ **C** Administer intravenous ceftriaxone and then transition to oral doxycycline once conduction improves, for a 14-day total course

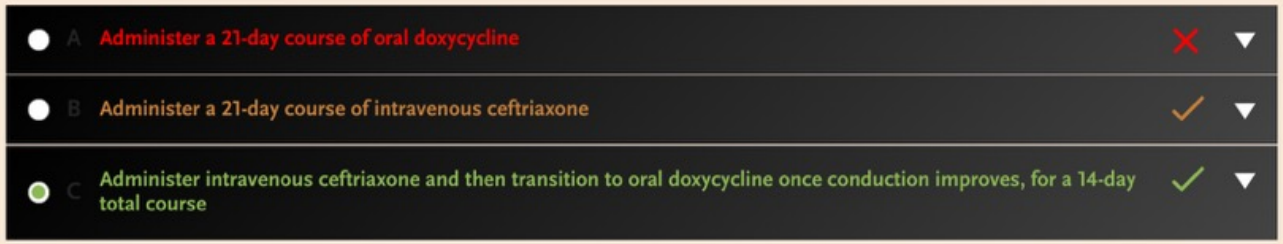

Epidemiology

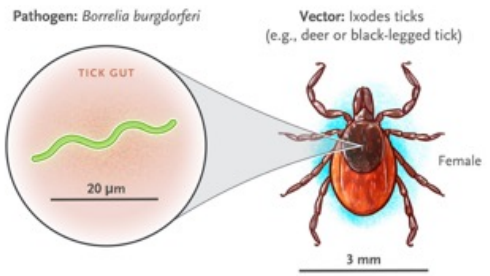

U.S. Lyme Disease Cases Reported to the CDC (2023)

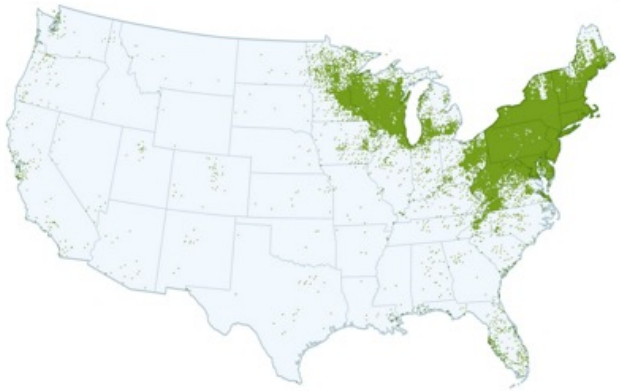

Source: Data are from the Centers for Disease Control and Prevention

- Lyme disease is the most common vector-borne illness in the United States. It is caused by the gram-negative spirochete, *Borrelia burgdorferi sensu stricto*. *B. burgdorferi* is transmitted by species of Ixodes tick (e.g., deer ticks or black-legged ticks). The range of this vector and the length of the season during which it is active have increased with climate change.
- Lyme carditis is a manifestation of early disseminated Lyme disease and occurs weeks to months after initial infection.
- Lyme carditis accounts for roughly 1% of Lyme disease cases reported to the Centers for Disease Control and Prevention.
- Lyme carditis occurs nearly three times as often in men as in women, despite the fact that the men account for just slightly over half of all Lyme disease cases.
- Lyme carditis is less common in Europe, where Lyme disease is primarily caused by other borrelia species.

Pathophysiology

Pathophysiology

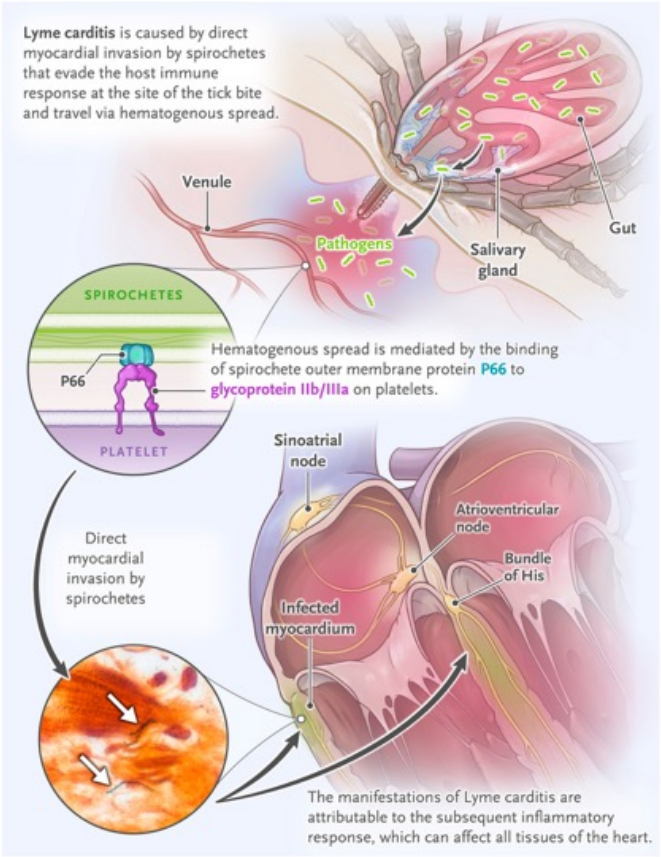

- Cardiac tropism may be driven by the binding of spirochetes to decorin, an extracellular matrix proteoglycan.
- Inflammation of the conduction system, and specifically the AV node, has been observed in autopsy specimens of patients with sudden cardiac death in the setting of Lyme disease.
- The AV block seen in Lyme carditis is most often found at the level of the AV node; blocks occurring further down the conduction system are uncommon.

Clinical Manifestations

Symptoms

- Symptoms of Lyme carditis include palpitations, exercise intolerance, presyncope, syncope, chest pain, dyspnea, and edema of the legs. In mild cases, patients may be asymptomatic.
- Patients may also report the constitutional or neurologic symptoms seen in early Lyme disease.
- Many patients will not recall having erythema migrans, the rash characteristically associated with early localized Lyme disease.

Clinical Findings

- The most common finding is AV block, ranging from first-degree AV block to complete heart block. AV block can progress if it is left untreated.
- Lyme carditis also causes other conduction abnormalities (e.g., bundle-branch block), myocarditis, pericarditis, and in very rare cases, valvular disease.

Management

Management

- Patients whose only manifestation is first-degree AV block with a PR interval of less than 300 msec can be treated with oral antibiotic agents in the outpatient setting. Oral antibiotic options include doxycycline, amoxicillin, cefuroxime axetil, and azithromycin.
- All other patients should be admitted for continuous cardiac monitoring and treatment. Intravenous ceftriaxone is the antibiotic of choice for patients who are hospitalized. Patients can be transitioned to oral antibiotics once there is improvement in conduction.
- When clinical suspicion for Lyme carditis is high, treatment can be initiated while diagnostic tests are pending. The negative predictive value for Lyme disease testing in patients with suspected Lyme carditis is high, so if testing is negative, alternate diagnoses should be considered.
- All patients should receive antibiotic treatment for 14 to 21 days.
- A temporary pacemaker may be placed for patients with unstable bradycardia, but placement of a permenant pacemaker should be avoided because conduction typically improves rapidly with appropriate antibiotic therapy.

Additional Imaging

Transthoracic echocardiography revealed a borderline dilated left ventricle (LV) but globally normal LV function without regional wall-motion abnormalities.

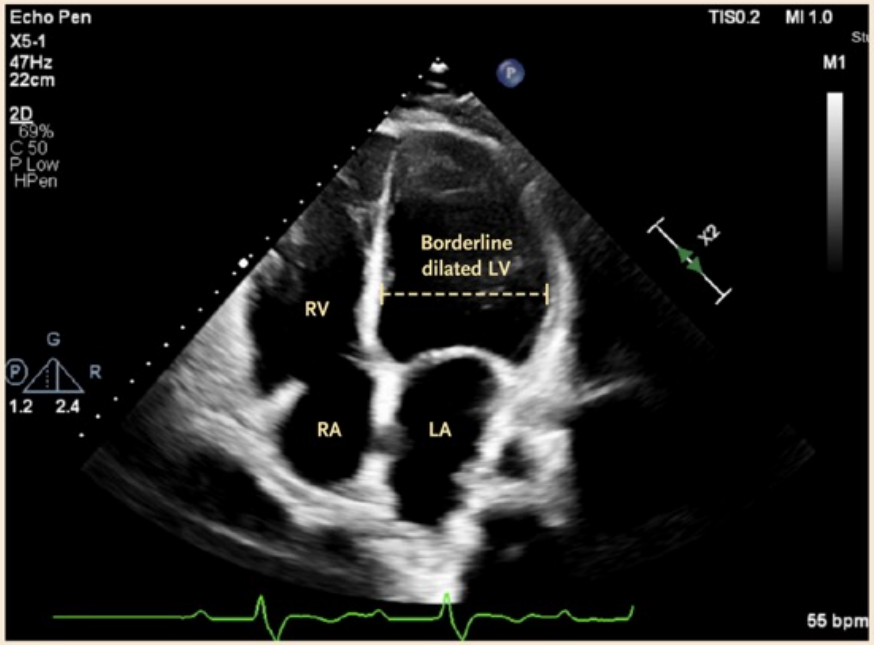

Given that in addition to AV block, the patient had RBBB, a finding less commonly associated with Lyme carditis, the decision was made to perform cardiac magnetic resonance imaging (MRI) to assess for an inflammatory process or scar.

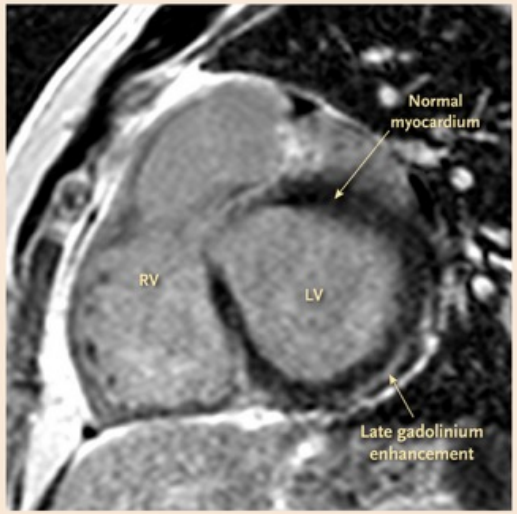

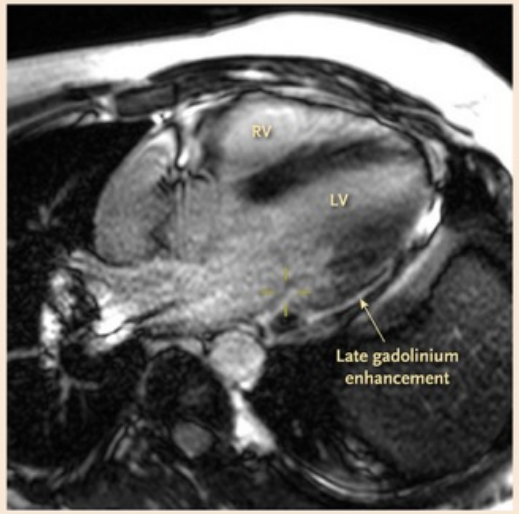

Findings on cardiac MRI were consistent with myocarditis with diffuse myocardial inflammation and a focus of recent injury in the epicardial inferolateral wall, as evidenced by late gadolinium enhancement.

Given the patient's lack of prior cardiac history and risk factors and the pattern of late gadolinium enhancement on cardiac MRI, the LV dilatation seen on the echocardiogram is probably explained by myocarditis. No previous imaging was available to assess the chronicity of the LV dilatation.

Ein **Rechtsschenkelblock (RSB)** hat bei ansonsten gesunden Menschen in der Regel **keinen nennenswerten Einfluss auf die Lebenserwartung**. Die Prognose hängt primär davon ab, ob eine zugrunde liegende Herz- oder Lungenerkrankung vorliegt.

Outcome and Management

Hospital

Day 3

Mobitz type I second-degree AV block resolved, with restoration of 1:1 AV conduction.

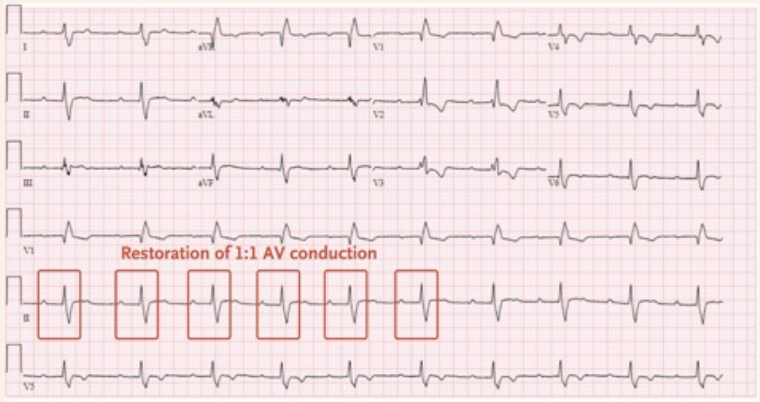

Day 4

Given sustained improvement in conduction, the patient was transitioned from intravenous ceftriaxone to oral doxycycline with a plan for a 14-day total course of antibiotics.

Day 5

The patient was discharged with a 2-week heart rhythm monitor, and cardiology follow-up was arranged.

Cardiology Follow-up 1 Month after Discharge

A 14-day heart rhythm monitor showed no evidence of recurrence of Mobitz type I second-degree AV block. ECG performed in the office showed resolution of AV block but persistent RBBB. It is possible that the patient's RBBB predated his Lyme carditis, but no previous ECGs were available to make this determination.

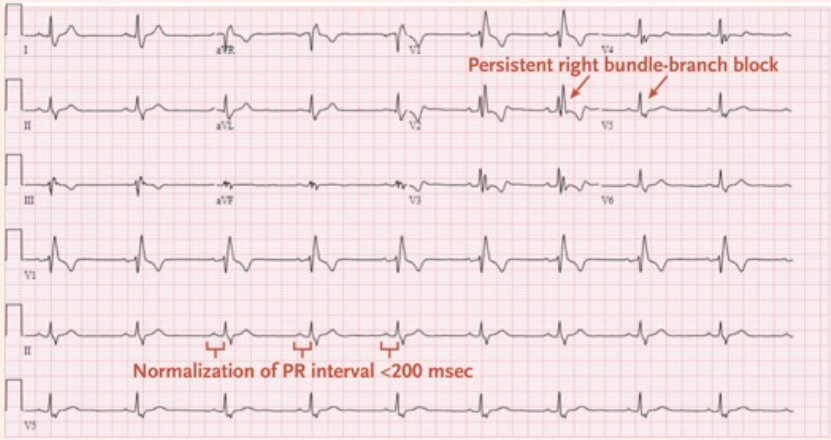

The patient reported feeling well, without recurrence of symptoms.

Teaching Points

- AV block refers to delayed, inconsistent, or absent conduction between the atria and the ventricles and has several possible causes.
- Lyme carditis should be considered in all patients presenting with new AV block in areas where the disease is endemic (or after travel to such areas), even in the absence of preceding erythema migrans.
- The AV block associated with Lyme carditis generally resolves with appropriate antibiotic therapy, and placement of a permanent pacemaker is not indicated.
- Advanced cardiac imaging can be a useful tool in the evaluation of conduction abnormalities.

INTERACTIVE MEDICAL CASE

A Fizzy Fix

A 63-year-old woman presented to the emergency department with a 1-month history of intractable and worsening nausea and vomiting....

Wie kann ein Mensch 16 Präparate schlucken?!?

Case Presentation

A 63-year-old woman presented to the emergency department with a 1-month history of intractable and worsening nausea and vomiting.

She reported decreased appetite during this period as well as nonbilious, nonbloody vomiting. She described burning abdominal pain over the previous month, occurring in the upper abdomen and right side and wrapping around to her back. She did not think that this pain was related to food intake. Over-the-counter omeprazole and famotidine did not decrease the pain or nausea. She attributed her symptoms to increased stress.

She reported weight loss of 18 kg (19.4% of total body weight) over the past year, which had accelerated in the past month. She attributed her weight loss to having started treatment with semaglutide 1 year earlier, when her body-mass index (the weight in kilograms divided by the square of the height in meters) was approximately 32.

Patient History

Medical History

Anxiety

Stage 2 chronic kidney disease (baseline creatinine level, approximately 1.0 mg per deciliter; baseline glomerular filtration rate, approximately 65 ml per minute per 1.73 m^2 of body-surface area)

Chronic obstructive pulmonary disease

Lumbar radiculopathy with chronic back pain

Depression

Gastroesophageal reflux disease

Hyperlipidemia

Essential hypertension

Opioid use disorder

Type 2 diabetes mellitus

Surgical History

Knee cartilage surgery 15 years before the current presentation

Throat surgery

Social History

Reports interpersonal stress and is in the process of a move to a different house

Smoked a half pack of cigarettes daily for 40 years but stopped more than 10 years before the current presentation

Reports no use of alcohol or illicit drugs

Reports long-term clinic-supervised use of methadone for back pain

Medications

Albuterol, 90 µg per actuation, one puff every 6 hours as needed

Alprazolam, 0.5-mg tablet once nightly

Amlodipine, 5 mg once daily

Aspirin, 81 mg once daily

Budesonide–formoterol, 160 µg and 5.6 µg per actuation, respectively, two puffs twice daily

Buspirone, 10 mg once daily

Gabapentin, 300 mg three times daily

Hydrochlorothiazide, 12.5 mg once daily

Lisinopril, 5 mg once daily

Metformin, 500 mg once daily

Methadone, 30 mg once daily

Omeprazole, 20 mg once daily

Roflumilast, 500 µg once daily

Rosuvastatin, 40 mg once daily

Semaglutide, 2 mg once weekly

Tramadol, 50 mg every 6 hours as needed for pain

Family History

Mother with ovarian cancer

Father with melanoma

Physical Examination

Vital signs

Temperature, 36.8°C (oral)
Heart rate, 60 beats per minute
Blood pressure, 109/47 mm Hg
Respiratory rate, 18 breaths per minute
Oxygen saturation, 96% while breathing ambient air
Height, 170.2 cm
Weight, 75 kg
Body-mass index, 25.9

General appearance

Uncomfortable-appearing but in no acute distress

Head, eyes, ears, nose, and throat

Mucous membranes moist

Heart

Regular rate and rhythm
No murmurs, rubs, or gallops

Skin

No erythema, rash, or cyanosis

Lungs

Clear on auscultation
No increased work of breathing or use of accessory muscles
No wheezes, rales, or rhonchi

Abdomen

Bowel sounds present
Negative Murphy's sign
Abdomen soft and nondistended
On admission tender to palpation over right abdomen

Arms and Legs

Warm and well-perfused
No edema
Capillary refill of less than 2 seconds

Lymph nodes

No palpable cervical lymphadenopathy

Nervous system

Awake and alert
Responds to questions appropriately
Oriented to time, person, place, and situation

Laboratory Evaluation

Variable	Result	Normal Range	Flag
Sodium (mmol/liter)	136	136–142	–
Potassium (mmol/liter)	3.2	3.5–5.0	Low
Chloride (mmol/liter)	97	98–108	Low
Bicarbonate (mmol/liter)	25	25–32	–
Urea nitrogen (mg/dl)	39	9–25	High
Creatinine (mg/dl)	3.07	0.70–1.30	High
Estimated glomerular filtration rate (ml/min/1.73 m^2)	16	>60	Low
Glucose (mg/dl)	109	<100 (fasting)	–
Alanine aminotransferase (U/liter)	13	10–50	–
Aspartate aminotransferase (U/liter)	24	10–50	–
Alkaline phosphatase (U/liter)	46	40–130	–
Total protein (g/dl)	6.8	6.4–8.3	–
Albumin (g/dl)	4.1	3.5–5.2	–
Total bilirubin (mg/dl)	0.3	0.0–1.0	–
Direct bilirubin (mg/dl)	<0.2	0.0–0.3	–

Urinstix, Sediment oder Proteinurie?!?
FENa ?

White-cell count (per mm^3)	7670	4000–10,000	–
Hematocrit (%)	29.4	36.0–48.0	Low
Hemoglobin (g/dl)	9.8	11.5–16.4	Low
Reticulocyte count (%)	0.9	0.6–2.8	–
Mean corpuscular volume (fl)	84.5	80.0–100.0	–
Red-cell distribution width (%)	12.9	12.1–16.0	–
Nucleated red cells (per 100 white cells)	0	0	–
Platelet count (per mm^3)	230,000	150,000–450,000	–
Iron (ug/dl)	71	37–145	–
Ferritin (ug/liter)	79	13–150	–
Iron saturation (%)	26	20–40	–
Total iron binding capacity (ug/dl)	272	250–450	–
Vitamin B_{12} (pg/ml)	535	211–946	–
Folate (ng/ml)	7.9	3.1–17.5	–

Imaging Studies

Computed Tomography (CT)

CT of the abdomen and pelvis, performed without contrast enhancement owing to acute kidney injury, showed moderate bile-duct dilatation to the level of the ampulla, without discernible radiodense stones. The stomach was moderately distended with semisolid material. No focal liver lesions were observed. Heavy stool burden was appreciated without evidence of bowel obstruction.

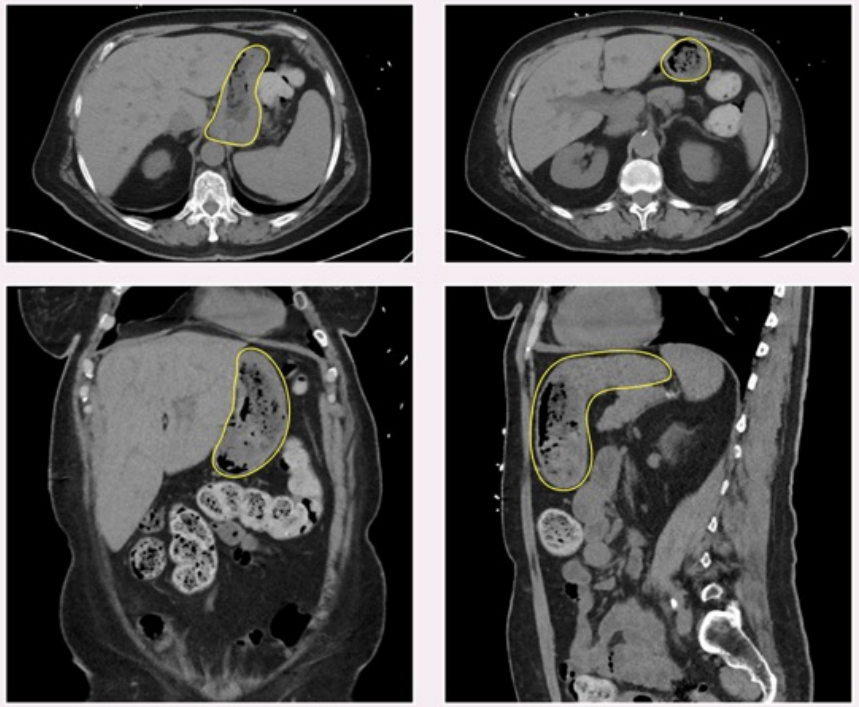

Magnetic Resonance Cholangiopancreatography

Magnetic resonance cholangiopancreatography showed extrahepatic ductal dilatation, with the common bile duct measuring up to 1.4 cm in diameter. No choledocholithiasis or obstructing mass was identified. These findings were considered to be most likely related to nonobstructive biliary dilation in the context of chronic opioid use.

Imaging also revealed a mass in the stomach with mottled features that were considered to be most likely caused by trapped air.

Clinical Course and Initial Management

The patient had persistent nausea and vomiting on the day of hospital admission. She provided additional history, reporting that a few months earlier she had taken approximately 24 tablets of ibuprofen in 1 week for her chronic back pain. Following magnetic resonance cholangiopancreatography, the differential diagnosis for the observed nonobstructive biliary dilatation included chronic opioid use, gastric bezoar, or potentially both. Use of semaglutide or opioids may cause delayed gastric emptying, which increases risk for bezoar formation. In addition, CT imaging aroused concern for accumulation of semisolid material in the stomach. Peptic ulcer disease was also considered, given her symptoms and use of ibuprofen. Esophagogastroduodenoscopy (EGD) was performed.

Initial EGD

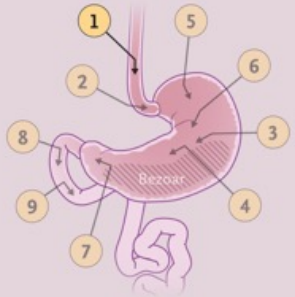

◀ 1 2 3 4 5 6 7 8 9 ▶

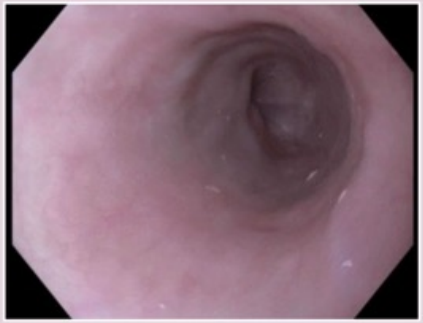

1. Lower Third of the Esophagus

Clinical Course and Initial Management

The patient had persistent nausea and vomiting on the day of hospital admission. She provided additional history, reporting that a few months earlier she had taken approximately 24 tablets of ibuprofen in 1 week for her chronic back pain. Following magnetic resonance cholangiopancreatography, the differential diagnosis for the observed nonobstructive biliary dilatation included chronic opioid use, gastric bezoar, or potentially both. Use of semaglutide or opioids may cause delayed gastric emptying, which increases risk for bezoar formation. In addition, CT imaging aroused concern for accumulation of semisolid material in the stomach. Peptic ulcer disease was also considered, given her symptoms and use of ibuprofen. Esophagogastroduodenoscopy (EGD) was performed.

Initial EGD

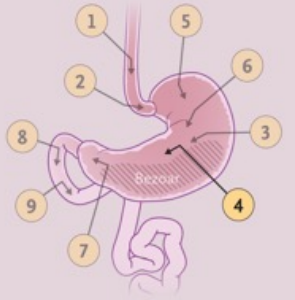

◀ 1 2 3 4 5 6 7 8 9 ▶

4. Gastric Body

Clinical Course and Initial Management

The patient had persistent nausea and vomiting on the day of hospital admission. She provided additional history, reporting that a few months earlier she had taken approximately 24 tablets of ibuprofen in 1 week for her chronic back pain. Following magnetic resonance cholangiopancreatography, the differential diagnosis for the observed nonobstructive biliary dilatation included chronic opioid use, gastric bezoar, or potentially both. Use of semaglutide or opioids may cause delayed gastric emptying, which increases risk for bezoar formation. In addition, CT imaging aroused concern for accumulation of semisolid material in the stomach. Peptic ulcer disease was also considered, given her symptoms and use of ibuprofen. Esophagogastroduodenoscopy (EGD) was performed.

Initial EGD

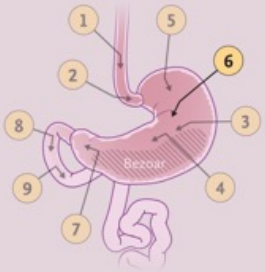

◀ 1 2 3 4 5 **6** 7 8 9 ▶

6. Gastric Body

Clinical Course and Initial Management

The patient had persistent nausea and vomiting on the day of hospital admission. She provided additional history, reporting that a few months earlier she had taken approximately 24 tablets of ibuprofen in 1 week for her chronic back pain. Following magnetic resonance cholangiopancreatography, the differential diagnosis for the observed nonobstructive biliary dilatation included chronic opioid use, gastric bezoar, or potentially both. Use of semaglutide or opioids may cause delayed gastric emptying, which increases risk for bezoar formation. In addition, CT imaging aroused concern for accumulation of semisolid material in the stomach. Peptic ulcer disease was also considered, given her symptoms and use of ibuprofen. Esophagogastroduodenoscopy (EGD) was performed.

Initial EGD

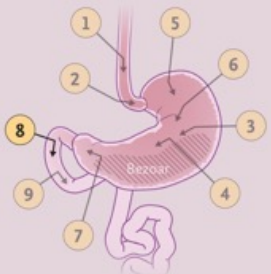

◀ 1 2 3 4 5 6 7 **8** 9 ▶

8. First Portion of Duodenum

The Basics of Gastric Bezoars

LEARNING MODULE

Presentation

Gastric bezoars may be found incidentally in an asymptomatic patient.

When symptomatic, patients may present with nonspecific gastrointestinal symptoms including pain, nausea, vomiting, and abdominal discomfort. Patients may also present with signs of bleeding due to ulceration, including bloody or tarry stool, hematemesis, and anemia.

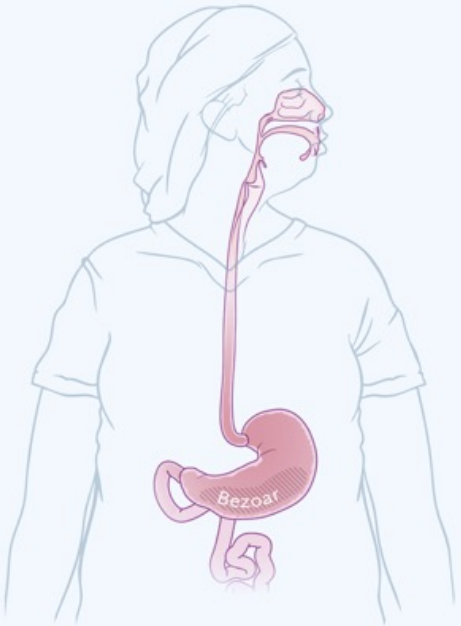

Etiologies

Bezoars are classified on the basis of their composite materials.

- **Phytobezoars** are formed from fruit or vegetable material.
- **Trichobezoars** are formed from ingested hair and are associated with trichotillomania and coincident psychiatric conditions.
- **Pharmacobezoars** are formed from medications and are associated with excessive pill consumption as seen in cases of attempted suicide. They may cause an extended period of drug absorption.

Other types are also described, including lactobezoars (composed of milk protein) in infants, and foreign-body bezoars.

Epidemiologic Features

Gastric bezoars are uncommon in the general population. The risk is higher in persons who ingest certain foods (e.g., persimmons, pineapples, raisins, and celery).

Available data suggest that gastric bezoars are detected in fewer than 0.5% of esophagogastroduodenoscopies. Reduced gastric motility may contribute to bezoar development. There are several possible contributing factors:

- **Anatomical causes** such as postsurgical changes (including changes related to bariatric or other gastric surgery).
- **Medical conditions** such as delayed gastric emptying, diabetes, and autonomic neuropathy.
- **Medications** affecting gastric motility, including glucagon-like peptide-1 receptor agonists, narcotic agents (both of which this patient was taking), and tricyclic antidepressants.

Diagnosis

Diagnosis may be made on the basis of imaging or upper endoscopy.

Computed tomography may show a gastric mass. The diagnosis is supported by the presence of a mass with a mottled appearance that is caused by air trapped within the bezoar.

The diagnosis is typically evident on endoscopy, where a collection of consumed material is found.

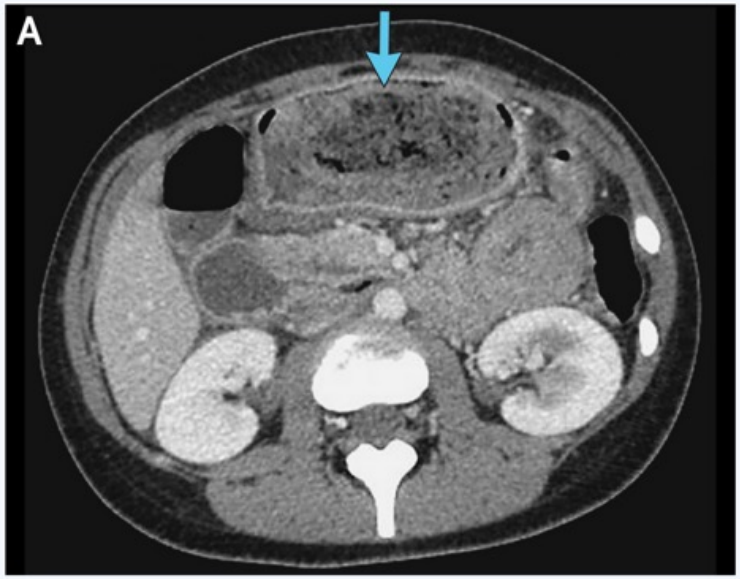

Panel A shows CT revealing a trichobezoar (arrow).

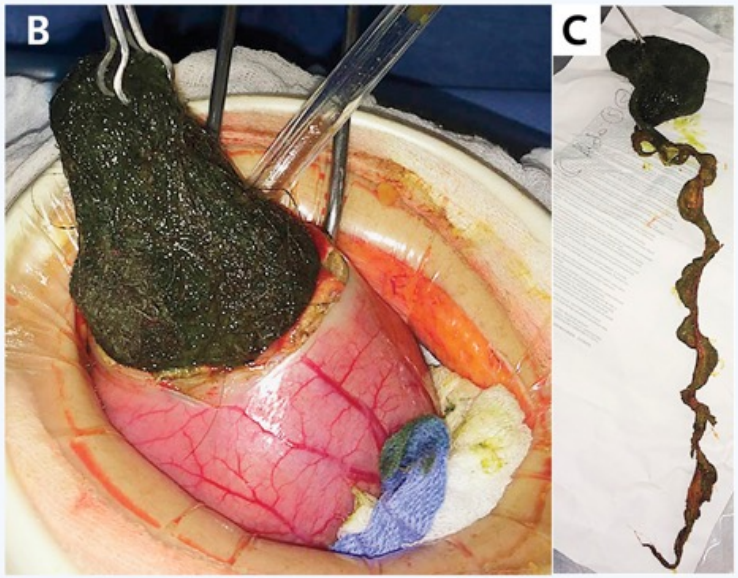

Panel B shows surgical removal of a trichobezoar, and Panel C a trichobezoar after removal.

What Would You Do?

In addition to the discontinuation of semaglutide, which of the following choices would be most appropriate for initial management of a gastric bezoar and persistent nausea and vomiting?

Select a strategy to see whether it is an appropriate choice and to learn about the probable outcome. You will be able to return to the list of choices to review the probable consequences of each choice.

Percentages associated with each management option represent reader responses.

- ○ **A** Monitor the patient and perform periodic EGD after 1 month.
- ○ **B** Initiate chemical dissolution of the bezoar.
- ○ **C** Initiate endoscopic therapy to mechanically disaggregate the bezoar.
- ○ **D** Perform laparoscopic gastrostomy.

Bezore (Bezoare) sind feste Ansammlungen von unverdaulichem Material im Magen-Darm-Trakt, die häufig aus Nahrungsfasern (Phytobezoare) oder Haaren (Trichobezoare) bestehen. Die chemische Auflösung ist eine therapeutische Methode, um diese Ansammlungen ohne Operation zu beseitigen.

Methoden der chemischen Auflösung:

- **Säure-Base-Reaktionen:** Aufgrund der Zusammensetzung, insbesondere bei Phytobezoaren, wird oft versucht, den Bezoar durch den Einsatz von sauren Getränken wie Coca-Cola aufzulösen. Die Säure (in Cola Phosphorsäure) kann die Fasern angreifen, während Kohlendioxid und Zucker den Bezoar lockern können.
- **Enzymatische Behandlung:** Enzyme wie Cellulase können eingesetzt werden, um die Pflanzenfasern von Phytobezoaren gezielt zu zersetzen.
- **Prokinetika:** Häufig wird die Auflösung durch den Einsatz von Medikamenten unterstützt, die die Magenbewegung anregen (Prokinetika), um die aufgelösten Bestandteile abzutransportieren.

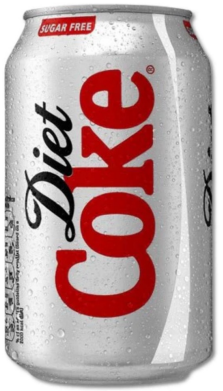

Chemical Dissolution

Semaglutide was discontinued on admission to the hospital.

Chemical dissolution with cola was attempted. Diet cola was recommended owing to the patient's history of diabetes. The plan to administer 3000 ml of cola over a 12-hour period was modified to administration of approximately 1500 ml per day because of the patient's reluctance to consume carbonated beverages, which she did not enjoy.

On the second day of administration of the diet cola, the patient reported a sudden tugging sensation in her abdomen, followed by a prompt decrease in her nausea and abdominal discomfort. A repeat EGD showed that the bezoar was no longer present.

EGD after Bezoar Removal

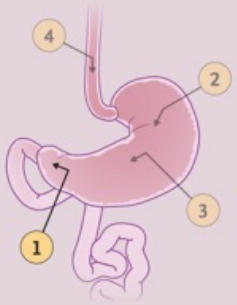

◀ 1 2 3 4 ▶

1. Prepyloric Stomach

Chemical Dissolution

Semaglutide was discontinued on admission to the hospital.

Chemical dissolution with cola was attempted. Diet cola was recommended owing to the patient's history of diabetes. The plan to administer 3000 ml of cola over a 12-hour period was modified to administration of approximately 1500 ml per day because of the patient's reluctance to consume carbonated beverages, which she did not enjoy.

On the second day of administration of the diet cola, the patient reported a sudden tugging sensation in her abdomen, followed by a prompt decrease in her nausea and abdominal discomfort. A repeat EGD showed that the bezoar was no longer present.

EGD after Bezoar Removal

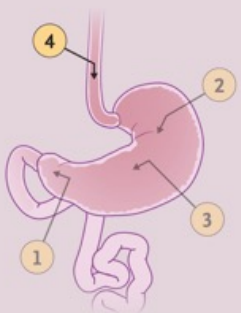

◀ 1 2 3 4 ▶

4. Lower Third of the Esophagus

Click each of the tabs below for information about GLP-1 agonists.

Mechanism of Action

GLP-1 is a peptide hormone released in response to food intake. In the gastrointestinal tract, it increases secretion of insulin and decreases secretion of glucagon in a glucose-dependent manner. GLP-1 also delays gastric emptying. In the brain, GLP-1 serves to down-regulate reward pathways associated with food intake and promote those associated with satiety. In the cardiovascular system, GLP-1 has a role in mitigating plaque development through mediating inflammation. GLP-1 also directly impacts adipose tissue. The cumulative effects of GLP-1 in the body remain under investigation but include improving glucose control, reducing appetite and drive for food, and improving lipid metabolism.

GLP-1 receptor agonist drugs emulate these effects. Exenatide, an early GLP-1–based drug, was limited by enzymatic inactivation, but subsequent drugs (e.g., liraglutide and semaglutide) were designed to be resistant to inactivation, enabling longer dosing intervals and improved absorption.

Derivation of Glucagon-like Peptide-1 (GLP-1) and the Biologic Actions of GLP-1 Medicines

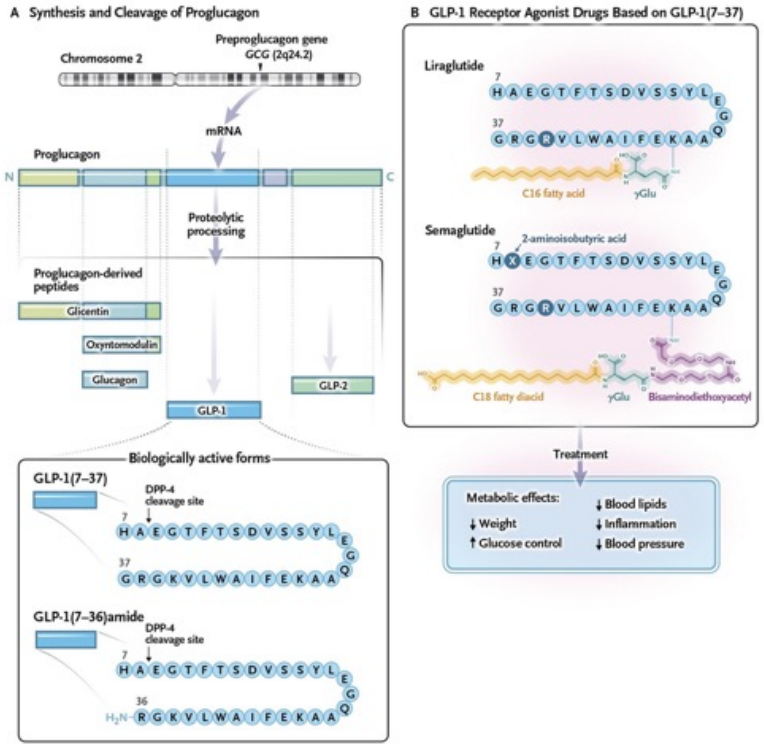

Dual-Acting Agents

Dual-acting agents may act as agonists at both GLP-1 receptors and glucose-dependent insulinotropic polypeptide (GIP) receptors. Similar to GLP-1, GIP is a gastrointestinal peptide that is released with satiety and also serves to slow digestion and modulate the release of insulin.

Tirzepatide is a commercially available dual-acting agent. When tirzepatide was compared with semaglutide in a controlled trial, tirzepatide was found to be superior with respect to weight loss.

Effect of Once-Weekly Tirzepatide as Compared with Semaglutide on Body Weight

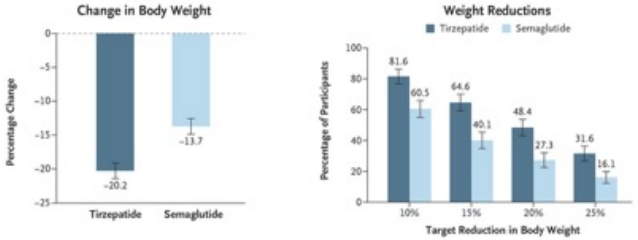

Figure adapted from Aronne LJ, Horn DB, le Roux CW, et al. Tirzepatide as compared with semaglutide for the treatment of obesity. N Engl J Med 2025;393:26-36.

Triple-Acting Agents

Triple-acting agents are also under investigation. These agents have agonist activity at GLP-1 receptors, GIP receptors, and glucagon receptors. Although glucagon increases the blood glucose level, it also serves to further slow gastric emptying and promote catabolic effects.

Retatrutide is one investigational agent in this class, with recently published phase 2 trial results showing a dose-dependent effect with up to 24% weight loss in patients with obesity and without diabetes.

Data that compare triple-acting agents with dual-acting or single-acting agents are unavailable at this time.

Percentage Changes in Body Weight with Retatrutide as Compared with Placebo

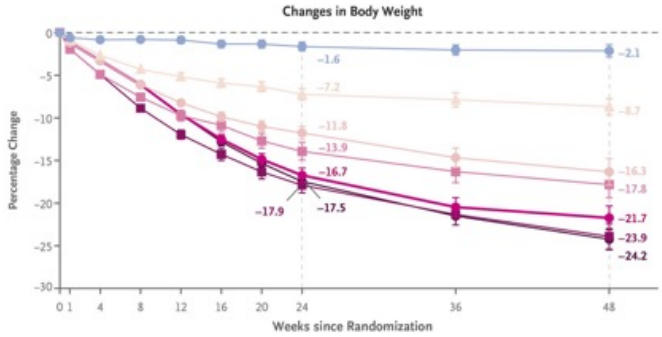

Indications

GLP-1 receptor agonists were initially approved by the Food and Drug Administration (FDA) for the treatment of type 2 diabetes. Several of these drugs were subsequently FDA-approved for the treatment of overweight and obesity. Semaglutide also has been approved for cardiovascular risk reduction in individuals with overweight and obesity with a history of myocardial infarction, stroke, or symptomatic peripheral artery disease, and tirzepatide for treatment of moderate-to-severe obstructive sleep apnea in individuals with obesity. Additional evidence supports use of semaglutide to reduce risk of progression of chronic kidney disease in patients with diabetes and improve symptoms in patients with heart failure. Other data suggest that these agents may reduce symptoms in patients with neurocognitive diseases and reduce craving and alcohol intake in persons with alcohol use disorder.

A full list of indications for GLP-1 receptor agonists approved by the FDA is provided in the accompanying table.

Trade name	Generic name	Indication
Byetta	Exenatide	Type 2 diabetes
Victoza	Liraglutide	Type 2 diabetes
Trulicity	Dulaglutide	Type 2 diabetes
Adlyxin	Lixisenatide	Type 2 diabetes
Xultophy	Liraglutide + insulin degludec	Type 2 diabetes
Soliqua	Liraglutide + insulin glargine	Type 2 diabetes
Bydureon BCise	Exenatide	Type 2 diabetes
Ozempic	Semaglutide	Type 2 diabetes
Rybelsus	Semaglutide	Type 2 diabetes
Mounjaro	Tirzepatide	Type 2 diabetes
Saxenda	Liraglutide	Obesity or overweight
Wegovy	Semaglutide	Obesity or overweight, cardiovascular risk reduction
Zepbound	Tirzepatide	Obesity or overweight, obstructive sleep apnea

Adverse Events

The most common adverse events reported with GLP-1 receptor agonists are gastrointestinal adverse effects including nausea, diarrhea, vomiting, dyspepsia, decreased appetite, and constipation.

Less commonly, delayed gastric emptying may occur; rarely, pancreatitis, gallbladder disease, and bowel obstruction may occur.

Gastrointestinal adverse effects are mitigated by increasing the dose gradually. If doses are missed, it may be necessary to resume a lower dose and increase the dose again over time.

Common Adverse Events Associated with GLP-1 Receptor Agonists

	Tirzepatide N=374	Semaglutide N=376
	no. of patients (%)	
Serious Adverse Events	**18 (4.8)**	**13 (3.5)**
Adverse Events		
Decreased appetite	17 (4.5)	19 (5.1)
Nausea	163 (43.6)	167 (44.4)
Vomiting	56 (15.0)	80 (21.3)
Dyspepsia	22 (5.9)	28 (7.4)
Abdominal pain	24 (6.4)	26 (6.9)
Diarrhea	88 (23.5)	88 (23.4)
Constipation	101 (27.0)	107 (28.5)

Data are from Aronne LJ, Horn DB, le Roux CW, et al. Tirzepatide as compared with semaglutide for the treatment of obesity. N Engl J Med 2025;393:26-36. In this trial, participants were randomly assigned to receive the maximum tolerated dose of tirzepatide (10 mg or 15 mg) or the maximum tolerated dose of semaglutide (1.7 mg or 2.4 mg).

Uptake and Consumer Access

A poll conducted by the Kaiser Family Foundation from April 23 to May 1, 2024, found that 12% of U.S. adults reported having taken a GLP-1 receptor agonist, and 6% reported currently taking one. One fifth of respondents who reported having taken a GLP-1 receptor agonist reported having obtained it from an online provider or a medical spa.

Direct-to-consumer platforms such as telehealth companies may provide access to GLP-1 receptor agonists, including compounded or unapproved products. However, concerns have been raised that these platforms may be associated with misleading advertising and are not generally associated with rigorous safety monitoring.

The cost of GLP-1 receptor agonists is currently high, and payer approvals are often difficult to obtain, thus limiting widespread access.

Semaglutid bewirkt eine deutliche Verzögerung der Magenentleerung. Dieser Mechanismus ist einer der Hauptgründe für die gewichtsreduzierende Wirkung des Medikaments, bringt jedoch auch spezifische Risiken und Verhaltensregeln mit sich.

Wichtige Risiken

- **Gastroparese (Magenlähmung)**: In seltenen Fällen kann die Entleerung so stark verzögert sein, dass eine klinische Magenlähmung auftritt. Dieses Risiko besteht laut Studien auch bei Personen ohne Diabetes.
- **Narkoserisiko**: Bei geplanten Operationen unter Vollnarkose besteht die Gefahr, dass trotz Einhalten der üblichen Fastenzeit noch Nahrung im Magen ist. Dies erhöht das Risiko einer **Aspiration** (Einatmen von Mageninhalt in die Lunge).

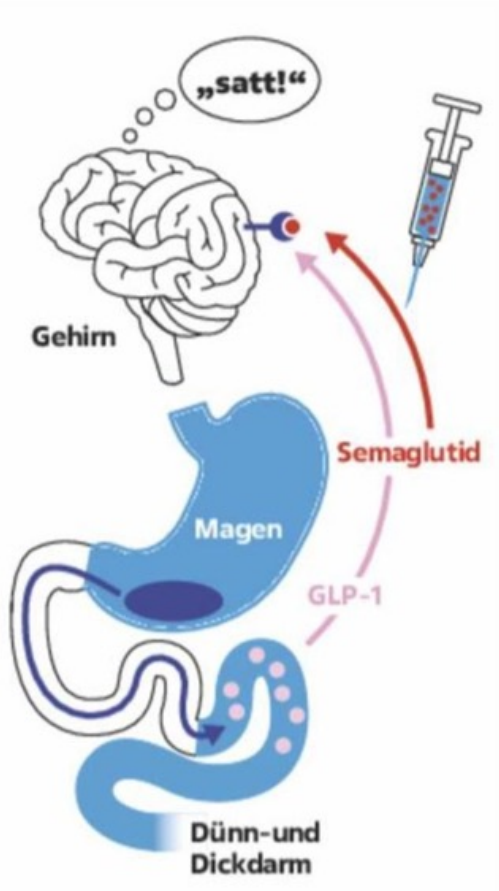

Patient Outcome

In the hospital, the patient transitioned to a regular diet with no adverse effects, and at the time of discharge, she had no nausea, vomiting, or abdominal pain. Semaglutide was not resumed; methadone and tramadol, as needed, were continued. The patient began treatment with twice-daily omeprazole. After discharge, she had an increase in appetite, and her weight increased from 74 kg at discharge to 84 kg 3 months later (BMI increased to 29). Her hemoglobin A1c was 6.6% 3 months after hospitalization (increased from 6.3% 2 months before hospitalization). She was advised to follow up with her primary care provider for a gastric-emptying study. Although this study has not yet been completed, she reported complete symptom resolution at subsequent primary care visits over the next several months.

Teaching Points

- GLP-1 receptor agonists are effective in weight reduction and treatment of type 2 diabetes, but they are associated with a range of gastrointestinal adverse effects including delayed gastric emptying, which may confer a predisposition to bezoar formation.
- Discontinuation or dose reduction of GLP-1 receptor agonists is not uncommon and may be indicated in the case of severe gastrointestinal adverse effects. Discontinuation of these drugs in the context of gastrointestinal adverse effects may be associated with weight gain and worsening glycemic control.
- Gastric bezoars often manifest with nonspecific gastrointestinal symptoms including nausea, vomiting, abdominal pain, and weight loss. Diagnosis requires a high index of suspicion.
- Bezoars formed from food material may be initially managed with oral administration of cola in patients in a clinically stable condition. This intervention is generally cost-effective and is associated with a lower risk of complications than invasive procedures.

Hoffentlich sind viele von den anderen 15 Sachen abgesetzt worden

Orforglipron ist ein neuartiger, einmal täglich einzunehmender **oraler Wirkstoff** zur Behandlung von **Typ-2-Diabetes** und **Adipositas** (Fettleibigkeit). Es gehört zur Klasse der GLP-1-Rezeptoragonisten, unterscheidet sich jedoch von bisherigen Medikamenten wie Semaglutid dadurch, dass es kein Peptid, sondern ein "kleines Molekül" (Small Molecule) ist.

Wichtigste Merkmale

- **Darreichungsform:** Im Gegensatz zu den meisten GLP-1-Therapien, die gespritzt werden müssen, wird Orforglipron als **Tablette** eingenommen.
- **Einfachere Anwendung:** Da es kein Peptid ist, unterliegt die Aufnahme im Körper nicht den strengen Nüchternheitsregeln (z. B. langes Warten vor dem Essen), wie sie bei der aktuellen oralen Semaglutid-Tablette (Rybelsus) gelten.
- **Wirksamkeit:** Klinische Studien (Phase 3) zeigten eine signifikante Senkung des Blutzuckerspiess (HbA1c) und eine deutliche Gewichtsreduktion.

THE LANCET

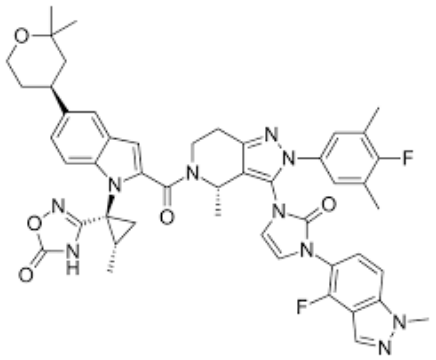

Efficacy and safety of once-daily oral orforglipron compared with oral semaglutide in adults with type 2 diabetes (ACHIEVE-3): a multinational, multicentre, non-inferiority, open-label, randomised, phase 3 trial

Summary

Background Orforglipron is a novel non-peptide (GLP-1) receptor agonist designed for daily oral administration without food or water restrictions. This study aimed to compare the efficacy and safety of orforglipron with oral semaglutide in individuals with type 2 diabetes inadequately controlled with metformin.

Methods In this 52-week, randomised, open-label, active-controlled, multicentre, multinational, phase 3 study, we enrolled adults (≥18 years) with type 2 diabetes inadequately controlled with metformin (≥1500 mg per day), glycated haemoglobin (HbA_{1c}) between 7·0% and 10·5% (53–91 mmol/mol), and BMI at least 25 kg/m² from 131 medical research centres and hospitals in Argentina, China, Japan, Mexico, and the USA. Participants were randomly assigned (1:1:1:1) to orforglipron (12 mg or 36 mg) or semaglutide (7 mg or 14 mg); all groups had an up to 4-week lead-in period and 52-week treatment period, with the drugs administered orally once per day. The primary objective of the study was to assess non-inferiority of orforglipron 36 mg versus semaglutide 14 mg and orforglipron 12 mg versus semaglutide 7 mg for mean change at week 52 from baseline in HbA_{1c} (with a non-inferiority margin of 0·3%) in the intention-to-treat population. Hierarchical analysis for superiority was prespecified after attainment of non-inferiority. The treatment regimen estimand, based on data from all randomly assigned participants regardless of intercurrent events, was the primary estimand; the efficacy estimand was considered supportive. The safety endpoints used data from all participants who received at least one dose of the study drug. This trial was registered on ClinicalTrials.gov (NCT06045221) and is completed.

Findings From Sept 22, 2023, to Aug 22, 2025, 1698 participants were recruited and randomly assigned to orforglipron (n=424 on 12 mg and n=423 on 36 mg) or semaglutide (n=426 on 7 mg and n=425 on 14 mg). For the treatment regimen estimand, mean changes at week 52 from a baseline HbA_{1c} of 8·3% were –1·71% (SE 0·07) with orforglipron 12 mg, –1·91% (0·08) with orforglipron 36 mg, –1·23% (0·05) with semaglutide 7 mg, and –1·47% (0·06) with semaglutide 14 mg. Estimated treatment differences were –0·48% (95% CI –0·65 to –0·31; p<0·0001) for orforglipron 12 mg versus semaglutide 7 mg; –0·44% (–0·62 to –0·26; p<0·0001) for orforglipron 36 mg versus semaglutide 14 mg; –0·24% (95% CI –0·41 to –0·072; p=0·0050) for orforglipron 12 mg versus semaglutide 14 mg; and –0·68% (–0·85 to –0·50; p<0·0001) for orforglipron 36 mg versus semaglutide 7 mg. The primary objective of non-inferiority was met and both orforglipron doses showed superiority to both semaglutide doses, including orforglipron 12 mg versus semaglutide 14 mg. The most frequent adverse events were gastrointestinal events (orforglipron: 249 [59%] of 424 on 12 mg and 245 [58%] of 423 on 36 mg; semaglutide: 157 [37%] of 426 on 7 mg and 193 [45%] of 425 on 14 mg), most of which were mild to moderate in severity. More participants in the orforglipron groups (37 [9%] on 12 mg and 41 [10%] on 36 mg) discontinued study treatment due to adverse events than in the semaglutide groups (19 (4%) on 7 mg and 21 (5%) on 14 mg), and mean increase in pulse rate was greater in the orforglipron groups (12 mg 3·7 bpm; 36 mg 4·7 bpm) than in the semaglutide groups (7 mg 1·0 bpm; 14 mg 1·5 bpm). Four deaths occurred during the study: one in the orforglipron 12 mg group, one in the orforglipron 36 mg group, and two in the semaglutide 7 mg group.

Interpretation In individuals with type 2 diabetes inadequately controlled with metformin, orforglipron 12 mg and 36 mg was non-inferior and superior to semaglutide 7 mg and 14 mg with respect to the mean change in HbA_{1c} from baseline to 52 weeks. Although the safety profiles of both orforglipron and semaglutide were generally consistent with the GLP-1 receptor agonist class, the incidence of gastrointestinal events, discontinuations due to adverse events, and mean increase in pulse rate were higher with orforglipron than oral semaglutide.

	Orforglipron 12 mg (n=424)	Orforglipron 36 mg (n=423)	Semaglutide 7 mg (n=426)	Semaglutide 14 mg (n=425)	Overall (n=1698)
Age, years	54·0 (11·3)	53·4 (11·4)	54·9 (11·2)	53·4 (10·5)	53·9 (11·1)
Sex					
Female	195 (46%)	218 (52%)	206 (48%)	206 (48%)	825 (48·6%)
Male	229 (54%)	205 (48%)	220 (52%)	219 (52%)	873 (51·4%)
Race					
White	250/418 (60%)	259/415 (62%)	266/419 (63%)	254/420 (60%)	1029/1672 (61·5%)
American Indian or Alaska Native	90/418 (22%)	79/415 (19%)	76/419 (18%)	89/420 (21%)	334/1672 (20·0%)
Asian	50/418 (12%)	51/415 (12%)	52/419 (12%)	49/420 (12%)	202/1672 (12·1%)
Black or African American	17/418 (4%)	16/415 (4%)	12/419 (3%)	20/420 (5%)	65/1672 (3·9%)
Ethnicity					
Hispanic or Latino	304 (72%)	304 (72%)	316 (74%)	310 (73%)	1234 (72·7%)
Not Hispanic or Latino	117 (28%)	117 (28%)	108 (25%)	113 (27%)	455 (26·8%)
Diabetes duration, years	9·0 (7·1)	8·2 (5·8)	8·7 (6·3)	8·6 (6·9)	8·6 (6·5)
HbA_{1c} concentration					
In %	8·3 (1·0)	8·3 (1·1)	8·3 (1·1)	8·3 (1·1)	8·3 (1·1)
In mmol/mol	66·8 (11·5)	67·0 (12·1)	67·3 (11·9)	67·2 (12·3)	67·1 (12·0)
≤8·0% [n (%)]	202 (48%)	217 (51%)	199 (47%)	200 (47%)	818 (48·2%)
>8·0% [n (%)]	222 (52%)	206 (49%)	227 (53%)	225 (53%)	880 (51·8%)
Fasting serum glucose					
In mg/dL	169 (54)	167 (52)	170 (51)	172 (52)	169 (52)
In mmol/L	9·4 (3·0)	9·3 (2·9)	9·4 (2·8)	9·6 (2·9)	9·4 (2·9)
BMI, kg/m^2	34·5 (7·1)	35·3 (7·2)	35·1 (7·0)	35·5 (7·1)	35·1 (7·1)
Weight, kg	96·1 (22·2)	96·5 (21·9)	97·1 (22·6)	98·4 (22·6)	97·0 (22·3)
Waist circumference, cm	111·4 (14·9)	112·3 (15·2)	112·3 (15·6)	113·4 (15·4)	112·3 (15·3)
Mean estimated glomerular filtration rate, mL per min per 1·73 m^2	90·4 (20·3)	92·4 (19·2)	88·9 (19·7)	90·5 (19·2)	90·6 (19·6)
Blood pressure, mm Hg					
Systolic	129·6 (13·8)	129·1 (13·1)	129·5 (13·4)	128·8 (13·7)	129·2 (13·5)
Diastolic	80·0 (9·2)	79·9 (8·3)	80·2 (9·1)	80·1 (8·9)	80·0 (8·9)
Pulse rate, bpm	74·7 (10·0)	75·1 (10·1)	74·8 (10·3)	76·2 (10·0)	75·2 (10·1)

Data are mean (SD) or n (%), unless otherwise indicated. This table includes all randomly assigned participants. Estimated glomerular filtration rate is calculated by use of the Chronic Kidney Disease Epidemiology cystatin-C equation.

Table 1: **Demographics and clinical characteristics of participants at baseline**

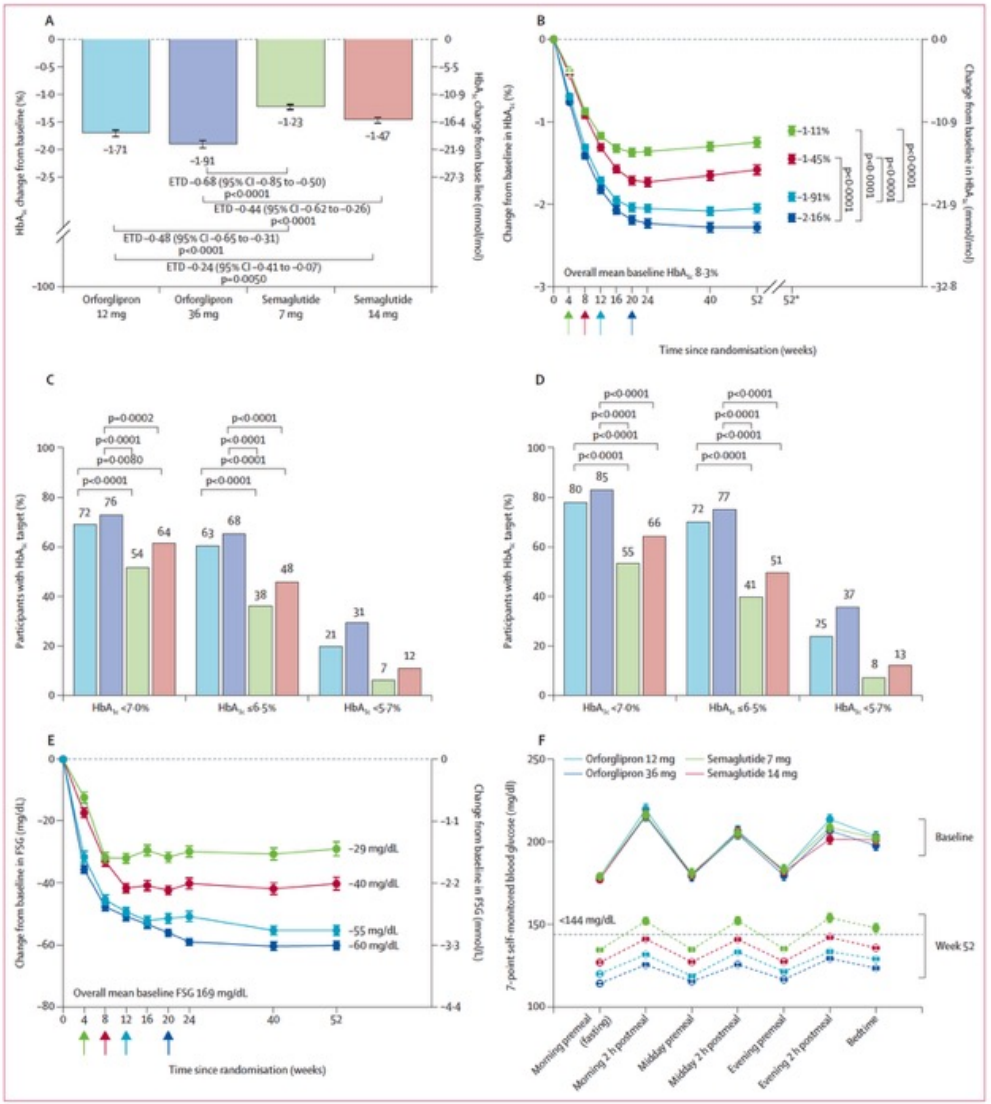

Figure 2: **HbA_{1c} changes, proportion of participants meeting HbA_{1c} targets, FSG, and 7-point self-monitored blood glucose profiles**

(A) Change from baseline in HbA_{1c} at 52 weeks from ANCOVA with multiple imputation by treatment for missing HbA_{1c} data at 52 weeks (treatment regimen estimand). (B) Change from baseline in HbA_{1c} over time. Data are observed mean (SE), with MBE (SE) and MMRM analysis (efficacy estimand) shown in the side panel. (C) Proportion of participants meeting HbA_{1c} targets <7·0%, ≤6·5%, and <5·7% at 52 weeks (treatment regimen estimand) with p values for risk difference; the proportion of participants with HbA_{1c} <5·7% was not controlled for type 1 errors; the proportion was calculated with imputed data from a logistic regression model with primary multiple imputation. (D) Proportion of participants with HbA_{1c} targets <7·0%, ≤6·5%, and <5·7% at 52 weeks (efficacy estimand) with p values for risk difference; the proportion of participants with HbA_{1c} <5·7% was not controlled for type 1 errors; the proportion was calculated with imputed data from logistic regression with multiple imputation under a missing at random assumption. (E) Change from baseline in FSG over time from MMRM analysis (efficacy estimand); this endpoint was not controlled for type 1 error. (F) 7-point self-monitored blood glucose profiles at baseline and week 52 from MMRM (efficacy estimand). Data are MBE (SE), unless otherwise noted, at 52 weeks for all randomly assigned participants. The primary and key secondary objectives were tested under a multiplicity-controlled procedure at a two-sided α level of 0·05 and p values presented are unadjusted two-sided for superiority. Arrows indicate when the randomly assigned dose of orforglipron 12 mg or 36 mg and semaglutide 7 mg or 14 mg were achieved (end of lead-in period). FSG=fasting serum glucose. ETD=estimated treatment differences. MBE=model-based estimate. MMRM=mixed model repeated measures. *MBE (SE).

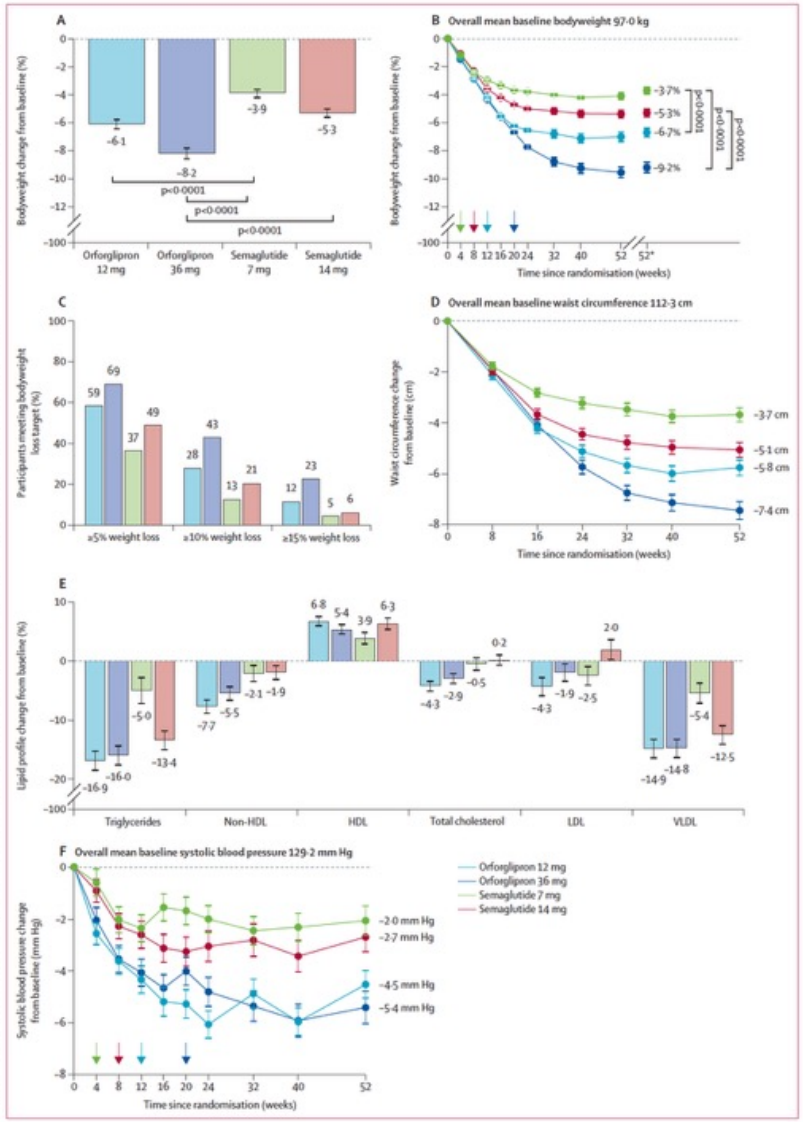

***Figure 3*: Bodyweight changes, proportion of participants achieving weight loss targets, lipid profiles, and systolic blood pressure changes**

(A) Percentage change from baseline in bodyweight at 52 weeks from ANCOVA with multiple imputation by treatment for missing weight at 52 weeks (treatment regimen estimand); orforglipron 12 mg versus semaglutide 14 mg was not controlled for type 1 errors. (B) Percentage change from baseline in bodyweight over time; data are observed mean (SE), with MBE (SE) and MMRM analysis (efficacy estimand) shown in the side panel; orforglipron 12 mg versus semaglutide 14 mg was not controlled for type 1 error. (C) Proportion of participants with weight loss ≥5%, ≥10%, and ≥15% (efficacy estimand); these endpoints were not controlled for type 1 errors; the proportion was calculated with imputed data from logistic regression with multiple imputation under a missing-at-random assumption. (D) Change from baseline in waist circumference over time from MMRM (efficacy estimand); this endpoint was not controlled for type 1 errors. (E) Percentage change from baseline in lipids at 52 weeks; data are estimated percentage means (SE) with log transformation; these endpoints were not controlled for type 1 errors. (F) Change from baseline in systolic blood pressure over time from MMRM (efficacy estimand); this endpoint was not controlled for type 1 errors. Data are MBE (SE), unless otherwise noted, at 52 weeks for all randomly assigned participants. Arrows indicate when the randomly assigned dose of orforglipron 12 mg or 36 mg and semaglutide 7 mg or 14 mg were achieved. The primary and key secondary objectives were tested under a multiplicity-controlled procedure at a two-sided α level of 0·05 and p values presented are unadjusted two-sided for superiority. MBE=model-based estimate. MMRM=mixed model repeated measures. *MBE (SE).

	Orforglipron 12 mg (n=424)	Orforglipron 36 mg (n=423)	Semaglutide 7 mg (n=426)	Semaglutide 14 mg (n=425)	Overall (n=1698)
Participants with ≥1 treatment-emergent adverse event	317 (75%)	318 (75%)	303 (71%)	308 (72%)	1246 (73·4%)
Serious adverse events	21 (5%)	40 (9%)	19 (4%)	24 (6%)	104 (6·1%)
Deaths	1 (<1%)	1 (<1%)	2 (<1%)	0	4 (0·2%)
Adverse event leading to study treatment discontinuation	37 (9%)	41 (10%)	19 (4%)	21 (5%)	118 (6·9%)
Gastrointestinal adverse events leading to study treatment discontinuation	26 (6%)	25 (6%)	11 (3%)	13 (3%)	75 (4·4%)
Nausea	6 (1%)	5 (1%)	3 (1%)	4 (1%)	18 (1·1%)
Vomiting	6 (1%)	9 (2%)	3 (1%)	4 (1%)	22 (1·3%)
Diarrhoea	2 (<1%)	5 (1%)	4 (1%)	0	11 (0·6%)
Abdominal pain	2 (<1%)	3 (1%)	0	0	5 (0·3%)
Dyspepsia	5 (1%)	1 (<1%)	0	0	6 (0·4%)
Decreased appetite	0	3 (1%)	1 (<1%)	0	4 (0·2%)
Constipation	0	0	0	1 (<1%)	1 (0·1%)
Treatment-emergent adverse events occurring in ≥5% of participants in any treatment group by preferred term					
Nausea	111 (26%)	114 (27%)	54 (13%)	90 (21%)	369 (21·7%)
Diarrhoea	91 (21%)	97 (23%)	55 (13%)	76 (18%)	319 (18·8%)
Vomiting	72 (17%)	70 (17%)	32 (8%)	44 (10%)	218 (12·8%)
Dyspepsia	47 (11%)	43 (10%)	18 (4%)	33 (8%)	141 (8·3%)
Decreased appetite	30 (7%)	29 (7%)	21 (5%)	27 (6%)	107 (6·3%)
Hyperglycaemia	25 (6%)	20 (5%)	68 (16%)	32 (8%)	145 (8·5%)
Eructation	42 (10%)	31 (7%)	17 (4%)	14 (3%)	104 (6·1%)
Abdominal distension	24 (6%)	34 (8%)	11 (3%)	14 (3%)	83 (4·9%)
Gastro-oesophageal reflux disease	23 (5%)	24 (6%)	12 (3%)	18 (4%)	77 (4·5%)
Constipation	56 (13%)	51 (12%)	32 (8%)	38 (9%)	177 (10·4%)
Abdominal pain	21 (5%)	25 (6%)	13 (3%)	14 (3%)	73 (4·3%)
Hypertension	10 (2%)	10 (2%)	14 (3%)	22 (5%)	56 (3·3%)
Flatulence	22 (5%)	12 (3%)	14 (3%)	7 (2%)	55 (3·2%)
All gastrointestinal adverse events	249 (59%)	245 (58%)	157 (37%)	193 (45%)	844 (49·7%)
Other adverse events of interest					
Hypoglycaemia (blood glucose <54 mg/dL)*	3 (1%)	4 (1%)	2 (<1%)	1 (<1%)	10 (0·6%)
Severe hypoglycaemia*	0	1 (<1%)	0	0	1 (0·1%)
Severe persistent hyperglycaemia requiring rescue therapy	15 (4%)	12 (3%)	56 (13%)	25 (6%)	108 (6·4%)
Adjudication-confirmed pancreatitis	2 (<1%)	0	0	2 (<1%)	4 (0·2%)
Thyroid malignancies†	1 (<1%)	0	0	1 (<1%)	2 (0·1%)
Gallbladder disorders	5 (1%)	6 (1%)	3 (1%)	4 (1%)	18 (1·1%)
Cholelithiasis	4 (1%)	6 (1%)	3 (1%)	3 (1%)	16 (0·9%)
Diabetic retinopathy, diabetic macular oedema, and related complications‡	21 (5%)	18 (4%)	26 (6%)	19 (4%)	84 (4·9%)
Adjudication-confirmed major adverse cardiovascular events	4 (1%)	4 (1%)	8 (2%)	3 (1%)	19 (1·1%)

Data are n (%) for safety participants (all participants who received at least one dose of the study drug). *Excluding hypoglycaemic events occurring after initiation of any new antihyperglycaemic therapy. †No cases of medullary thyroid cancer were reported, and papillary thyroid cancer was reported in one (<1%) participant in the orforglipron 12 mg group and one (<1%) participant in the semaglutide 14 mg group. ‡Based on MedDRA Preferred Term search defined in appendix (p 40).

Table 2: Adverse events in the safety population

In conclusion, oral orforglipron was non-inferior and superior to semaglutide in terms of efficacy, with meaningful improvements in glycaemic control and weight reduction compared with oral semaglutide in patients with type 2 diabetes, and with larger improvements in cardiometabolic risk factors and simplified administration. The overall safety profile of both orforglipron and semaglutide were consistent with the GLP-1 receptor agonist class, although patients receiving orforglipron had a higher incidence of gastrointestinal events and larger mean increases in pulse rate than those receiving oral semaglutide. Orforglipron represents a potential new therapeutic option for individuals with type 2 diabetes considering initiation of GLP-1 receptor agonist therapy who might prefer an alternative to the subcutaneous route of administration.

Research in context

Evidence before this study

GLP-1 receptor agonists have become a cornerstone in the management of type 2 diabetes, primarily due to their efficacy in improving glycaemic control and weight reduction. On Nov 20, 2025, we searched PubMed with the search terms "glucagon-like peptide-1 receptor agonist", AND "oral", AND "type 2 diabetes", AND "overweight" and limited our search to clinical trials, with no date or language restrictions. Most approved GLP-1 receptor agonists are peptide-based and require subcutaneous administration, with oral semaglutide, co-formulated with an absorption enhancer, sodium N-(8-[2-hydroxybenzoyl]amino) caprylate, being the only oral option. Oral semaglutide has restrictions on food and fluid intake to improve bioavailability. Phase 2 clinical trials showed that orforglipron, a non-peptide, orally available, small molecule GLP-1 receptor agonist, could achieve dose-dependent reductions in glycated haemoglobin (HbA_{1c}) and bodyweight over 26 weeks. In addition to type 2 diabetes and an ongoing cardiovascular outcomes trial, orforglipron is under development for obesity (NCT05869903 and NCT05872620), obstructive sleep apnoea (NCT06649045), stress urinary incontinence (NCT07202884), and peripheral artery disease (NCT07223593). ACHIEVE-1, the first phase 3 clinical trial of orforglipron, showed clinically meaningful efficacy for reduction in HbA_{1c} and bodyweight and safety consistent with the GLP-1 receptor agonist class in individuals with early type 2 diabetes inadequately controlled with diet and exercise alone. In individuals with type 2 diabetes and obesity or overweight (ATTAIN-2), orforglipron was superior for HbA_{1c} and weight reduction than placebo. For individuals or health-care providers considering initiating an oral GLP-1 receptor agonist, there is no evidence on the comparative efficacy and safety of orforglipron versus oral semaglutide.

Added value of this study

ACHIEVE-3 is a multicentre, open-label, international, randomised, active-controlled phase 3 trial to directly compare orforglipron (12 mg or 36 mg) with oral semaglutide (7 or 14 mg) in adults with type 2 diabetes inadequately controlled with metformin. The findings show that orforglipron was non-inferior and superior to semaglutide for HbA_{1c} reduction. Orforglipron 12 mg was significantly better than semaglutide 7 mg and orforglipron 36 mg was significantly better than both semaglutide 7 mg and 14 mg for achieving glycaemic targets and robust weight reduction. Additionally, orforglipron 12 mg was superior to semaglutide 14 mg for HbA_{1c} change from baseline and the proportion of participants achieving HbA_{1c} of less than 7·0% and 6·5% or less. The frequency of gastrointestinal adverse events and treatment discontinuation due to gastrointestinal adverse events, and the increase from baseline in pulse rate, were higher in orforglipron groups than semaglutide groups. The overall safety profiles of both orforglipron and semaglutide were overall consistent with the GLP-1 receptor agonist class.

Implications of all the available evidence

Together with previous research, the results of the ACHIEVE-3 study suggest that orforglipron represents an important advancement in the oral treatment landscape for type 2 diabetes. Its efficacy, safety, tolerability, and simple dosing could address important barriers associated with current incretin-based therapies, offering a new highly efficacious and safe option for individuals seeking effective glycaemic and weight control without the use of injections or administration restrictions.

THE LANCET

GRAFIK

Fraktionelle Flussreserve (FFR): Definition und Werte

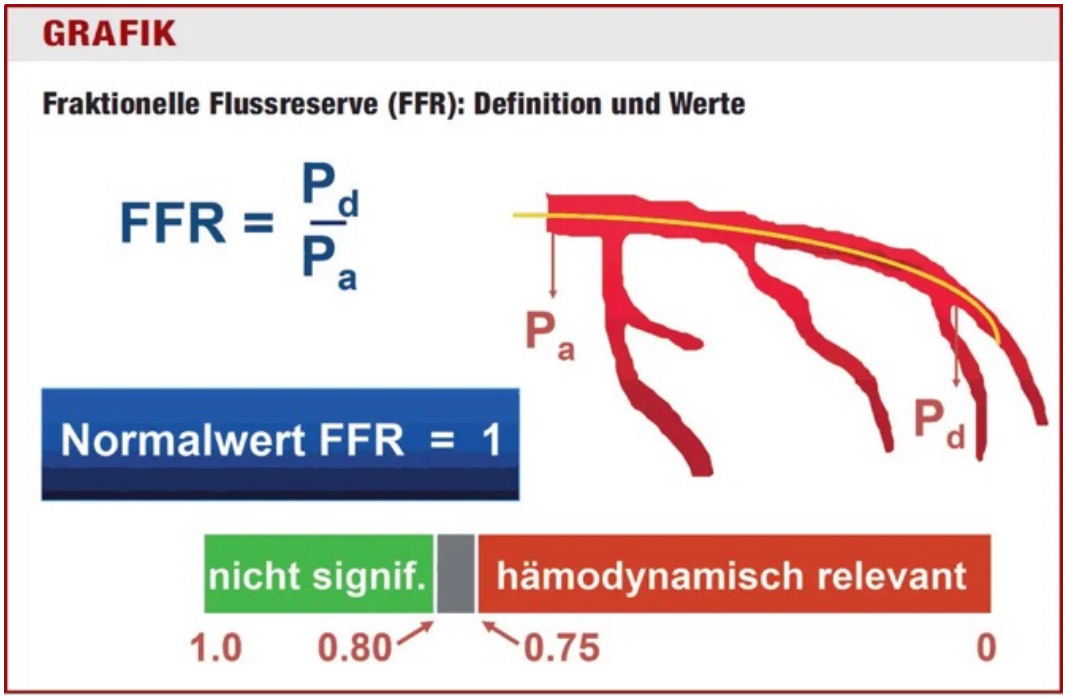

Die FFR ist definiert als der Quotient aus distalem Druck im Koronargefäß (pd, gemessen mit Druckdraht) zu Aortendruck (pa, gemessen mit Führungskatheter) unter Hyperämie. Der Normalwert der FFR ist 1,0. Bei einer FFR > 0,80 besteht keine hämodynamische Relevanz, bei einer FFR < 0,75 liegt eine relevante Läsion vor. Dazwischen liegt ein für ein biologisches System typischer Graubereich.

Die fraktionelle Flussreserve (FFR) ist ein invasiver kardiologischer Messwert zur Beurteilung der hämodynamischen Relevanz von Verengungen (Stenosen) in den Herzkranzgefäßen. Durch eine Druckmessung hinter der Engstelle während der Herzkatheteruntersuchung wird bestimmt, ob ein Stent notwendig ist. Ein FFR-Wert zeigt meist eine behandlungsbedürftige Minderdurchblutung an.

Kernfakten zur FFR:

- **Definition:** Verhältnis des maximalen Blutflusses in einer stenosierten Arterie zum normalen maximalen Fluss.
- **Messung:** Erfolgt mittels eines speziellen Druckdrahtes während der Koronarangiographie, oft unter medikamentös induzierter maximaler Durchblutung (Hyperämie)
- **Nutzen:** Hilft zu entscheiden, ob eine Engstelle den Blutfluss tatsächlich einschränkt und eine Behandlung (Revaskularisation) erfordert, was unnötige Eingriffe reduziert.
- **Klinische Relevanz:** Ein FFR-Wert von 1,0 gilt als normal. Werte weisen auf eine signifikante Stenose hin, die das Myokard (Herzmuskel) unterversorgt.
- **Vorteil:** Bietet eine präzisere funktionelle Beurteilung als die reine visuelle Einschätzung im Angiogramm.

Angiography-derived fractional flow reserve versus coronary angiography to guide coronary artery bypass grafting in patients undergoing surgical valve procedures with concomitant coronary artery disease in China (FAVOR IV-QVAS): a multicentre, triple-blind, randomised trial

Summary

Background For patients undergoing surgical valve procedures with concomitant coronary artery disease, current guidelines recommend that coronary artery bypass grafting (CABG) should be anatomically guided on the basis of stenosis severity, as assessed by coronary angiography. We aimed to test whether a physiologically guided strategy using angiography-derived fractional flow reserve (FFR) could improve clinical outcomes in this population.

Methods FAVOR IV-QVAS is an investigator-initiated, multicentre, randomised, triple-blind trial done at 12 tertiary hospitals in China. Eligible patients were aged 18 years or older and were scheduled for valve surgery, with at least one clinically significant stenosis in a major coronary artery. Patients were randomly assigned (1:1) to undergo physiologically guided CABG (for lesions with an angiography-derived FFR value ≤0·80) or anatomically guided CABG (for lesions with a stenosis diameter ≥50% on coronary angiography). Randomisation was done using a web-based program and stratified by site with fixed blocks of four. Patients, surgeons, follow-up physicians, and outcome assessors were masked to treatment allocation. The primary outcome was a composite of death, myocardial infarction, stroke, unplanned coronary revascularisation, and new renal failure requiring dialysis within 30 days after surgery. The key secondary outcome was a composite of death, myocardial infarction, stroke, unplanned coronary revascularisation, and hospitalisation for unstable angina or heart failure at a minimum follow-up of 1 year. The primary analysis of the primary and key secondary outcomes was done in a modified intention-to-treat population that included all randomly assigned patients who underwent surgery and had available data for the primary outcome. Missing data for the primary outcome were planned to be analysed using complete-case analysis or multiple imputation, with a proportion of missing data of 2% as the threshold. This trial is registered at ClinicalTrials.gov (NCT03977129); extended follow-up is ongoing.

Findings Between Aug 4, 2019, and Aug 13, 2024, 793 patients were enrolled. 396 were randomly assigned to the angiography-derived FFR group and 397 to the coronary angiography group; one patient in the coronary angiography group declined surgery and was excluded from the modified intention-to-treat population. The median age was 65 years (IQR 59–70), 221 (28%) patients were female, and 571 (72%) were male. Concomitant CABG was done in 223 (56%) patients in the angiography-derived FFR group and in 388 (98%) patients in the coronary angiography group. The primary outcome occurred in 31 (7·8%) patients in the angiography-derived FFR group and 53 (13·4%) in the coronary angiography group (absolute difference –5·6 percentage points [95% CI –9·9 to –1·3]; risk ratio 0·58 [95% CI 0·38 to 0·89]; p=0·011). Death within 30 days occurred in 11 (2·8%) patients in the angiography-derived FFR group and 17 (4·3%) patients in the coronary angiography group. At a median follow-up of 27 months (28 months [IQR 18–44] in the angiography-derived FFR group and 27 months [18–42] in the coronary angiography group), the key secondary outcome occurred in 82 (20·7%) patients in the angiography-derived FFR group and in 106 (26·8%) patients in the coronary angiography group (hazard ratio 0·74 [95% CI 0·55–0·98]; p=0·036).

Interpretation Among patients undergoing valve surgery with concomitant coronary artery disease, physiologically guided CABG using angiography-derived FFR reduced the incidence of the composite perioperative outcome compared with anatomically guided CABG. These findings support a selective approach to surgical coronary revascularisation guided by physiological assessment in patients undergoing valve procedures.

Funding Shanghai Hospital Development Center, Shanghai Municipal Science and Technology Commission, and Ministry of Science and Technology of the People's Republic of China.

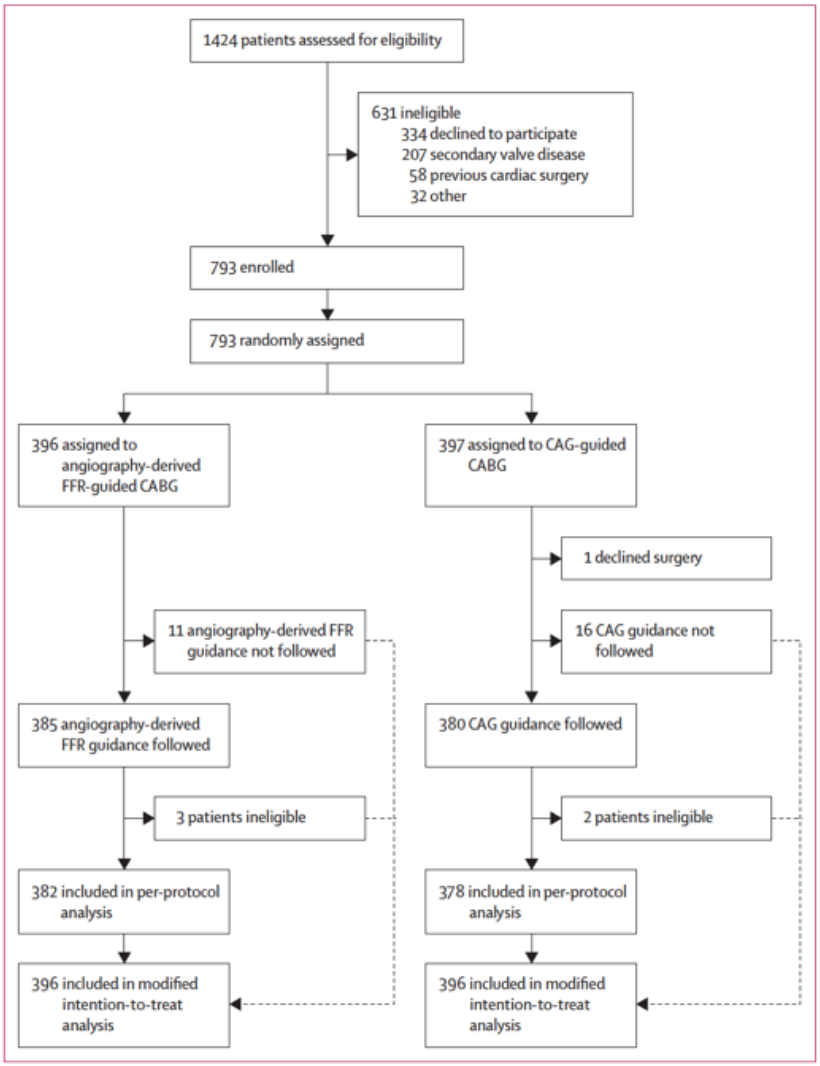

Figure 1: **Trial profile**
CABG=coronary artery bypass grafting. CAG=coronary angiography. FFR=fractional flow reserve.

	Angiography-derived FFR group (n=396)	Coronary angiography group (n=396)
Age, years	65 (59-70)	65 (59-70)
Sex		
Female	112 (28%)	109 (28%)
Male	284 (72%)	287 (72%)
Race or ethnicity		
East Asian	396 (100%)	396 (100%)
BMI, kg/m²	24·6 (22·6-27·0)	24·2 (22·0-26·6)
Aetiology of valvular disease		
Degenerative	293 (74%)	293 (74%)
Rheumatic	93 (23%)	81 (20%)
Other	10 (3%)	22 (6%)
Types of valvular pathology		
Aortic stenosis	96 (24%)	90 (23%)
Aortic regurgitation	131 (33%)	158 (40%)
Mitral stenosis	60 (15%)	56 (14%)
Mitral regurgitation	206 (52%)	218 (55%)
Isolated aortic valve disease	146 (37%)	144 (36%)
Isolated mitral valve disease	192 (48%)	174 (44%)
Combined aortic and mitral valve disease	56 (14%)	77 (19%)
Tricuspid regurgitation	82 (21%)	86 (22%)
Previous myocardial infarction	16 (4%)	29 (7%)
Previous stroke	50 (13%)	53 (13%)
Hypertension	284 (72%)	274 (69%)
Diabetes	91 (23%)	106 (27%)
Atrial fibrillation	125 (32%)	113 (29%)
Current or former smoker	179 (45%)	181 (46%)
Left ventricular ejection fraction	61% (54-65)	61% (55-66)
SYNTAX score*	7 (5-12)	8 (5-13)
Coronary artery lesion		
Left main artery	10 (3%)	15 (4%)
Single vessel	230 (58%)	216 (55%)
Two vessels	95 (24%)	107 (27%)
Three vessels	70 (18%)	72 (18%)
STS-PROM score, %†	2·7% (1·7-4·3)	2·9% (1·9-4·8)

Data are n (%) or median (IQR). FFR=fractional flow reserve. STS-PROM=Society of Thoracic Surgeons predicted risk of mortality. SYNTAX=synergy between percutaneous coronary intervention with taxus and cardiac surgery.
*The SYNTAX score reflects a comprehensive angiographic assessment of the coronary vasculature; a higher score denotes higher anatomical complexity, and a score of 22 or less typically indicates low anatomical complexity of coronary artery disease. The score was calculated by the core laboratory. †The STS-PROM score reflects operative mortality defined as: (1) all-cause death during the hospital stay for the operation, even if after 30 days (including patients transferred to other acute care facilities); and (2) all-cause deaths after discharge from the hospital but before the end of the 30th postoperative day. The score was calculated as valve surgery plus coronary artery bypass grafting here.

Table 1: **Patient characteristics at baseline (modified intention-to-treat population)**

	Angiography-derived FFR group (n=396)	Coronary angiography group (n=396)	Absolute difference, percentage points (95% CI)	Risk ratio (95% CI)	p value
Primary composite outcome					
Death, myocardial infarction, stroke, unplanned revascularisation, or new renal failure requiring dialysis	31 (7·8%)	53 (13·4%)	−5·6 (−9·9 to −1·3)	0·58 (0·38–0·89)	0·011
Individual components of the primary outcome					
Death	11 (2·8%)	17 (4·3%)	−1·5 (−4·3 to 1·1)	0·65 (0·31–1·36)	..
Cardiovascular death	8 (2·0%)	12 (3·0%)	..	..	..
Non-cardiovascular death	3 (0·8%)	5 (1·3%)	..	..	..
Myocardial infarction	6 (1·5%)	22 (5·6%)	−4·0 (−6·9 to −1·5)	0·27 (0·11–0·67)	..
Stroke	6 (1·5%)	9 (2·3%)	−0·8 (−2·9 to 1·3)	0·67 (0·24–1·86)	..
Unplanned revascularisation	5 (1·3%)	1 (0·3%)	1·0 (−0·4 to 2·7)	5·00 (0·59–42·60)	..
New renal failure requiring dialysis	9 (2·3%)	18 (4·6%)	−2·3 (−5·0 to 0·3)	0·50 (0·23–1·10)	..

Data are n (%) unless otherwise specified. FFR=fractional flow reserve.

Table 2: Primary outcome at 30 days (modified intention-to-treat population)

	Angiography-derived FFR group (n=396)				Coronary angiography group (n=396)			
	Number of patients with events (%)	Patients with events per 100 patient-years	Cumulative incidence at 1 year, % (95% CI)	Cumulative incidence at 3 years, % (95% CI)	Number of patients with events (%)	Patients with events per 100 patient-years	Cumulative incidence at 1 year, % (95% CI)	Cumulative incidence at 3 years, % (95% CI)
Key secondary composite outcome								
Death, myocardial infarction, stroke, unplanned revascularisation, hospitalisation for unstable angina, and hospitalisation for heart failure	82 (20·7%)	8·8	14·4% (10·9–17·8)	21·3% (16·7–25·7)	106 (26·8%)	12·1	19·0% (15·0–22·8)	29·3% (24·0–34·2)
Component outcomes								
Death	42 (10·6%)	4·2	7·4% (4·7–9·9)	11·8% (8·2–15·3)	57 (14·4%)	5·8	8·1% (5·4–10·8)	16·5% (12·0–20·7)
Myocardial infarction	13 (3·3%)	1·3	2·8% (1·6–5·0)	3·3% (1·8–5·8)	28 (7·1%)	3·0	6·3% (4·3–9·2)	7·5% (5·2–10·8)
Stroke	29 (7·3%)	3·0	4·8% (3·1–7·5)	6·9% (4·7–10·1)	19 (4·8%)	2·0	3·0% (1·7–5·3)	5·4% (3·5–8·5)
Unplanned revascularisation	8 (2·0%)	0·8	1·8% (0·8–3·7)	2·1% (1·0–4·1)	1 (0·3%)	0·1	0·3% (0–1·8)	0·3% (0–1·8)
Hospitalisation for unstable angina	1 (0·3%)	0·1	0·3% (0–1·8)	0·3% (0–1·8)	2 (0·5%)	0·2	0·5% (0·1–2·0)	0·5% (0·1–2·0)
Hospitalisation for heart failure	11 (2·8%)	1·1	1·3% (0·5–3·0)	3·1% (1·6–5·8)	27 (6·8%)	2·9	4·6% (2·9–7·2)	7·3% (4·9–11·1)

FFR=fractional flow reserve.

Table 3: Key secondary outcome at 1 year and 3 years (modified intention-to-treat population)

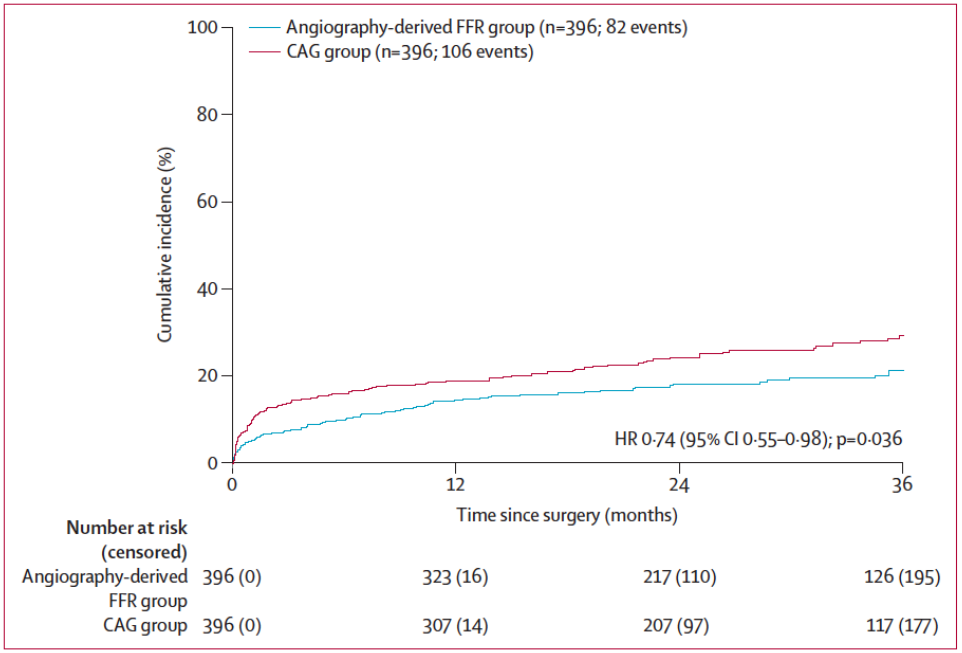

Figure 2: **Kaplan–Meier estimates of the key secondary outcome (modified intention-to-treat population)**
The key secondary outcome was a composite of all-cause death, myocardial infarction, stroke, unplanned revascularisation, hospitalisation for unstable angina, and hospitalisation for heart failure. There was no significant interaction between randomised treatment and log(time) in the extended Cox model (p=0·18). CAG=coronary angiography. FFR=fractional flow reserve.

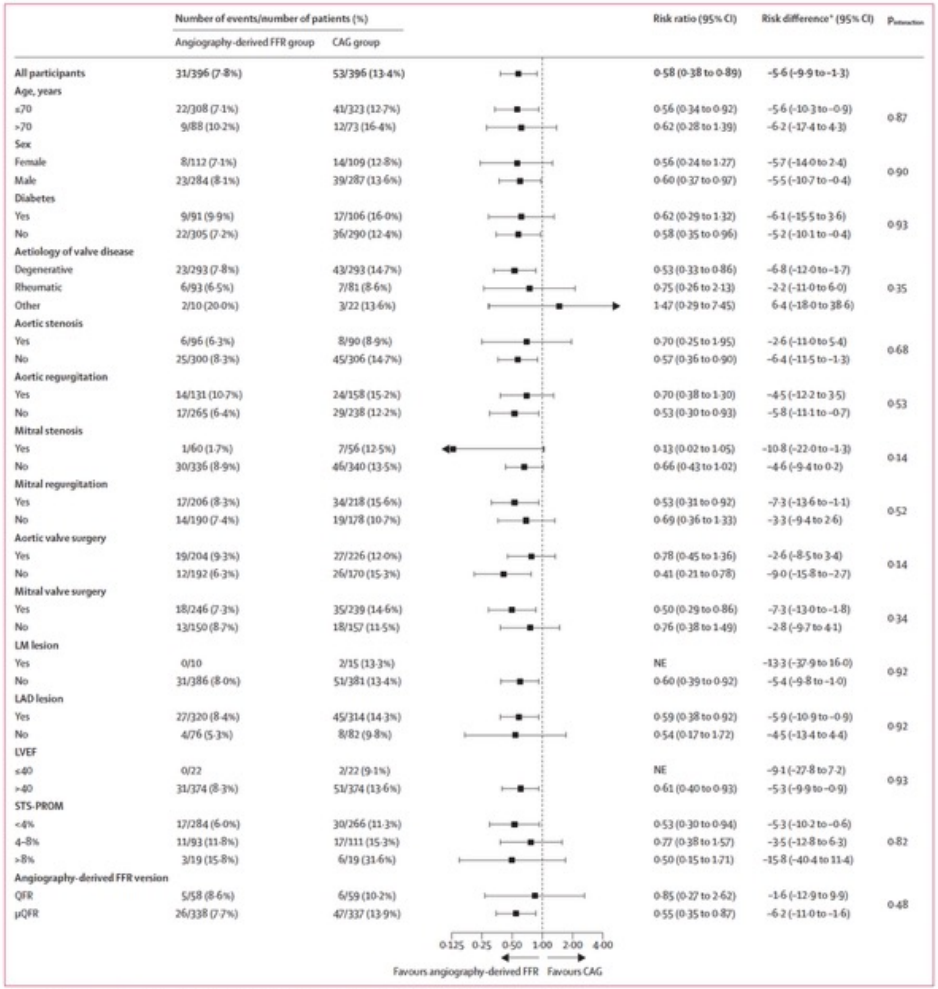

	Number of events/number of patients (%)		Risk ratio (95% CI)	Risk difference* (95% CI)	$p_{interaction}$
	Angiography-derived FFR group	CAG group			
All participants	31/396 (7·8%)	53/396 (13·4%)	0·58 (0·38 to 0·89)	−5·6 (−9·9 to −1·3)	
Age, years					
≤70	22/308 (7·1%)	41/323 (12·7%)	0·56 (0·34 to 0·92)	−5·6 (−10·3 to −0·9)	0·87
>70	9/88 (10·2%)	12/73 (16·4%)	0·62 (0·28 to 1·39)	−6·2 (−17·4 to 4·3)	
Sex					
Female	8/112 (7·1%)	14/109 (12·8%)	0·56 (0·24 to 1·27)	−5·7 (−14·0 to 2·4)	0·90
Male	23/284 (8·1%)	39/287 (13·6%)	0·60 (0·37 to 0·97)	−5·5 (−10·7 to −0·4)	
Diabetes					
Yes	9/91 (9·9%)	17/106 (16·0%)	0·62 (0·29 to 1·32)	−6·1 (−15·5 to 3·6)	0·93
No	22/305 (7·2%)	36/290 (12·4%)	0·58 (0·35 to 0·96)	−5·2 (−10·1 to −0·4)	
Aetiology of valve disease					
Degenerative	23/293 (7·8%)	43/293 (14·7%)	0·53 (0·33 to 0·86)	−6·8 (−12·0 to −1·7)	
Rheumatic	6/93 (6·5%)	7/81 (8·6%)	0·75 (0·26 to 2·13)	−2·2 (−11·0 to 6·0)	0·35
Other	2/10 (20·0%)	3/22 (13·6%)	1·47 (0·29 to 7·45)	6·4 (−18·0 to 38·6)	
Aortic stenosis					
Yes	6/96 (6·3%)	8/90 (8·9%)	0·70 (0·25 to 1·95)	−2·6 (−11·0 to 5·4)	0·68
No	25/300 (8·3%)	45/306 (14·7%)	0·57 (0·36 to 0·90)	−6·4 (−11·5 to −1·3)	
Aortic regurgitation					
Yes	14/131 (10·7%)	24/158 (15·2%)	0·70 (0·38 to 1·30)	−4·5 (−12·2 to 3·5)	0·53
No	17/265 (6·4%)	29/238 (12·2%)	0·53 (0·30 to 0·93)	−5·8 (−11·1 to −0·7)	
Mitral stenosis					
Yes	1/60 (1·7%)	7/56 (12·5%)	0·13 (0·02 to 1·05)	−10·8 (−22·0 to −1·3)	0·14
No	30/336 (8·9%)	46/340 (13·5%)	0·66 (0·43 to 1·02)	−4·6 (−9·4 to 0·2)	
Mitral regurgitation					
Yes	17/206 (8·3%)	34/218 (15·6%)	0·53 (0·31 to 0·92)	−7·3 (−13·6 to −1·1)	0·52
No	14/190 (7·4%)	19/178 (10·7%)	0·69 (0·36 to 1·33)	−3·3 (−9·4 to 2·6)	
Aortic valve surgery					
Yes	19/204 (9·3%)	27/226 (12·0%)	0·78 (0·45 to 1·36)	−2·6 (−8·5 to 3·4)	0·14
No	12/192 (6·3%)	26/170 (15·3%)	0·41 (0·21 to 0·78)	−9·0 (−15·8 to −2·7)	
Mitral valve surgery					
Yes	18/246 (7·3%)	35/239 (14·6%)	0·50 (0·29 to 0·86)	−7·3 (−13·0 to −1·8)	0·34
No	13/150 (8·7%)	18/157 (11·5%)	0·76 (0·38 to 1·49)	−2·8 (−9·7 to 4·1)	
LM lesion					
Yes	0/10	2/15 (13·3%)	NE	−13·3 (−37·9 to 16·0)	0·92
No	31/386 (8·0%)	51/381 (13·4%)	0·60 (0·39 to 0·92)	−5·4 (−9·8 to −1·0)	
LAD lesion					
Yes	27/320 (8·4%)	45/314 (14·3%)	0·59 (0·38 to 0·92)	−5·9 (−10·9 to −0·9)	0·92
No	4/76 (5·3%)	8/82 (9·8%)	0·54 (0·17 to 1·72)	−4·5 (−13·4 to 4·4)	
LVEF					
≤40	0/22	2/22 (9·1%)	NE	−9·1 (−27·8 to 7·2)	0·93
>40	31/374 (8·3%)	51/374 (13·6%)	0·61 (0·40 to 0·93)	−5·3 (−9·9 to −0·9)	
STS-PROM					
<4%	17/284 (6·0%)	30/266 (11·3%)	0·53 (0·30 to 0·94)	−5·3 (−10·2 to −0·6)	
4–8%	11/93 (11·8%)	17/111 (15·3%)	0·77 (0·38 to 1·57)	−3·5 (−12·8 to 6·3)	0·82
>8%	3/19 (15·8%)	6/19 (31·6%)	0·50 (0·15 to 1·71)	−15·8 (−40·4 to 11·4)	
Angiography-derived FFR version					
QFR	5/58 (8·6%)	6/59 (10·2%)	0·85 (0·27 to 2·62)	−1·6 (−12·9 to 9·9)	0·48
μQFR	26/338 (7·7%)	47/337 (13·9%)	0·55 (0·35 to 0·87)	−6·2 (−11·0 to −1·6)	

Figure 3: **Prespecified subgroup analyses of the primary outcome at 30 days (modified intention-to-treat population)**
The primary outcome was a composite of all-cause death, myocardial infarction, stroke, unplanned revascularisation, or new renal failure requiring dialysis within 30 days after surgery. CAG=coronary angiography. FFR=fractional flow reserve. LM=left main coronary artery. LAD=left anterior descending artery. LVEF=left ventricular ejection fraction. NE=not estimable. QFR=quantitative flow ratio. STS-PROM=Society of Thoracic Surgeons predicted risk of mortality. μQFR=upgraded Murray law-based version of QFR. *Risk difference shown as percentage points change.

Research in context

Evidence before this study

For patients undergoing valve surgery with concomitant coronary artery disease, current guidelines recommend that coronary artery bypass grafting (CABG) be anatomically guided on the basis of stenosis severity as assessed by coronary angiography. In percutaneous coronary intervention, physiologically guided revascularisation improves outcomes by avoiding treatment of non-ischaemic lesions, but its role in CABG remains uncertain, and few previous studies have addressed this question. We searched PubMed for randomised controlled trials and observational studies published from database inception to Oct 29, 2025, without language restrictions, using the search terms "fractional flow reserve" OR "FFR" OR "quantitative flow ratio" OR "QFR" OR "angiography-derived FFR" OR ("angioFFR" AND "coronary artery bypass grafting") OR ("CABG" AND "valve surgery"). Our search identified only small observational studies that assessed wire-based or angiography-derived indices to guide CABG, and none provided adequately powered evidence in patients undergoing valve surgery with concomitant coronary disease.

Added value of this study

To the best of our knowledge, FAVOR IV-QVAS is the first large, multicentre, triple-blind, randomised trial of physiologically guided CABG using angiography-derived fractional flow reserve (FFR) in patients undergoing valve surgery. In this trial, conducted at 12 Chinese sites and enrolling 793 patients, angiography-derived FFR guidance significantly reduced the mean number of grafts placed per patient, shortened bypass times, and reduced the composite of death, myocardial infarction, stroke, unplanned revascularisation or new dialysis at 30 days, with benefits maintained at a median follow-up of 27 months.

Implications of all the available evidence

These findings support a selective, physiologically guided approach to concomitant CABG for patients undergoing valve surgery. Physiological assessment can identify non-ischaemic lesions for which surgery can be deferred, simplifying surgery and reducing perioperative morbidity. Further research is needed to ascertain the long-term durability of this approach, its applicability to broader patient populations and health-care systems, and its impact on health-related quality of life and cost-effectiveness.

THE LANCET

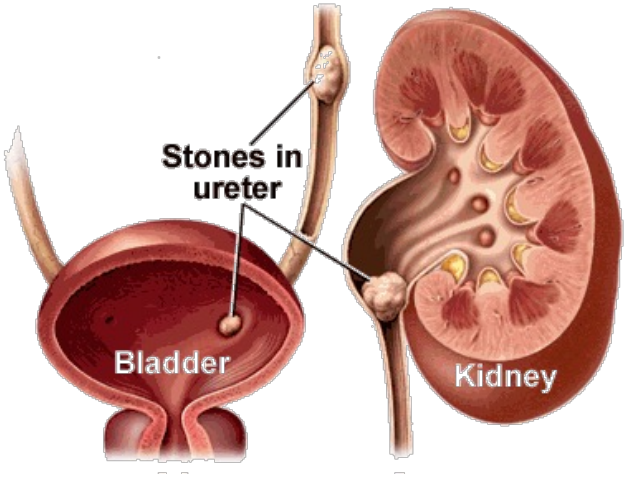

Vorbeugung

- **Viel Trinken:** Ausreichende Flüssigkeitszufuhr (min. 2,5 Liter pro Tag) verdünnt den Urin.
- **Ernährungsumstellung:** Reduzierung von Salz und tierischem Eiweiß, ausgewogene Ernährung.

Harnsteine (Urolithiasis) sind feste Ablagerungen aus Mineralien und Salzen in den Nieren, Harnleitern oder der Blase, die oft durch Dehydrierung, Ernährung oder Stoffwechselstörungen entstehen. Symptome reichen von starken Flankenschmerzen (Koliken) über Blut im Urin bis hin zu Schmerzen beim Wasserlassen. Behandlung umfasst Schmerztherapie, Steinentfernung (Schallwellen/OP) und viel Trinken.

Ursachen und Risikofaktoren

- **Wassermangel:** Zu wenig Flüssigkeitsaufnahme führt zu konzentriertem Urin, was die Kristallisation fördert.
- **Ernährung:** Hoher Konsum von purinreichen Lebensmitteln (Fleisch, Fisch, Meeresfrüchte) kann Harnsäuresteine verursachen.
- **Stoffwechsel/Gesundheit:** Übergewicht, Diabetes und chronische Harnwegsinfektionen (Struvitsteine).
- **Andere Faktoren:** Bewegungsmangel und erblich bedingte Erkrankungen (z. B. Zystinurie).

Prevention of urinary stones with hydration: a randomised clinical trial of an adherence intervention

Summary

Background Increased fluid intake is universally recommended to decrease the risk of recurrent urinary stones; however, adherence is challenging. The effectiveness of interventions to maintain high fluid intake has not been well studied. We sought to determine whether a multicomponent behavioural intervention programme to promote high fluid intake reduces symptomatic stone recurrence, compared with a control.

Methods In this randomised clinical trial, participants aged 12 years and older with a history of urinary stone disease and low 24 h urine volumes based on current guidelines were enrolled at six academic medical centres in the USA. Participants were randomly assigned in a 1:1 ratio to a multicomponent behavioural intervention designed to promote increased fluid intake or to the control group receiving guideline-concordant care. The intervention consisted of a fluid prescription, financial incentives to adhere to fluid prescription, health coaching to overcome barriers to consuming more fluids, and patient-selected approaches such as text messaging to maintain increased fluid intake. Randomisation assignment was computer-generated remotely, and investigators, treating physicians, outcome assessors, and adjudicators were masked to group assignment. The primary outcome was symptomatic stone recurrence defined as stone passage or procedural intervention for stone(s) during a 2-year follow-up period, analysed in the intention-to-treat population. Secondary outcomes included change in 24 h urine volume, urinary symptoms, radiographic stone recurrence or growth, and a composite outcome of symptomatic stone recurrence, new stone formation, and growth of existing stone(s); hyponatremia requiring hospitalisation was the safety endpoint. This trial is registered with ClinicalTrials.gov, NCT03244189.

Findings Between Oct 26, 2017, and Feb 18, 2022, 1658 participants were randomly assigned to intervention (n=826) and control (n=832) groups (median age 44 years [IQR 29–59]; 946 [57%] female). At a median follow-up of 738 days (IQR 711–778), symptomatic stone events occurred in 154 (19%) participants in the intervention group and 165 (20%) in the control group (hazard ratio 0·96, 95% CI 0·77–1·20). Among these 1658 participants, 1104 (66·6%) were recurrent stone formers. 24 h urine volume increased from baseline in both groups and was higher in the intervention group at months 6, 12, 18, and 24 compared with the control group. Urinary storage symptoms of frequency, urgency, and nocturia were greater in the intervention group versus control at months 6 and 12 but not at other timepoints. There was no difference in stone growth of at least 2 mm or new stones between groups from baseline to end-of-study imaging, and the composite outcome of symptomatic stone recurrence, new stone formation, or stone growth of at least 2 mm was also not statistically different between groups. No episodes of hyponatremia requiring hospitalisation (safety endpoint) were reported; 12 (1%) participants in the intervention group had asymptomatic hyponatraemia versus two (<1%) participants in the control group.

Interpretation A behavioural intervention programme to promote fluid intake for secondary stone prevention did not reduce recurrent stone events but modestly increased urine volume compared with guideline-based care during a 2-year follow-up period.

Funding National Institute of Diabetes and Digestive and Kidney Diseases.

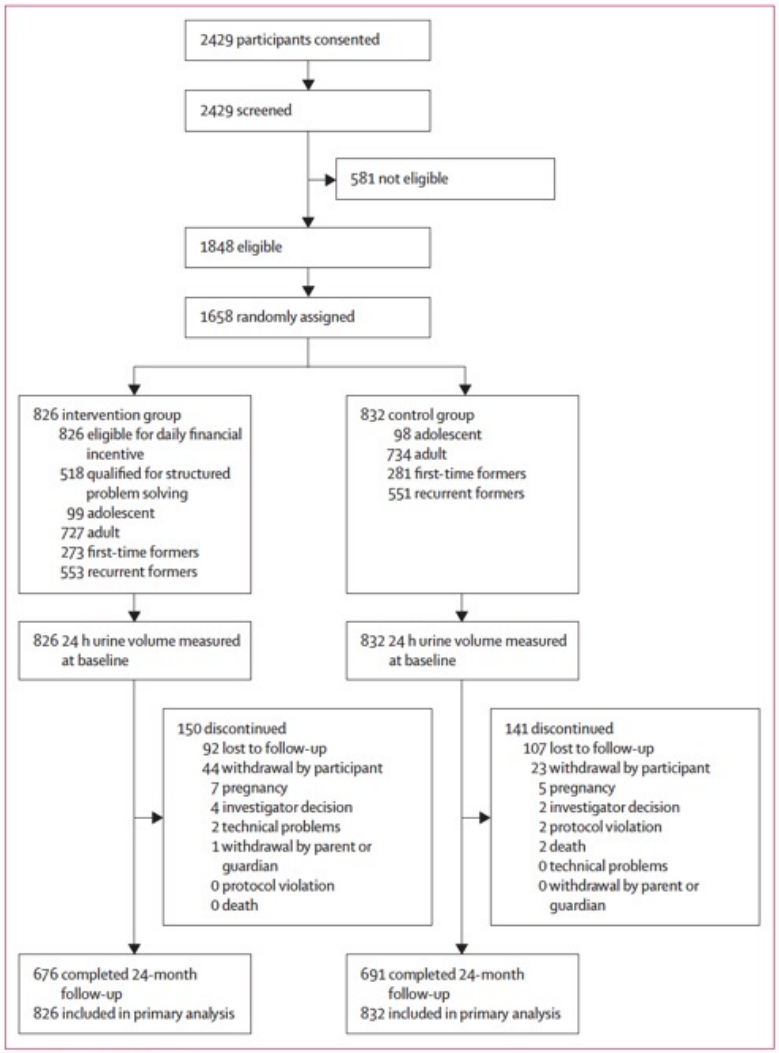

Figure 1: **CONSORT diagram**
All randomly assigned patients included in the primary analysis.

	Intervention group (n=826)	Control group (n=832)	Total (n=1658)
Age, median (IQR), years	45 (30–60)	44 (27–58)	44 (29–59)
Age group, median (IQR), years			
Adult	49 (35–61)	48 (34–59)	48 (36–60)
Adolescent	15 (14–16)	16 (14–16)	15 (14–16)
Female	469 (56·8%)	477 (57·3%)	946 (57·1%)
Male	357 (43·2%)	355 (42·7%)	712 (42·9%)
Race			
White	732 (88·6%)	719 (86·4%)	1451 (87·5%)
Black or African American	55 (6·7%)	58 (7·0%)	113 (6·8%)
Native American	0 (0·0%)	3 (0·4%)	3 (0·2%)
Asian	22 (2·7%)	25 (3·0%)	47 (2·8%)
Native Hawaiian or other Pacific Islander	2 (0·2%)	2 (0·2%)	4 (0·2%)
Other or unknown*	8 (1·0%)	11 (1·2%)	19 (1·1%)
Multiracial	7 (0·8%)	14 (1·7%)	21 (1·3%)
Ethnicity			
Not Hispanic or Latino	761 (92·1%)	757 (91·0%)	1518 (91·6%)
Hispanic or Latino	46 (5·6%)	56 (6·7%)	102 (6·2%)
Not reported	13 (1·6%)	10 (1·2%)	23 (1·4%)
Unknown	6 (0·7%)	9 (1·1%)	15 (0·9%)
Household income			
<$90 000	323 (39·1%)	305 (36·7%)	628 (37·9%)
≥$90 000	365 (44·2%)	371 (44·6%)	736 (44·4%)
Other*	138 (16·7%)	156 (18·8%)	294 (17·7%)
Thiazide diuretic at baseline	61 (7·4%)	60 (7·2%)	121 (7·3%)
Potassium citrate at baseline	92 (11·1%)	96 (11·5%)	188 (11·3%)
Median baseline 24 h urine total volume, L, median (IQR), number of adolescents	0·85 (0·66–1·14), 99	0·85 (0·65–1·05), 98	0·85 (0.66–1·10), 197
Median baseline 24 h urine total volume, L, (IQR), number of adults	1·29 (0·98–1·61), 727	1·30 (1·01–1·56), 734	1·30 (1·00–1·58), 1461
Baseline 24 h urine calcium, mg per total volume, median (IQR), number of adults	190 (129–261), 552	190 (127–256), 544	190 (128–259), 1096
Baseline 24 h urine citrate, mg per total volume, median (IQR), number of adults	553 (383–757), 538	534 (376–729), 532	544 (378–746), 1070
Baseline 24 h urine pH, mean (IQR), number of adults	6·00 (5·65–6·41), 671	6·04 (5·66–6·41), 685	6·02 (5·65–6·41), 1356
Baseline 24 h urine osmolality, mOsm/kg, median (IQR), number of adults	662 (471–847), 432	653 (463–815), 469	657 (469–834), 901
Baseline 24 h urine sodium mEq/TV, median (IQR), number of adults	140 (103–183), 549	134 (99–177), 540	137 (101–179),1089
Baseline 24 h urine potassium, mEq/TV, median (IQR), number of adults	50 (36–66), 538	48 (36–62), 525	49 (36–64), 1063

Data are number (%), unless otherwise indicated. mEq/TV=milliEquivalents per total volume. mOsm=milliosmole osmotic concentration. TV=total volume. $=US$.*Includes "don't know" and "prefer not to answer" responses.

Table: **Demographic and clinical characteristics of study participants**

Kein Unterschied hier!

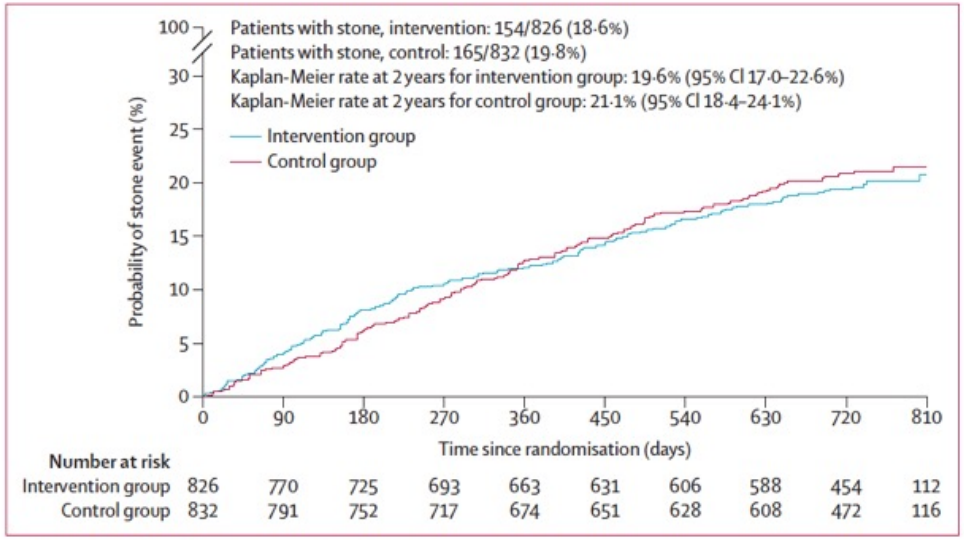

Figure 2: Symptomatic recurrence of urinary stones

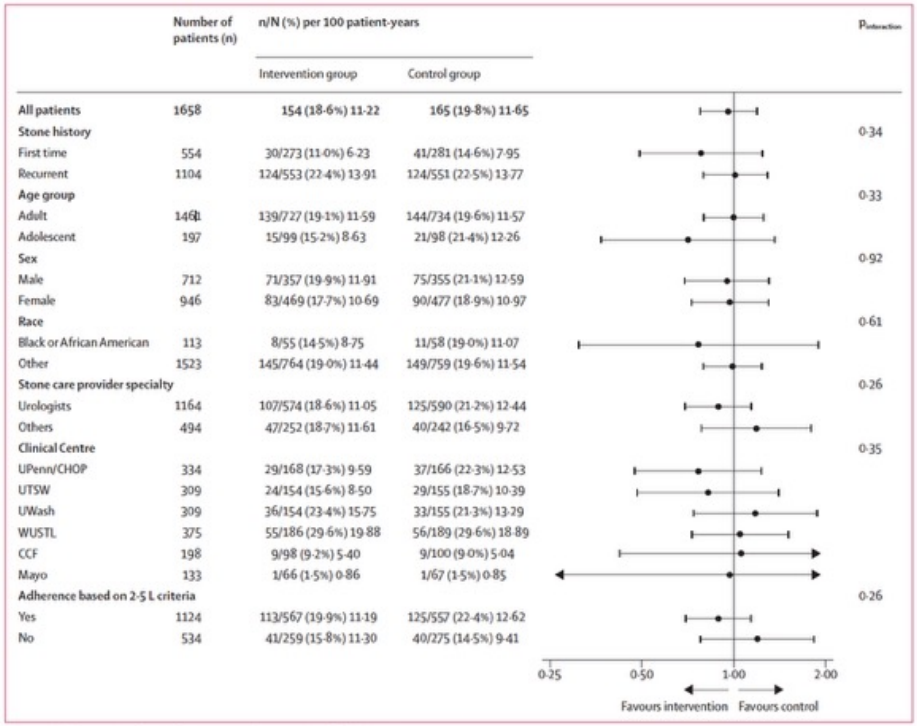

	Number of patients (n)	n/N (%) per 100 patient-years		$P_{interaction}$
		Intervention group	Control group	
All patients	1658	154 (18·6%) 11·22	165 (19·8%) 11·65	
Stone history				0·34
First time	554	30/273 (11·0%) 6·23	41/281 (14·6%) 7·95	
Recurrent	1104	124/553 (22·4%) 13·91	124/551 (22·5%) 13·77	
Age group				0·33
Adult	1461	139/727 (19·1%) 11·59	144/734 (19·6%) 11·57	
Adolescent	197	15/99 (15·2%) 8·63	21/98 (21·4%) 12·26	
Sex				0·92
Male	712	71/357 (19·9%) 11·91	75/355 (21·1%) 12·59	
Female	946	83/469 (17·7%) 10·69	90/477 (18·9%) 10·97	
Race				0·61
Black or African American	113	8/55 (14·5%) 8·75	11/58 (19·0%) 11·07	
Other	1523	145/764 (19·0%) 11·44	149/759 (19·6%) 11·54	
Stone care provider specialty				0·26
Urologists	1164	107/574 (18·6%) 11·05	125/590 (21·2%) 12·44	
Others	494	47/252 (18·7%) 11·61	40/242 (16·5%) 9·72	
Clinical Centre				0·35
UPenn/CHOP	334	29/168 (17·3%) 9·59	37/166 (22·3%) 12·53	
UTSW	309	24/154 (15·6%) 8·50	29/155 (18·7%) 10·39	
UWash	309	36/154 (23·4%) 15·75	33/155 (21·3%) 13·29	
WUSTL	375	55/186 (29·6%) 19·88	56/189 (29·6%) 18·89	
CCF	198	9/98 (9·2%) 5·40	9/100 (9·0%) 5·04	
Mayo	133	1/66 (1·5%) 0·86	1/67 (1·5%) 0·85	
Adherence based on 2·5 L criteria				0·26
Yes	1124	113/567 (19·9%) 11·19	125/557 (22·4%) 12·62	
No	534	41/259 (15·8%) 11·30	40/275 (14·5%) 9·41	

Figure 3: Subgroup analyses of symptomatic recurrence of urinary stones
UWash=University of Washington. WUSTL=Washington University in St.Louis. CCF=Cleveland Clinic. Mayo=Mayo Clinic. UPenn/CHOP=University of Pennsylvania/Children's Hospital of Philadelphia. UTSW=University of Texas Southwestern. *Adherence defined as at least 2·5 L urine output per 24 h on at least two 24 h collections for adult participants. Additionally, the 24 h urine collection group is required to have creatinine mg/kg per day within 2 SD of mean Cr mg/kg per day for the cohort.

Bisschen mehr Urin!

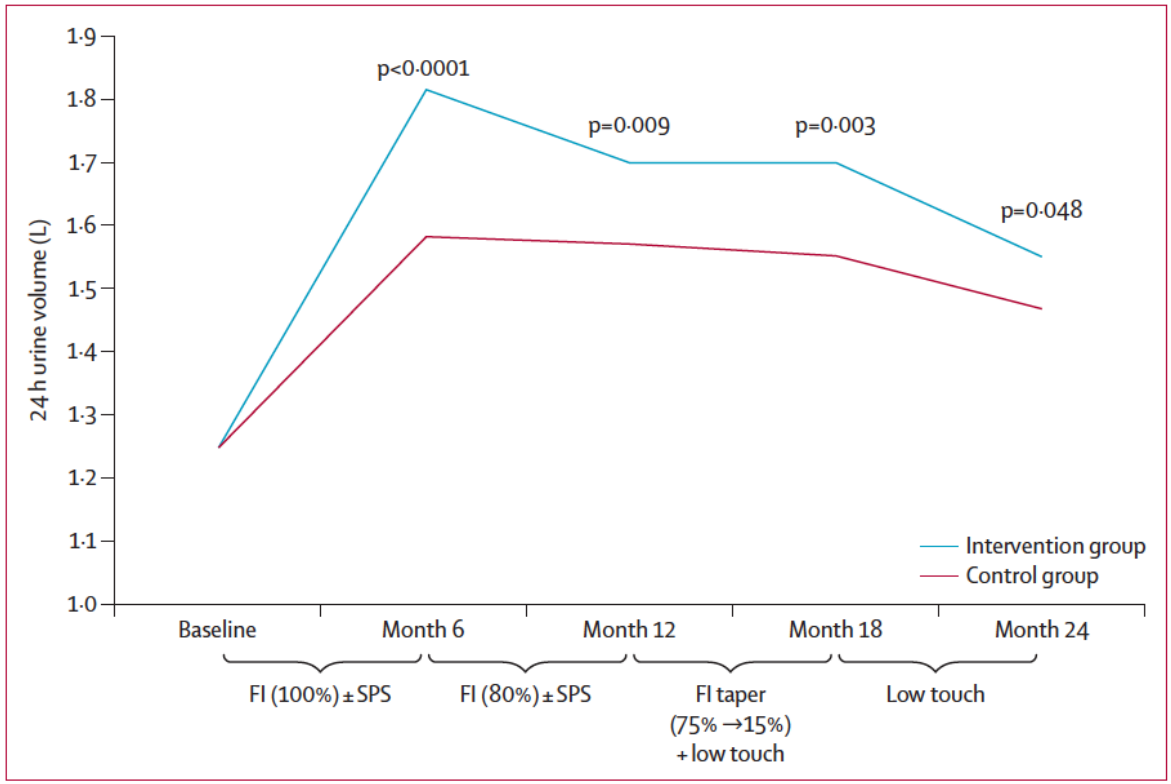

Figure 4: **24 h urine volume by timepoint and treatment group (mixed-effects model)**
FI (%)=loss-framed financial incentive. % indicates percentage of days loss-framed incentive was available to participants. FI Taper=financial incentive taper. Availability tapered from 75% of days (month 13) to 15% of days (month 18). Participants blinded to which day(s) financial incentive was available. No financial incentive available in months 19–24. SPS=structured problem solving. Low touch=low touch interventions to promote adherence (eg, support partner, reminder via text communication).

Research in context

Evidence before this study

We performed a systematic search of PubMed for randomised trials testing interventions to promote adherence to fluid intake for secondary prevention of urinary stone disease. We searched PubMed (from Jan 1, 1995, to June 2, 2025); the detailed search strategy is available in the appendix (p 4). We also searched ClinicalTrials.gov (from inception to June 2, 2025) to identify similar trials in progress or without published results.

We identified 222 publications and five ClinicalTrials.gov listings. Of these, we identified six trials (including one published only as a conference abstract) testing adherence interventions for fluid intake for secondary stone prevention. Of these six trials, two were initiated before 2017, when our Prevention of Urinary Stones with Hydration (PUSH) trial began. The Hidrate Me study (NCT02938884) randomly assigned participants with a history of urinary stone disease and low urine volume to a smart water bottle (Hidrate Spark) versus standard water bottle, facilitating self-monitoring of behaviour in the intervention group. The results of this trial were reported in 2022. Among 85 participants enrolled, 51 (60%) completed 24 h urine collections at 6 weeks, with a greater mean increase in urine volume over baseline in the smart water bottle group than in the control group (+1·37 [SD 0·94] L per day *vs* +0·79 [SD 0·97] L per day, p=0·04). Stone recurrence was not ascertained as an outcome. The second study, initiated before 2017, was an observational cohort study (NCT01928108) enrolling adults with a history of urinary stone disease. This study compared use of two different smartphone applications to manually track water consumption, also using a behaviour change technique of self-monitoring. Neither the literature search nor ClinicalTrials.gov reported study results. The other four trials of adherence interventions for fluid intake in prevention of urinary stone disease were initiated after PUSH started. The protocol describing the sipIT2 trial (with a primary endpoint of 24 h urine volume) was published in 2024. Two randomised controlled trials identified only via ClinicalTrials.gov compared a smartphone application delivering prevention education versus a control group receiving no stone prevention information. The sixth trial (comparing the mobile app care plan versus the standard kidney stone follow-up pathway) was identified only via a conference abstract; no ClinicalTrials.gov registration was identified. Current guidance for water intake for secondary stone prevention is based on a Cochrane Systematic Review (2020) that found a single randomised controlled trail (Borghi, 1996) comparing the effects of high water intake versus low water intake for secondary urinary stone disease prevention. Cochrane assessed this randomised controlled trial as low-certainty evidence.

Added value of this study

The PUSH trial advances the field by testing an adaptive, multicomponent behavioural health approach to promoting fluid intake adherence in a large population of patients with urinary stone disease and low urine volume. The PUSH intervention is grounded in contingency management, leveraging a loss-framed financial incentive, along with an adaptive structured problem-solving intervention that is responsive to participant non-adherence. In addition to examining 24 h urine output, PUSH is the first adherence study to assess the clinical endpoint of urinary stone recurrence.

Implications of all the available evidence

Very little evidence is available to guide clinicians about the best strategies that will increase and sustain high fluid intake for secondary urinary stone disease prevention. The PUSH trial results suggest that for many patients with urinary stone disease and low urine volume, it might be difficult to sustain high fluid intake and thereby reduce stone recurrence. Taken together, these results suggest that investigators might need to focus on alternative adherence strategies and secondary prevention strategies that go beyond simply increasing fluid intake.

THE LANCET

Video-assisted thorascopic surgery

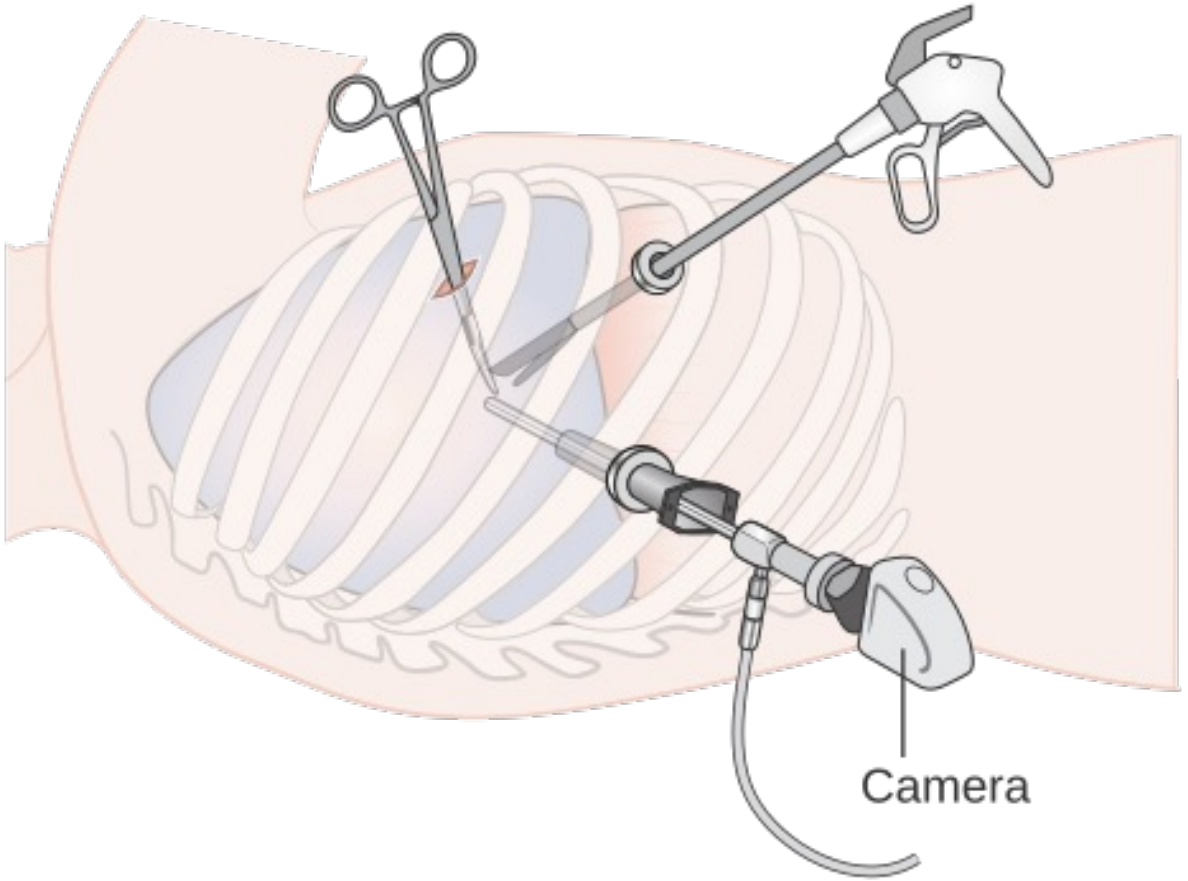

Eine **Lobektomie** ist der chirurgische Eingriff, bei dem ein ganzer Lungenlappen entfernt wird. Sie gilt als **Goldstandard** für die Behandlung von lokalisiertem Lungenkrebs, insbesondere beim nicht-kleinzelligen Lungenkarzinom (NSCLC) im Frühstadium.

Warum eine Lobektomie durchgeführt wird

Der Hauptgrund ist die vollständige Entfernung eines Tumors, bevor dieser in andere Bereiche streuen kann.

- **Krebskontrolle**: Durch die Entfernung des gesamten Lappens wird ein Sicherheitsabstand um den Tumor gewährleistet.
- **Lymphknoten**: Zusammen mit dem Lappen werden umliegende Lymphknoten entfernt, um eine mögliche Ausbreitung zu prüfen und das Rückfallrisiko zu senken.
- **Heilungschance**: Bei Tumoren über 2 cm bietet die Lobektomie die besten Aussichten auf eine langfristige Heilung.

Survival outcome of VATS compared with open lobectomy for lung cancer: an individual patient data meta-analysis of randomised trials

Summary

Background Video-assisted thoracoscopic surgery (VATS) is currently the most common approach for pulmonary lobectomy in early-stage lung cancer. Reported advantages include less pain, fewer complications, faster recovery, and improved postoperative quality of life. The widespread adoption of VATS lobectomy is principally based on non-oncological benefits. Its oncological equivalence to open surgery remains assumed as no single trial has been powered for survival. To address this important question, we sought to conduct an individual patient data meta-analysis of eligible randomised trials.

Methods We systematically reviewed PubMed, MEDLINE, Embase, and the Cochrane Central Register of Controlled Trials, limiting the searches to papers published between Jan 1, 2000, and June 13, 2025. We included completed randomised controlled trials comparing VATS versus open lobectomy performed after the year 2000 conducted for clinical early-stage non-small-cell lung cancer in adults aged 18 years or older that collected information on mortality and disease recurrence. Individual patient data were extracted from the included studies, and authors were contacted where data were unavailable. The primary outcome was overall survival, and the secondary outcome was disease-free survival. Risk of bias was assessed using the Cochrane risk of bias tool for randomised trials. The primary analytical strategy was a one-stage random effects Cox proportional hazards model. A two-stage approach was performed to assess consistency.

Findings We screened 554 articles and three studies were eligible for inclusion. Data were provided for 1185 patients (586 randomised to VATS and 599 randomised to open lobectomy). Overall survival favoured VATS lobectomy, reflecting a 21% mortality risk reduction (pooled hazard ratio [HR] 0·79 [95% CI 0·65–0·96]). Disease-free survival was similar in both groups (pooled HR 0·91 [0·75–1·12]). There was no evidence of statistical heterogeneity across trials for either outcome.

Interpretation This meta-analysis provides evidence that surgical access by VATS lobectomy improved overall survival compared with open surgery without any compromise to disease-free survival. These results underscore the importance of prioritising VATS when technically feasible as the access of choice for surgical resection of early-stage non-small-cell lung cancer.

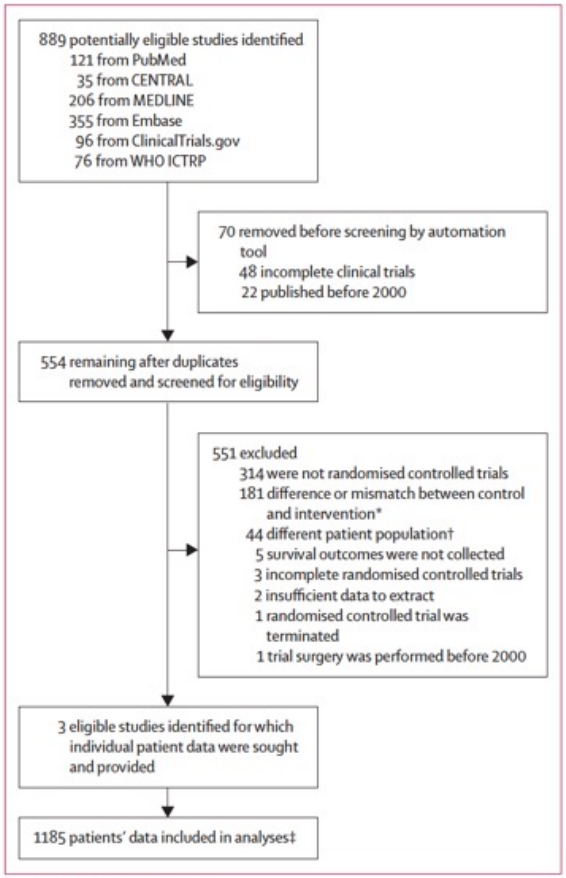

Figure 1: **PRISMA diagram**
*This includes studies investigating and comparing robotic-assisted thoracic surgery surgical approaches, sublobar resection (non-pulmonary lobectomy) or RCTs evaluating entirely different interventions including surgical staples, general or regional anaesthesia techniques, and different lung ventilation approaches in the context of early-stage lung cancer resection. †This includes studies examining patients with clinical stage III and above non-small-cell lung cancer, small-cell lung cancer, or pulmonary metastasis. ‡Data for five patients were not provided (one consent withdrawn after randomisation, four were lost to follow-up).

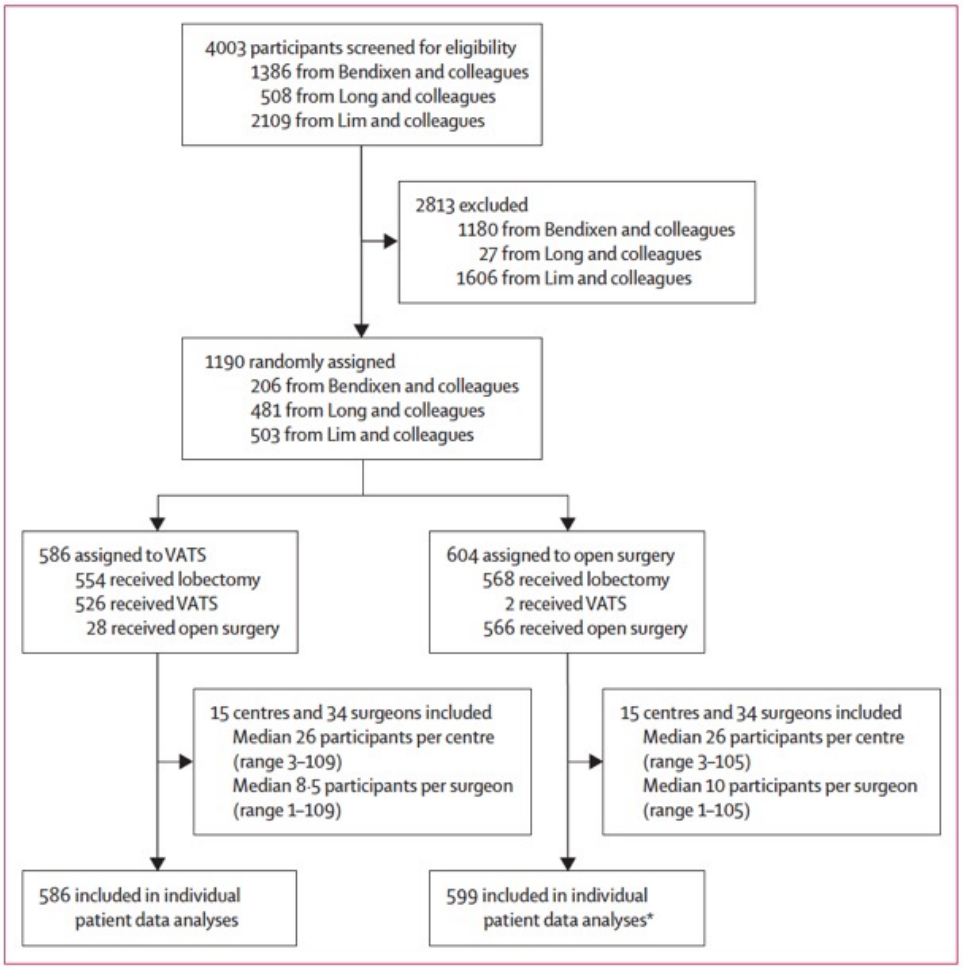

Figure 2: **Trial profile**
*One patient withdrew and four were lost to follow-up.

	Bendixen and colleagues (n=202)		Long and colleagues (n=481)		Lim and colleagues (n=502)		Overall (n=1185)	
	Randomised to VATS (n=103)	Randomised to open surgery (n=99)	Randomised to VATS (n=236)	Randomised to open surgery (n=245)	Randomised to VATS (n=247)	Randomised to open surgery (n=255)	Randomised to VATS (n=586)	Randomised to open surgery (n=599)
Age, years								
Median (IQR)	66·0 (61·0–72·0)	65·0 (60·0–72·0)	58·0 (51·0–64·0)	59·0 (52·0–64·0)	69·5 (63·6–74·5)	70·3 (63·2–76·3)	64·0 (57·0–71·4)	64·8 (57·0–71·7)
Sex								
Male	50 (49%)	47 (48%)	122 (52%)	126 (51%)	119 (48%)	130 (51%)	291 (50%)	303 (51%)
Female	53 (51%)	52 (52%)	114 (48%)	119 (49%)	128 (52%)	125 (49%)	295 (50%)	296 (49%)
Spirometric measures								
Predicted FEV1*	85% (19·3)	81% (20·1)	93% (18·2)	91% (17·4)	83% (19·8)	82% (21·2)	87% (19·6)	85% (20·0)
Predicted FVC†	97% (18·4)	95% (19·8)	94% (17·7)	91% (17·6)	95% (17·1)	95% (18·3)	95% (17·5)	93% (18·2)
Preoperative details								
Stage of primary tumour								
T1	68/102 (67%)	51/97 (53%)	119/174 (68%)	119/181 (66%)	165/247 (67%)	173/255 (68%)	352/523 (67%)	343/533 (64%)
T2	26/102 (25%)	27/97 (28%)	53/174 (31%)	62/181 (34%)	63/247 (26%)	63/255 (25%)	142/523 (27%)	152/533 (29%)
T3	7/102 (7%)	19/97 (20%)	1/174 (1%)	0/181	19/247 (8%)	19/255 (7%)	27/523 (5%)	38/533 (7%)
T4	1/102 (1%)	0/97	1/174 (1%)	0/181	0/247	0/255	2/523 (<1%)	0/533
Regional lymph node involvement								
N0	102/102 (100%)	97/97 (100%)	165/174 (95%)	171/181 (94%)	232/247 (94%)	238/255 (93%)	499/523 (95%)	506/533 (95%)
N1	0/102	0/97	6/174 (3%)	8/181 (4%)	15/247 (6%)	17/255 (7%)	21/523 (4%)	25/533 (5%)
N2	0/102	0/97	3/174 (2%)	2/181 (1%)	0/247	0/255	3/523 (1%)	2/533
Postoperative details and outcomes								
Pathological tumour stage								
T1	37/100 (37%)	40/93 (43%)	120/226 (53%)	96/215 (45%)	132/226 (58%)	136/234 (58%)	289/552 (52%)	272/542 (50%)
T2	50/100 (50%)	35/93 (38%)	88/226 (39%)	93/215 (43%)	69/226 (31%)	73/234 (31%)	207/552 (38%)	201/542 (37%)
T3	12/100 (12%)	16/93 (17%)	10/226 (4%)	25/215 (12%)	21/226 (9%)	19/234 (8%)	43/552 (8%)	60/542 (11%)
T4	1/100 (1%)	2/93 (2%)	8/226 (4%)	1/215 (<1%)	4/226 (2%)	6/234 (3%)	13/552 (2%)	9/542 (2%)
Pathological staging of nodal involvement								
N0	81/100 (81%)	71/93 (76%)	172/226 (76%)	149/215 (69%)	200/233 (86%)	207/237 (87%)	453/559 (81%)	427/545 (78%)
N1	12/100 (12%)	11/93 (12%)	20/226 (9%)	25/215 (12%)	18/233 (8%)	18/237 (8%)	50/559 (9%)	54/545 (10%)
N2	7/100 (7%)	11/93 (12%)	33/226 (15%)	39/215 (18%)	15/233 (6%)	12/237 (5%)	55/559 (10%)	62/545 (11%)
N3	0/100	0/93	0/226	2/215 (1%)	0/233	0/237	0/559	2/545 (<1%)
NX	0/100	0/93	1/226 (<1%)	0/215	0/233	0/237	1/559 (<1%)	0/545
Lymph node upstaging								
cN0 to pN1								
Yes	12/101 (12%)	11/96 (11%)	15/231 (6%)	19/238 (8%)	15/244 (6%)	13/252 (5%)	42/576 (7%)	43/586 (7%)
No	88/101 (87%)	82/96 (85%)	208/231 (90%)	189/238 (79%)	211/244 (86%)	219/252 (87%)	507/576 (88%)	490/586 (84%)
Not cancer	1/101 (1%)	3/96 (3%)	8/231 (3%)	30/238 (13%)	18/244 (7%)	20/252 (8%)	27/576 (5%)	53/586 (9%)
cN0 to pN2								
Yes	7/101 (7%)	10/95 (11%)	27/228 (12%)	29/238 (12%)	11/244 (5%)	10/252 (4%)	45/573 (8%)	49/585 (8%)
No	93/101 (92%)	82/95 (86%)	193/228 (85%)	179/238 (75%)	215/244 (88%)	222/252 (88%)	501/573 (87%)	483/585 (83%)
Not cancer	1/101 (1%)	3/95 (3%)	8/228 (4%)	30/238 (13%)	18/244 (7%)	20/252 (8%)	27/573 (5%)	53/585 (9%)
cN1 to pN2								
Yes	0/101	0/95	0/228	3/238 (1%)	4/244 (2%)	2/252 (1%)	4/573 (1%)	5/585 (1%)
No	100/101 (99%)	92/95 (97%)	220/228 (96%)	205/238 (86%)	222/244 (91%)	230/252 (91%)	542/573 (95%)	527/585 (90%)
Not cancer	1/101 (1%)	3/95 (3%)	8/228 (4%)	30/238 (13%)	18/244 (7%)	20/252 (8%)	27/573 (5%)	53/585 (9%)
Complete (R0) resection	99/101 (98%)	97/97 (100%)	225/227 (99%)	217/221 (98%)	210/215 (98%)	219/224 (98%)	534/543 (98%)	533/542 (98%)
Received adjuvant chemotherapy	23/100 (23%)	22/96 (23%)	115/231 (50%)	112/239 (47%)	33/241 (14%)	32/245 (13%)	171/572 (30%)	166/580 (29%)

(Table continues on next page)

(Continued from previous page)

	Bendixen and colleagues (n=202)		Long and colleagues (n=481)		Lim and colleagues (n=502)		Overall (n=1185)	
	Randomised to VATS (n=103)	Randomised to open surgery (n=99)	Randomised to VATS (n=236)	Randomised to open surgery (n=245)	Randomised to VATS (n=247)	Randomised to open surgery (n=255)	Randomised to VATS (n=586)	Randomised to open surgery (n=599)
Disease recurrence and new cancer								
Locoregional recurrence	34/103 (33%)	31/99 (31%)	15/236 (6%)	13/245 (5%)	10/247 (4%)	11/255 (4%)	59/586 (10%)	55/599 (9%)
Distant recurrence	38/103 (37%)	42/99 (42%)	71/236 (30%)	62/245 (25%)	7/247 (3%)	8/255 (3%)	116/586 (20%)	112/599 (19%)
New cancer	25/103 (24%)	23/99 (23%)	1/236 (<1%)	0/245	4/247 (2%)	6/255 (2%)	30/586 (5%)	29/599 (5%)

Data are n (%) or mean (SD) unless otherwise stated. Primary tumour and pathological tumour were staged using the TNM classification.[10] NX means regional lymph nodes could not be assessed or evaluated. R0 resection means there is no residual tumour. FEV1=forced expiratory volume in 1 s. FVC=forced vital capacity. VATS=video-assisted thoracoscopic surgery. *59 patients had missing data (12 Bendixen VATS, 3 Bendixen open surgery; 15 Long VATS, 17 Long open surgery; 7 Lim VATS, 5 Lim open surgery). †166 patients had missing data (68 Bendixen VATS, 52 Bendixen open surgery; 15 Long VATS, 16 Long open surgery; 8 Lim VATS, 7 Lim open surgery).

Table: Baseline characteristics and postoperative details in the intention-to-treat population

All-cause death

2-stage model

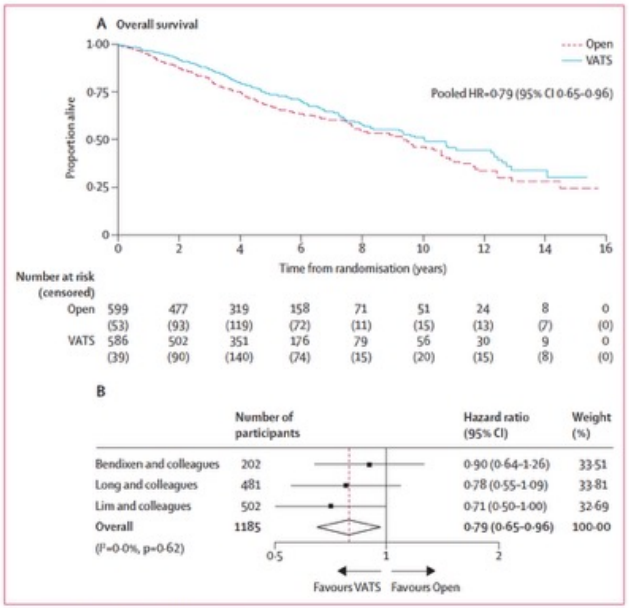

years

Figure 3: Kaplan–Meier (A) and forest plot (B) of overall survival

(A) Kaplan–Meier showing overall survival in intention-to-treat population. Overall survival was defined as time from randomisation to death from any cause. Number of events in individual trials were: Bendixen and colleagues 133 (66 VATS, 67 open); Long and colleagues 135 (63 VATS, 72 open); Lim and colleagues 133 (56 VATS, 77 open). 5-year event rate: 26% (VATS) versus 32% (open); 10-year event rate: 49% (VATS) versus 54% (open); 15-year event rate: 70% (VATS) versus 76% (open). (B) Pooled estimates of overall survival from two-stage model.

Disease-
Free

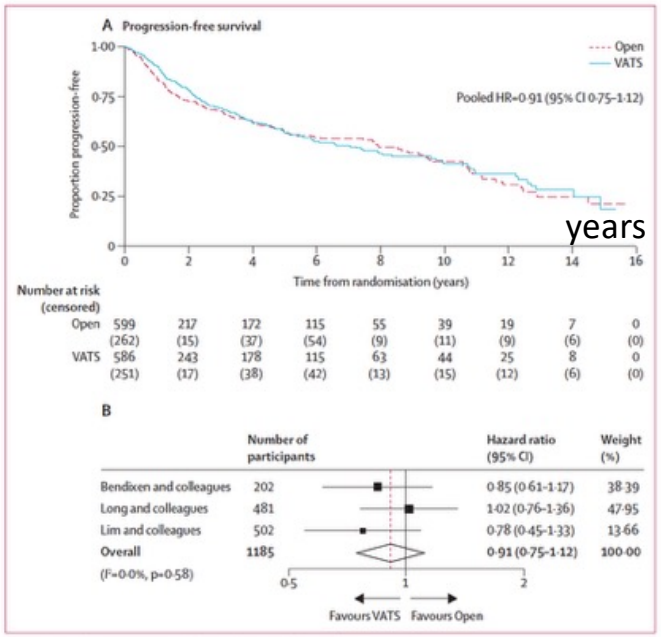

Figure 4: **Kaplan–Meier (A) and forest plot (B) of disease-free survival**
(A) Kaplan–Meier showing disease-free survival in intention-to-treat population. Disease-free survival was defined as time from randomisation to disease recurrence or death from any cause, whichever occurred first. Number of events in individual trials were: Bendixen and colleagues 148 (73 VATS, 75 open), Long and colleagues 185 (96 VATS, 89 open), Lim and colleagues 55 (23 VATS, 32 open). 5-year event rate: 43% (VATS) versus 42% (open); 10-year event rate: 59% (VATS) versus 58% (open); 15-year event rate: 81% (VATS) versus 79% (open). (B) Pooled estimates of disease-free survival from two-stage model.

Research in context

Evidence before this study

Video-assisted thoracoscopic surgery (VATS) is the predominant surgical approach for pulmonary lobectomy in early-stage non-small-cell lung cancer. Previous randomised controlled trials have shown the advantages of VATS over open thoracotomy, including reduced pain, faster recovery, and improved quality of life. However, definitive conclusions regarding overall and disease-free survival differences remain unclear, as no single randomised trial has been adequately powered to detect an important difference. Three aggregate meta-analyses of predominantly non-randomised studies and one real-world registry study suggested the possibility of survival benefit with VATS, but the findings are limited by selection bias and residual confounding.

Added value of this study

By pooling participant-level data from three randomised trials, we identified beneficial effects of VATS access above and beyond that of improved postoperative pain, shorter hospital stays, fewer one-year complications and readmissions, and better quality of life. The cumulative benefits also extend to improved overall survival.

Implications of all the available evidence

Our results affirm VATS as the standard of care for the surgical approach when technically feasible for early-stage non-small-cell lung cancer surgery, showing a long-term overall survival advantage in addition to the established non-oncological benefits and superior perioperative outcomes as reported in previous randomised trials.

THE LANCET

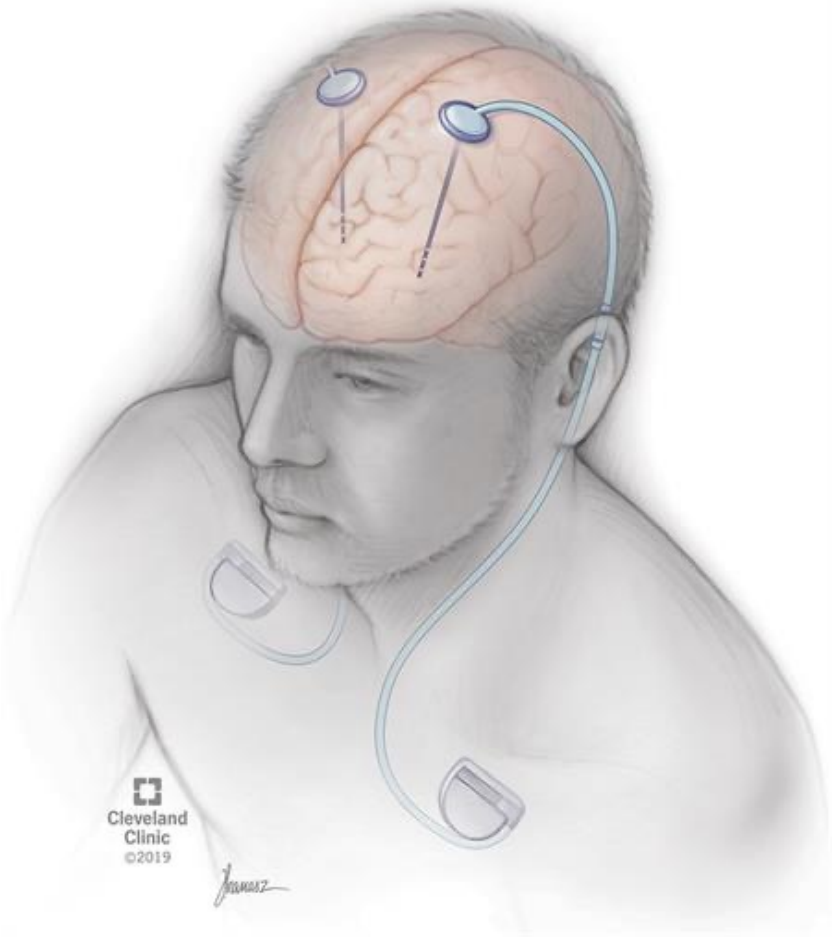

Adaptive deep brain stimulation in Parkinson's disease

(smart)

With the introduction of adaptive deep brain stimulation (aDBS) for Parkinson's disease, new questions emerge regarding who, why, and how to treat. This paper outlines the pathophysiological rationale for aDBS, which provides real-time modulation of the stimulation amplitude based on subthalamic beta (range 13–30 Hz) activity and related physiomarkers. We review clinical evidence comparing aDBS with conventional DBS in terms of motor improvement, side-effect reduction, energy efficiency, and technical developments, including sensing-enabled device characteristics, stimulation algorithms, and potential clinical indications. We also discuss limitations, such as physiomarker variability, signal artifacts, and the absence of standardised programming protocols. Finally, we explore the readiness for clinical implementation and future directions, and estimate the scope of eligible patients. In our view, aDBS marks a fundamental change in approach from fixed stimulation towards physiomarker-guided neuromodulation. This evolution necessitates new infrastructure, clinician training, and real-world studies, but holds promise for more personalised and responsive treatment.

Die adaptive tiefe Hirnstimulation (aDBS) ist eine Weiterentwicklung der herkömmlichen Parkinson-Therapie, die Hirnsignale in Echtzeit misst und die elektrische Stimulation automatisch an den momentanen Bedarf des Patienten anpasst. Im Gegensatz zu konstanter Stimulation ermöglicht dies eine präzisere Symptomkontrolle, weniger Nebenwirkungen und eine längere Akkulaufzeit.

In der Medizintechnik steht **beta-informed aDBS** für eine Form der **adaptiven Tiefenhirnstimulation** (adaptive Deep Brain Stimulation), bei der die Hirnstromaktivität im sogenannten **Beta-Frequenzband** (etwa 13–30 Hz) als Steuersignal genutzt wird.

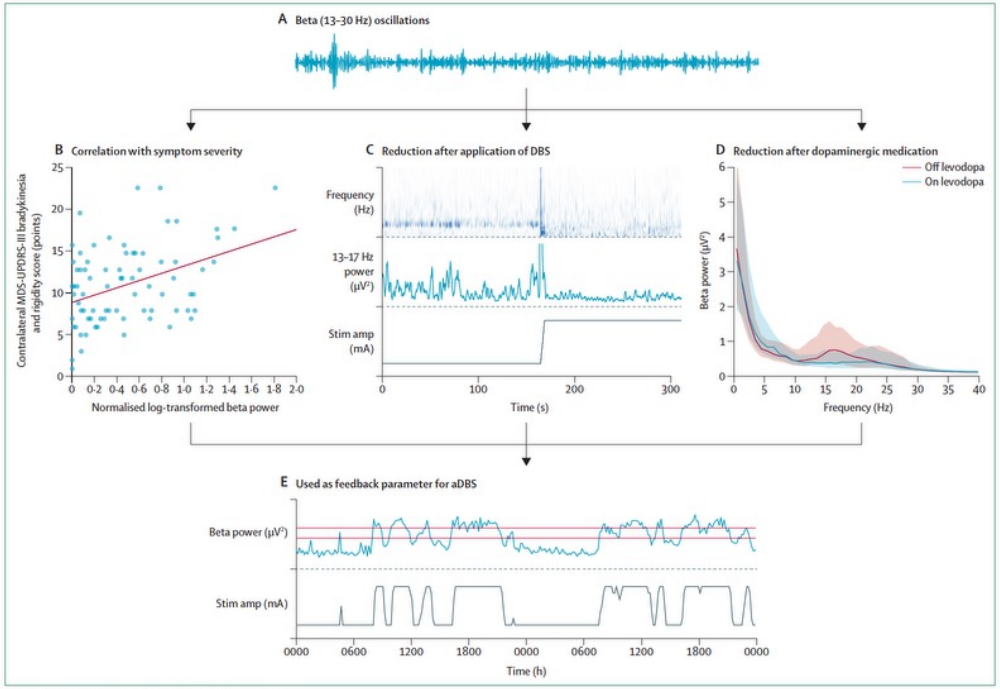

Figure 1: **Mechanism of action for beta-informed aDBS**
(A) LFP recordings from the subthalamic nucleus or internal segment of the globus pallidus show time-varying fluctuations in the amplitude of beta band (13–30 Hz) neural oscillations. (B) Adapted from Beudel et al,[34] by permission of John Wiley and Sons. In patients, the average amplitude of beta oscillations is correlated with the severity of contralateral bradykinesia and rigidity, as measured with the MDS-UPDRS-III. (C) Adapted from Swinnen et al.[35] Amplitude of beta oscillations decreases after the application of DBS (bottom), as observed from the time-frequency spectrum of the LFP recording (top) or the extracted beta amplitude envelope (middle) in this example case. (D) Amplitude of beta oscillations decreases after the intake of dopaminergic medication, as seen in the average power spectra from LFP recordings obtained in 52 patients (100 hemispheres). Unpublished data from a prospective observational cohort study.[36] (E) Excerpt of data from a patient treated with aDBS in our centre. aDBS automatically adjusts the stimulation amplitude (bottom) based on the signal strength of a specific physiomarker, in this case beta power (top). Red horizontal lines represent the lower and upper thresholds of the dual threshold aDBS control algorithm. The slight mismatch between the threshold crossings of beta power and the corresponding stimulation amplitude adjustments arises due to a difference in time resolution at which the beta power estimates are stored (10-min averages) compared with what is used by the control algorithm (s to min). aDBS=adaptive deep brain stimulation. DBS=deep brain stimulation. LFP=local field potential. MDS-UPDRS-III=Movement Disorder Society Unified Parkinson's Disease Rating Scale part III.

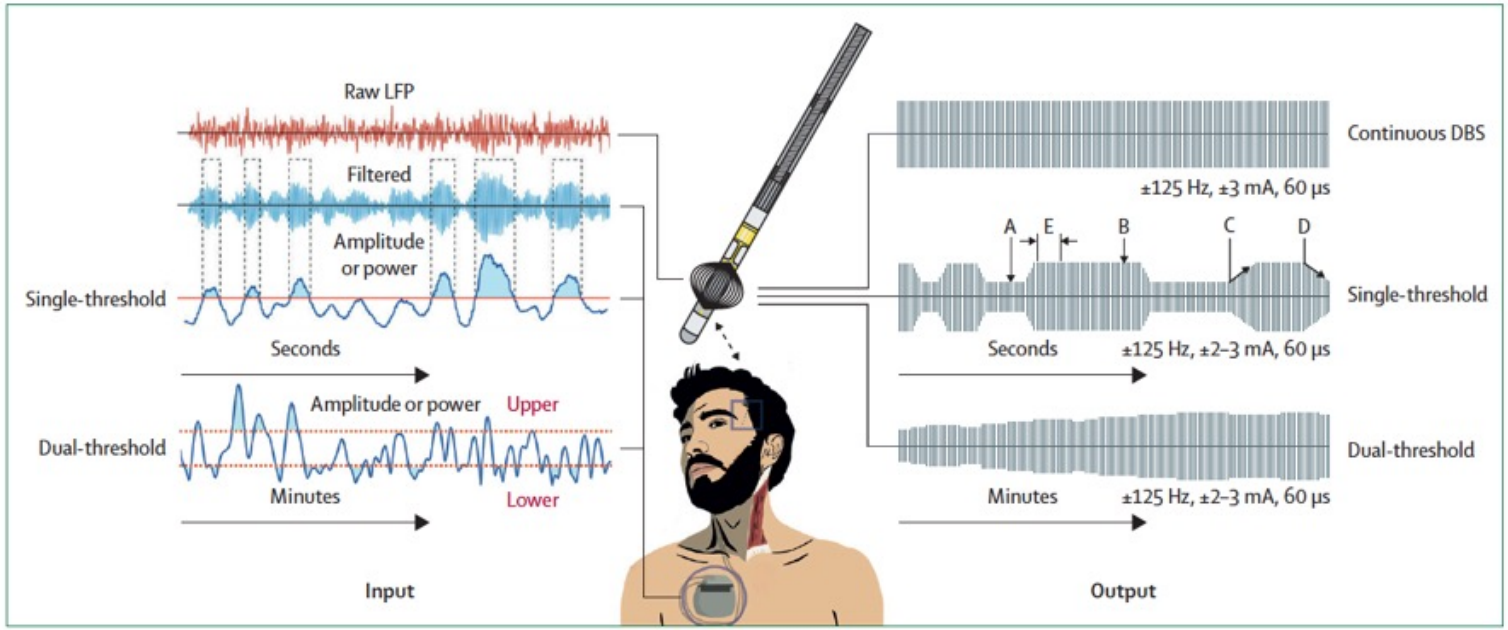

Figure 2: **Schematic of the workings of aDBS**

In the centre, a patient is depicted with a fully implanted DBS system consisting of electrodes in the subthalamic nucleus and a pulse generator. A magnified DBS electrode is depicted above (real size=1·57 mm in diameter). LFP recordings (in red) are used by the pulse generator to extract a physiomarker. The continuously measured physiomarker acts as feedback signal to control the stimulation. The two different types of aDBS control algorithms—single-threshold and dual-threshold—are depicted on the left. The stimulation amplitude (depicted on the right) changes between a low (A) and high (B) value following a transition time up (C) and down (D), over a period of seconds. A refractory (blanking) period (E) can be chosen, during which the stimulation amplitude cannot change. For single-threshold aDBS, stimulation is applied on either the low (A) or high (B) amplitude values, whereas for dual-threshold aDBS, the stimulation amplitude transitions more gradually between these two limits. aDBS=adaptive deep brain stimulation. DBS=deep brain stimulation. LFP=local field potential.

	Setting	Feedback signal	Control algorithm	Patients undergoing aDBS (N; male/female)	Clinical outcome measure	aDBS compared with no stimulation	aDBS compared with cDBS
Single-target STN-DBS, STN beta power-informed							
Little et al, 2013[41]	Acute postoperative	Subthalamic 13–35 Hz peak frequency amplitude (bandwidth 2–6 Hz); one hemisphere	Single-threshold; stimulation either OFF or ON	8 (unknown)	MDS-UPDRS-III hemibody	49·7% improvement	More improvement (27·0% [SD 7·8]) for aDBS
Rosa et al, 2015[48]	Acute postoperative	Subthalamic 13–17 Hz band power	No threshold; linear adaptation between 0 V and 2 V	1 (1/0)	MDS-UPDRS-III upper limb hemibody; Rush-DRS	NA	Lower MDS-UPDRS-III scores for aDBS; no statistical difference in dyskinesia scores; no numerical outcome values reported
Little et al, 2016[49]	Acute postoperative	Amplitude of subthalamic activity with an individualised frequency and bandwidth encompassing peaks within 13–30 Hz	Single-threshold; stimulation either OFF or ON	4 (4/0)	MDS-UPDRS-III full motor examination	43% improvement	NA
Little et al, 2016[50]	Acute postoperative	Subthalamic 13–35 Hz peak frequency amplitude; one hemisphere	Single-threshold; stimulation either OFF or ON	8 (unknown)	MDS-UPDRS-III excluding rigidity; SIT	No difference in speech intelligibility (67·9% [SD 9·2] *vs* 70·4% [SD 6·4])	Lower MDS-UPDRS-III scores (19·7 points [SD 1·0] *vs* 31·6 points [SD 4·3]) and better speech intelligibility (70·4% [SD 6·4] *vs* 60·5% [SD 8·2]) for aDBS
Rosa et al, 2017[51]	Acute postoperative	Power of frequency window within subthalamic 13–30 Hz band; selection method unclear	Single-threshold; stimulation either OFF or ON	10 (unknown)	MDS-UPDRS-III; UDysRS	NA	Similar MDS-UPDRS-III improvement ON medication (−46·1% [SD 10·5] *vs* −40·1% [SD 17·5]); lower dyskinesia scores (11·7 points [SD 6·7] *vs* 15·0 points [SD 8·7]) for aDBS
Arlotti et al, 2018[52]	Acute postoperative	Power of subthalamic 11–35 Hz peak frequency ±2 Hz	No threshold; linear adaptation between 0 V and clinically effective amplitude	11 (7/4)	MDS-UPDRS-III; UDysRS	Lower MDS-UPDRS-III score OFF medication (22·2 points [SD 3·3] *vs* 29·4 points [SD 3·9]) for aDBS and similar scores ON medication (17·9 points [SD 2·0] *vs* 15·5 points [SD 2·3]); no differences in dyskinesia scores in both OFF and ON medication	NA
Herz et al, 2018[53]	Acute postoperative	Power of subthalamic 13–30 Hz peak frequency	Single-threshold; stimulation either OFF or ON, with 250 ms ramping	7 (unknown)	MDS-UPDRS-III; response time during decision making task	Reduction in response time (−8·8%) but not accuracy for aDBS	No difference in MDS-UPDRS-III score OFF medication (22·2% *vs* 22·9%); no difference in response time or accuracy

(Table continues on next page)

	Setting	Feedback signal	Control algorithm	Patients undergoing aDBS (N; male/female)	Clinical outcome measure	aDBS compared with no stimulation	aDBS compared with cDBS
(Continued from previous page)							
Velisar et al, 2019[24]	Acute postoperative	Subthalamic 13–30 Hz band power	Dual-threshold; adaptation between 0 V and clinically effective amplitude	13 (11/2)	Kinematic measures of bradykinesia and tremor (only tremor-dominant patients)	Improvement of bradykinesia for aDBS; no numerical outcome values reported; median time below tremor detection threshold 95·4% (95% CI 65·4–100·0)	NA
Piña-Fuentes et al, 2020[25]	Chronically implanted during battery replacement	Power of subthalamic 12–35 Hz peak frequency ±3 Hz	Single-threshold; stimulation either OFF or ON	13 (11/2)	MDS-UPDRS-III upper limb bradykinesia and tremor; SIT; tablet-based bradykinesia test	Lower MDS-UPDRS-III subscore (12·30 points [SD 0·85] *vs* 15·81 points [SD 0·75]) for aDBS; no difference in speech intelligibility or bradykinesia	No difference in MDS-UPDRS-III score or bradykinesia
Petrucci et al, 2020[26]	Unknown	Subthalamic 12–18 Hz band power	Dual-threshold; adaptation between 0 V and clinically effective amplitude; different for up and down	1 (1/0)	Percentage freezing during stepping in place task	Less freezing OFF medication (5·2% vs 54·9%)	Similar freezing with aDBS compared with clinical cDBS (5·2% *vs* 2·3%) but lower compared with cDBS matched to aDBS in contact and settings (5·2% vs 23·5%)
Bocci et al, 2021[27]	Acute postoperative	Power of subthalamic 11–35 Hz peak frequency ±2 Hz	No threshold; linear adaptation within therapeutic window	8 (6/2)	MDS-UPDRS-III relative score; MDS-UPDRS-III subscores for rest tremor, bradykinesia, and rigidity; Rush-DRS	NA	Lower MDS-UPDRS-III relative score (0·33 [SD 0·04] *vs* 0·46 points [SD 0·05]) for aDBS; lower MDS-UPDRS-III rigidity subscore (2·14 points [SD 0·50] *vs* 2·91 points [SD 0·66]) for aDBS but no differences in rest tremor and bradykinesia subscores; lower dyskinesia scores (1·67 points [SD 0·53] *vs* 2·50 points [SD 1·13]) for aDBS
Gilron et al, 2021[28]	Chronic	Power of subthalamic 12–30 Hz peak frequency ±4 Hz	Dual-threshold; adaptation within therapeutic window	1 (0/1)	No clinical outcomes for STN-aDBS	NA	NA
Nakajima et al, 2021[29]	Chronic	Power of subthalamic 16·60 Hz ±2·5 Hz; selection method unclear	Dual-threshold; adaptation within therapeutic window	1 (1/0)	MDS-UPDRS-IV parts A (dyskinesias) and B (motor fluctuations)	NA	No difference in dyskinesia scores (0 points vs 0 points); lower motor fluctuation scores (0 points vs 3 points) for aDBS
He et al, 2023[30]	Acute postoperative	Power of subthalamic 13–30 Hz peak frequency ±3 Hz	Single-threshold; adaptation between 0 mA and clinically effective amplitude	13 (7/6)	Reaching task; finger tapping movements with blinded bradykinesia ratings; tremor assessment with accelerometer; estimation of effect β with GLME model	Improvement of reaction time (β=−0·0253 [SD 0·0094]) and velocity (β=0·0128 [SD 0·0045]) during reaching task; increased acceleration during finger tapping (β=0·0339 [SD 0·0149]) and reduction of blinded bradykinesia ratings (β=−0·1738 [SD 0·0593]) and lower resting tremor (β=−0·5726 [SD 0·1256])	No difference in task performance metrics and bradykinesia, but more resting tremor (k=0·7605 [SD 0·2179]) for aDBS
Busch et al, 2024[61]	Acute postoperative	Subthalamic 12–30 Hz band power	Single-threshold; adaptation between 0 V and clinically effective amplitude	12 (8/4)	No clinical outcome measure	NA	NA
Patel et al, 2025[62]	Chronic	Subthalamic beta power; details unknown	Unknown	1 (1/0)	Complete MDS-UPDRS; PDQ-39	NA	Reduction in complete MDS-UPDRS score (70 points to 50 points) and MDS-UPDRS-III score (42 points to 28 points); increase in PDQ-39 score (no numerical outcome given)

(Table continues on next page)

	Setting	Feedback signal	Control algorithm	Patients undergoing aDBS (N; male/female)	Clinical outcome measure	aDBS compared with no stimulation	aDBS compared with cDBS
(Continued from previous page)							
Busch et al, 2025[43]	Chronic	Power of subthalamic 13–30 Hz peak frequency ±2·5 Hz	Dual-threshold; adaptation between two clinically relevant stimulation amplitudes	8 (5/3)	Ecological momentary assessments (7-point scales) on overall wellbeing, general movement, tremor, dyskinesias, and clinical status	NA	Improvement in overall wellbeing (5·92 points [SD 1·01] to 6·73 points [SD 1·33]); no significant differences in motor symptoms and clinical status; only group-level results reported
Emura et al, 2025[44]	Chronic	Power of subthalamic 13–30 Hz peak frequency ±2·5 Hz	Dual-threshold; adaptation between two clinically relevant stimulation amplitudes	19 (8/11)	MDS-UPDRS-I; MDS-UPDRS-II; MDS-UPDRS-III in four conditions; MDS-UPDRS-IV; PDQ-39; Berg Balance Scale; 10-minute timed up and go	Reduction in MDS-UPDRS-III scores without medication at 12 months (26 points [range 23–32] *vs* 53 points [range 42–57]); not statistically compared	Reduction in MDS-UPDRS-III score OFF medication and ON stimulation (baseline 33 points [range 28–38] to 26 points [range 23–32] at 12 months); no differences in other outcomes but correlation between age at initiation and PDQ-39 improvement at 12 months (r=0·616)
Ferrucci et al, 2025[45]	Acute postoperative	Power of subthalamic 11–35 Hz peak frequency ±2 Hz	No threshold; linear adaptation within stimulation window; limits unclear	16 (12/4)	Cognitive assessments of attention, language, and memory	NA	Fluctuations in reaction time between OFF and ON medication conditions during cDBS (n=4) but not during aDBS (n=16); other cognitive outcomes did not fluctuate between medication conditions
Bronte-Stewart et al, 2025[46]	Chronic	Power of subthalamic 8–30 Hz peak frequency ±2·5 Hz	Single-threshold or dual-threshold; adaptation between two clinically relevant stimulation amplitudes	68 (48/20)	Self-reported home diary; CGI-C; MDS-UPDRS-I; MDS-UPDRS-II; MDS-UPDRS-III; MDS-UPDRS-IV; PDQ-39	NA	Clinically meaningful increase in ON time without troublesome dyskinesias for dual-threshold (+1·3 h [SD 0·5]) but not for single-threshold (+0·6 h [SD 0·6]); clinically meaningful reduction in MDS-UPDRS-III score (−3·73 points [SD 1·17]) and UPDRS-IV (−1·6 points [SD 3·32]) scores on the selected aDBS mode
Single-target STN-DBS, gamma-informed							
Swann et al, 2018[17]	Chronic	Power of cortical 80 Hz ±1·25 Hz (half the stimulation frequency)	Single-threshold; adaptation within therapeutic window	2 (2/0)	MDS-UPDRS-III upper body bradykinesia; UDysRS	NA	Only one patient with clinical outcomes; similar bradykinesia and dyskinesia scores; no statistical tests done
Gilron et al, 2021[18]	Chronic	Power of cortical 50–90 Hz peak frequency ±4 Hz	Dual-threshold; linear adaptation within therapeutic window	1 (0/1)	Kinematic data and patient diary	NA	Increase in ON time during aDBS; no statistical tests done
Oehrn et al, 2024[45]	Chronic	Cortical 64–66 Hz or 64–69 Hz band power (n=3) or subthalamic 64–66 Hz band power (n=1)	Single-threshold (n=3) and dual-threshold (n=1); adaptation within therapeutic window	4 (4/0)	Daily questionnaire on symptoms and quality of life (EQ-5D-5L); estimation of effect β with GLME model	NA	Less time with most bothersome symptom (β=−16·3% [SD 4·4]) without worsening time with opposite symptom (β=−2·5% [SD 2·2]) and higher quality of life (β=6·9% [SD 1·7]) for aDBS
Cernera et al, 2025[48]	Chronic; 8 month follow-up of one patient from Oehrn et al, 2024[45]	Cortical 64–66 Hz band power	Dual-threshold (n=1); adaptation within therapeutic window	1 (1/0)	Daily questionnaire on symptoms and quality of life (EQ-5D-5L); bradykinesia and dyskinesia severity with a wearable device; estimation of effect β with GLME model	NA	Less time with bradykinesia (β=−10·22% [SD 1·67]) for aDBS without worsening time with dyskinesia (β=0·26% [SD 0·29]); higher quality of life (β=10·38% [SD 1·37]) for aDBS; wearable device outcomes: reduction of fluctuations in bradykinesia (β=−8·66% [SD 1·74]; p<0·001) for aDBS

(Table continues on next page)

	Setting	Feedback signal	Control algorithm	Patients undergoing aDBS (N; male/female)	Clinical outcome measure	aDBS compared with no stimulation	aDBS compared with cDBS
(Continued from previous page)							
Other configurations							
Malekmohammadi et al, 2016[69]	Chronic (STN)	4–8 Hz tremor power measured with a wearable device	Dual-threshold; adaptation between 0 V and highest tolerable amplitude	5 (3/2)	4–8 Hz tremor power measured with a wearable device	Improvement of 36·6% with aDBS	NA
Piña-Fuentes et al, 2019[70]	Chronically implanted during battery replacement (GPi)	Pallidal 18 Hz ±3 Hz band power	Single-threshold; stimulation either OFF or ON	1 (0/1)	MDS-UPDRS-III upper body	Improvement of 64% (4 points *vs* 11 points) for aDBS	Greater improvement (64% *vs* 37%; scores of 4 points *vs* 7 points compared with 11 points without stimulation) for aDBS
Molina et al, 2021[71]	Chronic (GPi and PPN)	2·5–7·5 Hz band power within PPN	Single-threshold; stimulation either OFF or ON for PPN lead	5 (3/2)	Number of FoG episodes; gait performance with three dimensional motion capture	>40% improvement in 3 of 5 patients (average 29% [range −63% to 93%]) for aDBS; no difference at group level; no change in velocities and stride lengths at group level	NA
Smyth et al, 2023[72]	Chronic (STN)	Cortical delta (0·5–4·5 Hz) and beta (12–30 Hz) power	Linear discriminant analysis model for sleep stage classification	1 (unknown)	No clinical outcome measure	NA	NA
Schmidt et al, 2024[73]	Chronic (STN and GPi)	Subthalamic 13–30 Hz band power	Proportional-integral controller; adaptation between 0 mA and cDBS amplitude	6 (4/2)	MDS-UPDRS-III ON and OFF medication (in-clinic); dyskinesia and tremor measured with wearable device (at home, n=3)	NA	Similar improvement in MDS-UPDRS-III scores both ON (mean difference=−1) and OFF medication (mean difference=0·25); at-home: similar reduction in tremor; dyskinesias not routinely observed

When available, outcomes of aDBS compared with no stimulation or with cDBS are provided and reported as the mean (SD) unless indicated otherwise. CGI-C=Clinical Global Impression of Change Scale. DBS=deep brain stimulation. aDBS=adaptive deep brain stimulation. cDBS=continuous deep brain stimulation. EQ-5D-5L=EuroQol Five-Dimensional, Five-Level Questionnaire. FoG=freezing of gait. GLME=generalised linear mixed-effects. GPi=internal segment of the globus pallidus. MDS-UPDRS=Movement Disorder Society Unified Parkinson's Disease Rating Scale. NA=not applicable. PDQ-39=39-item Parkinson's Disease Questionnaire. PPN=pendunculopontine nucleus. Rush-DRS=Rush Dyskinesia Rating Scale. SIT=speech intelligibility test. STN=subthalamic nucleus. UDysRS=Unified Dyskinesia Rating Scale.

Table: **Literature overview of aDBS in Parkinson's disease**

Conclusion

Adaptive DBS represents an advancement in Parkinson's disease therapy by dynamically addressing motor fluctuations and reducing stimulation-induced side-effects. Its promise lies in integrating multiple physiomarkers, wearable sensors, and artificial intelligence-driven algorithms for more precise, personalised therapy. Future applications might extend to gait, sleep, and other non-motor symptoms. However, technical and clinical challenges remain—particularly in physiomarker selection and standardisation. Continued investment in robust clinical trials, real-world studies, and technology development is essential to establish the safety, efficacy, and accessibility of aDBS. As aDBS enters clinical practice, interdisciplinary collaboration will be key to translating innovation into long-term patient benefit.

THE LANCET

Clinical Rounds

CERVICAL CANCER IN PREGNANCY

Challenges, Treatment, and Care Planning

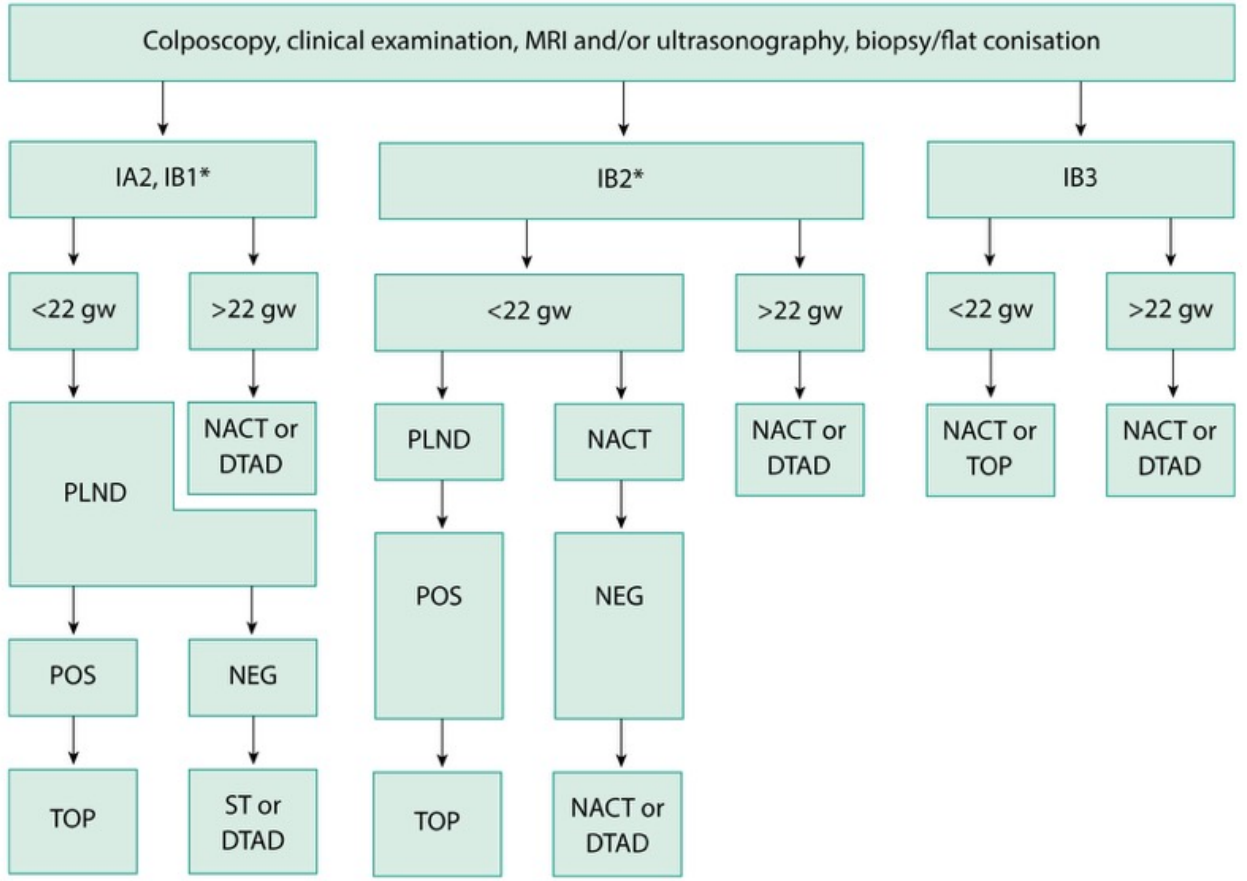

Flow chart summarising cervical cancer management during pregnancy.[1] AC = adjuvant chemotherapy; DTAD = delayed treatment after delivery; gw = gestational weeks; MRI = magnetic resonance imaging; NACT = neoadjuvant chemotherapy; NEG = negative; PLND = pelvic lymph node dissection; POS = positive; ST = simple trachelectomy; TOP = termination of pregnancy.

A multidisciplinary management approach to cervical cancer during pregnancy

Patient presentation

A 39-year-old woman, gravida 3, para 1, presented to the emergency department with vaginal bleeding at 10 weeks and 4 days gestation after spontaneous conception. Her obstetric history was notable for one miscarriage and one spontaneous preterm delivery at 35 weeks 5 days gestation. She reported a history of high-grade squamous intraepithelial lesion (HSIL) of the cervix, diagnosed 1 year before without further diagnostic evaluation or follow-up. At initial prenatal consultation, cervical cancer testing showed HSIL and a viable intrauterine pregnancy was confirmed with normal adnexa. The patient was haemodynamically stable, with minimal vaginal bleeding and no associated cramping. Transvaginal ultrasound confirmed a viable intrauterine singleton pregnancy. On colposcopic examination, the cervix appeared asymmetrical; an opaque acetowhite lesion with vascular mosaicism, measuring 20 mm, was present from 10 o'clock to 2 o'clock. Cervical biopsy showed an invasive squamous cell carcinoma with stromal invasion depth of 3·8 mm and lymphovascular space invasion. The patient was referred to a tertiary oncologic and obstetric centre for staging and treatment planning.

Learning points for management of cervical cancer during pregnancy

- Invasive cervical cancer can be diagnosed during early pregnancy, and a high index of suspicion is warranted in patients with a history of high-grade squamous intraepithelial lesion of the cervix presenting with vaginal bleeding
- Multidisciplinary management, including obstetrics, oncology, neonatology, and surgery, is essential to balance maternal oncological outcomes with fetal wellbeing
- Sentinel lymph node biopsy using indocyanine green is a feasible staging method during pregnancy, providing crucial information for treatment planning; however, more robust data are needed to confirm its oncological safety in this context
- Neoadjuvant chemotherapy can be administered safely in the second trimester, but requires careful maternal and fetal monitoring, including surveillance for maternal haematotoxicity, preterm labour, and fetal growth restriction

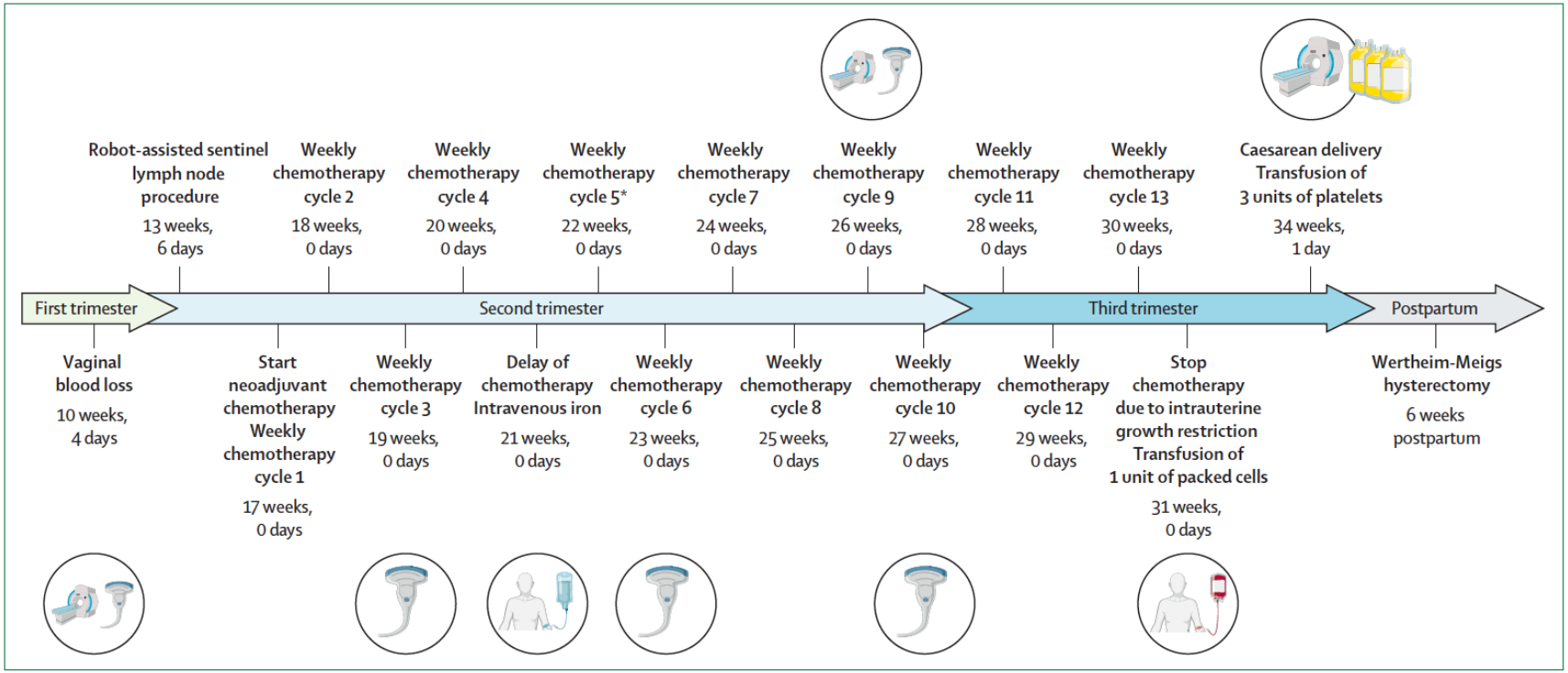

Figure: **Timeline of cervical cancer interventions during pregnancy and postpartum**
Weekly chemotherapy=paclitaxel 60 mg/m² and carboplatin area under the curve (AUC) 2·7 (with a dose reduction of carboplatin to AUC 2·0 from cycle 5*). *Administration of cycle 5 at 21 weeks' gestation was delayed due to thrombocytopenia but was administered at 22 weeks gestation following platelet recovery.

Despite advances in the management of cancer during pregnancy, particularly cervical cancer, this Clinical Rounds highlights the complexity and need for individualised management. This patient's course reflects the complex interplay between chemotherapy-related toxicity, pre-existing obstetric risk factors, and progressive fetal compromise. The staged approach allowed for delivery of the fetus at an appropriate gestational age, avoiding extreme prematurity, while ensuring optimal conditions for curative surgery. It underscores the need for dynamic, multidisciplinary treatment planning, necessitating collaboration between oncology, obstetrics, and neonatology teams within a tertiary care centre. Given the heterogeneity in staging, gestational age at diagnosis, maternal comorbidities, and patient preferences, management strategies must be highly individualised, and treatment decisions in such cases cannot be readily generalised.

Neurodermitis, auch als
atopisches Ekzem bekannt, ist eine chronisch-entzündliche Hauterkrankung, die meist in Schüben verläuft. Sie zeichnet sich durch extrem trockene Haut, Rötungen und einen teils unerträglichen Juckreiz aus.

Die wichtigsten Merkmale auf einen Blick
•**Symptome:** Typisch sind rote, schuppige und manchmal nässende Hautstellen. Bei chronischem Verlauf kann die Haut verhärten und ein gröberes Relief ("Baumrindenoptik") entwickeln.
•**Ursachen:** Eine Kombination aus genetischer Veranlagung, einer gestörten Hautbarriere (die Haut verliert zu viel Feuchtigkeit) und einer Überreaktion des Immunsystems.
•**Verbreitung:** Besonders häufig bei Babys und Kindern (ca. 10 % in Deutschland), oft bessert sich das Krankheitsbild bis zum Erwachsenenalter deutlich

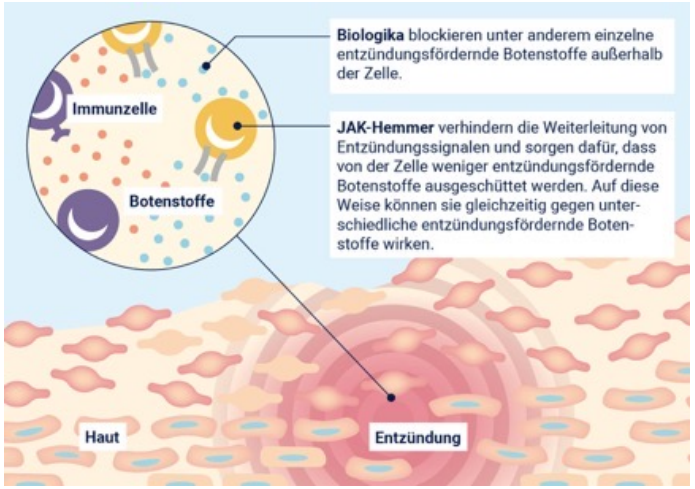

A neuroimmune circuit links stress to skin inflammation

Psychological stress exacerbates inflammatory skin diseases, such as atopic dermatitis, but the neurobiological mechanisms underpinning this connection are poorly understood. Stress mobilizes two main neuroendocrine systems: the brain (hypothalamus)–pituitary–adrenal gland axis, which leads to the production of cortisol, and the sympathetic nervous system–adrenal gland axis, which triggers the release of catecholamines such as epinephrine and norepinephrine. Tian *et al*. report a previously unrecognized neuroimmune axis that links psychological stress with worsening of atopic dermatitis in mice. The authors identified a population of norepinephrine-producing sympathetic neurons that specifically innervate hairy skin and mediate stress-induced aggravation of skin inflammation in an eosinophil-dependent manner. A better understanding of how the brain communicates with the immune system could open possibilities for targeted therapeutic interventions in stress-related skin disorders.

...t

Atopic dermatitis is the most prevalent chronic inflammatory skin disease, affecting 5 to 10% of adults. This disease is mainly driven by a dysregulated immune response that triggers eczema associated with an intense itching sensation. Atopic dermatitis is exacerbated by stress. To model the effects of stress on skin inflammation, Tian *et al*. subjected mice with chemically induced atopic dermatitis to three types of stressful situations: placement on a high platform with no guardrails, restraint in a tight conical tube, and cage changes. Using an injectable dye, the authors selectively identified a population of sympathetic neurons that innervate the skin and that stoke atopic dermatitis flares during stress. Single-cell RNA sequencing revealed that these neurons express prodynorphin (PDYN) and form a dense network in the dermis and around muscles associated with hair follicles in the skin. These PDYN$^+$ neurons do not regulate vascular constriction in response to stress, as might be expected of sympathetic neurons. Instead, they attract eosinophils to inflamed skin and stimulate the b-2 adrenergic receptor (ADRB2) at their surface, causing them to release toxic granules that amplify skin inflammation. This mechanism highlights the functional heterogeneity of sympathetic neurons and their capacity to modulate immune responses in a tissue-specific manner.

Stress stokes skin inflammation
Psychological stress stimulates PDYN-expressing (PDYN$^+$) sympathetic neurons in stellate ganglia. These neurons activate the CCL11-CCR3 signaling axis and promote the recruitment of eosinophils to inflamed skin. PDYN$^+$ neurons also release norepinephrine, which stimulates ADRB2 at the surface of the recruited eosinophils, activating them and worsening skin inflammation.

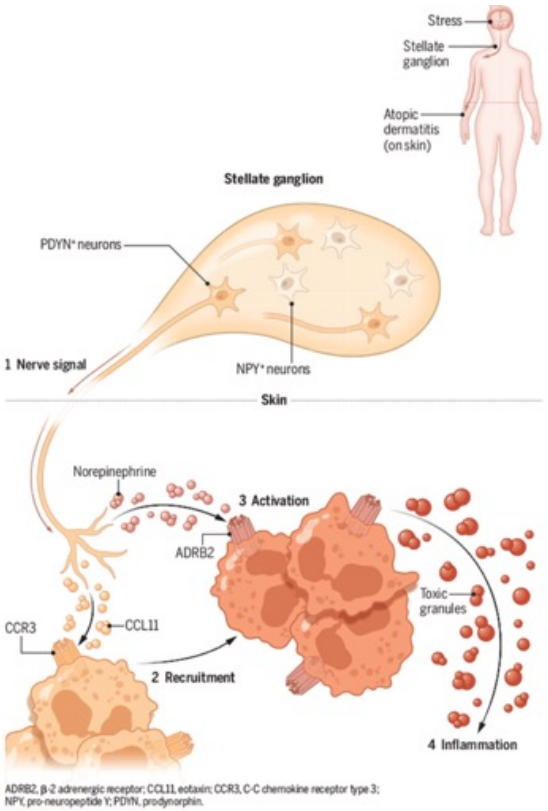

ADRB2, β-2 adrenergic receptor; CCL11, eotaxin; CCR3, C-C chemokine receptor type 3; NPY, pro-neuropeptide Y; PDYN, prodynorphin.

A sympathetic-eosinophil axis orchestrates psychological stress to exacerbate skin inflammation

Psychological stress is believed to exacerbate dermatitis, yet the neurobiological mechanisms linking stress to immune processes remain elusive. We identified a subset of prodynorphin-positive (Pdyn$^+$) noradrenergic sympathetic neurons in mice that specifically innervate hairy skin, mediating stress-induced exacerbation of skin inflammation in an eosinophil-dependent manner. Genetic ablation of Pdyn$^+$ sympathetic neurons or eosinophils mitigated stress-evoked worsening of inflammation in atopic dermatitis–like mice, whereas optogenetic activation of these neurons precipitated inflammation through eosinophils. Pdyn$^+$ sympathetic neurons recruited eosinophils through the ccL11-ccr3 axis and activated them through the adrenergic receptor beta2 (adrb2) in inflamed skin. Our findings reveal a neuroimmunological mechanism underlying psychological stress–induced exacerbation of dermatitis, emphasizing the Pdyn$^+$ sympathetic-eosinophil axis as a crucial interface between the brain and skin inflammation, with potential therapeutic implications.

RESULTS: To determine the immune mediators and neural pathways through which stress signals aggravate skin inflammation, we conducted a retrospective analysis of AD patients and studied stress-challenged murine AD models. Our analysis revealed a specific association between stress-induced eosinophilia and skin inflammation severity in AD patients.

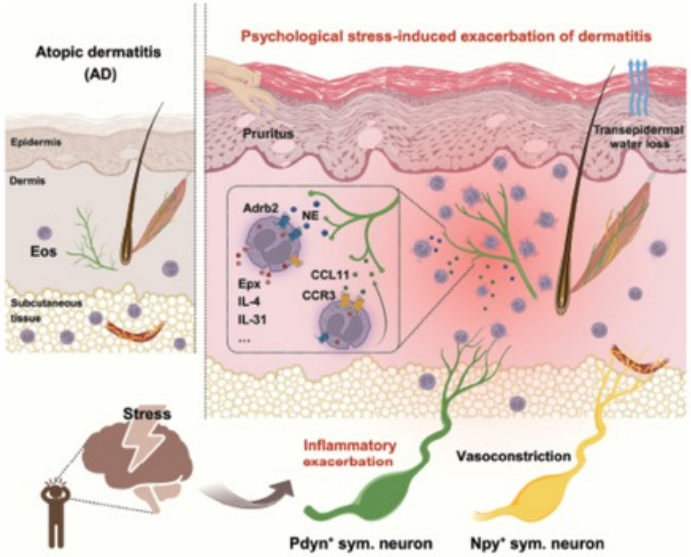

Pdyn$^+$ sympathetic neurons mediate psychological stress–evoked eosinophilia and dermatitis. Skin-projecting Pdyn$^+$ sympathetic (sym.) neurons, but not their Npy$^+$ counterparts, orchestrate stress-aggravated dermatitis by recruiting eosinophils (Eos) through the CCL11-CCR3 axis. Additionally, these neurons release norepinephrine (NE), which activates eosinophils through Adrb2 receptors, triggering the release of cytotoxic granule proteins (e.g., Epx) and proinflammatory cytokines (e.g., IL-31) within the inflamed skin.

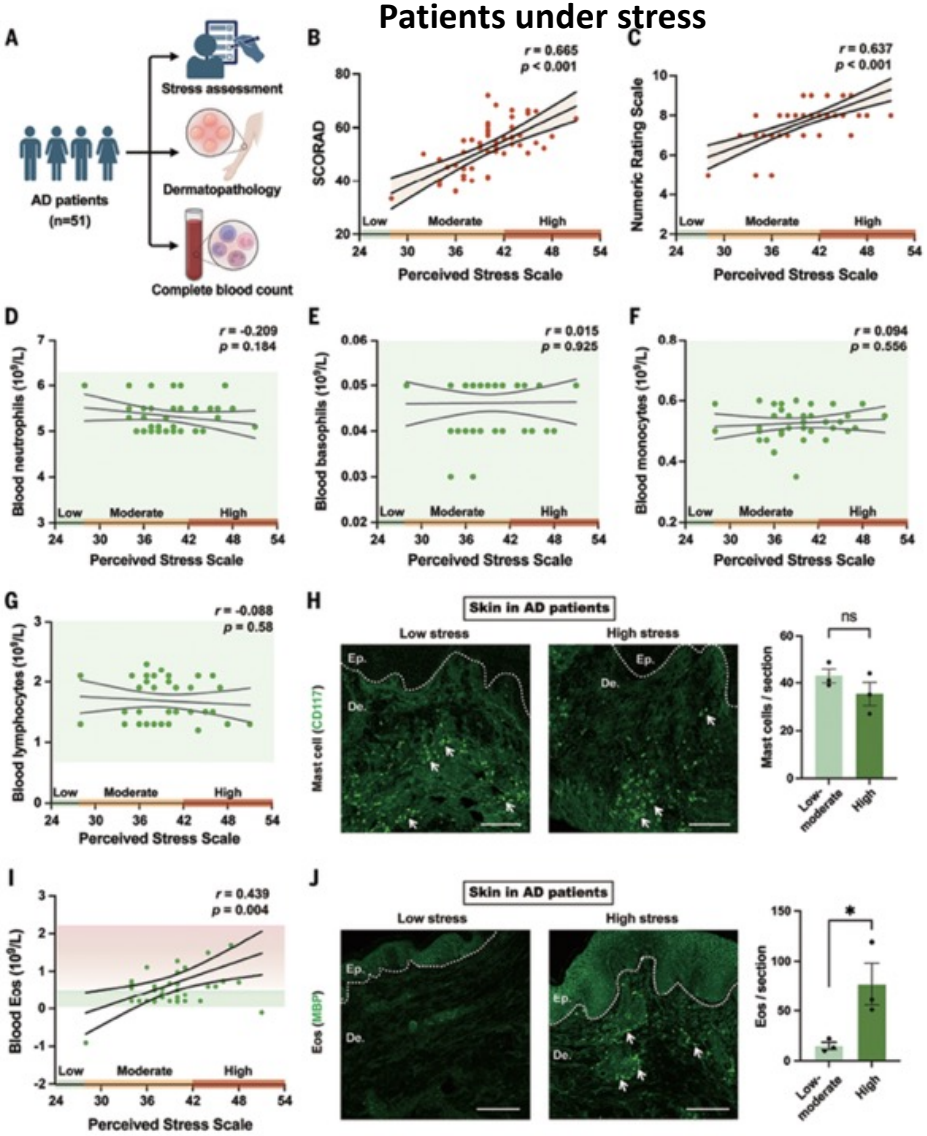

Fig. 1. Perceived stress correlates with eosinophil infiltration and disease severity in AD patients. (**A**) Schematic representation of the retrospective cohort study evaluating the effect of psychosocial stress on AD severity. (**B** and **C**) PSS score was positively correlated with SCORAD score (B) and NRS score (C) in AD patients. Perceived stress levels were categorized as low (PSS ≤ 28), moderate (PSS 29 to 42), and high (PSS ≥ 43). n = 51 AD patients. For (B), r = 0.665, $^{***}P < 0.001$; for (C), r = 0.637, $^{***}P < 0.001$ (two-tailed correlation test). (D to G) Counts of blood neutrophils (D), basophils (E), monocytes (F), and T/B lymphocytes (G) had a nonsignificant (ns) correlation with perceived stress levels in AD patients. Green shading indicates normal reference ranges for different blood immune cell populations. n = 42 AD patients. For (D), r = –0.209, ns, P = 0.184; for (E), r = 0.015, ns, P = 0.925; for (F), r = 0.094, ns, P = 0.556; and for (G), r = –0.088, ns, P = 0.58 (two-tailed correlation test). (**H**) The number of skin mast cells showed no significant difference between AD patients with low and moderate stress versus high stress levels. Quantification was performed on three to five sections per patient. The dashed line represents the boundary between the dermis (De.) and the epidermis (Ep.). White arrows indicate mast cells within the dermal layer. n = 3 AD patients per group. t_4 = 1.326, P = 0.256 (two-tailed unpaired Student's t test). (**I**) Positive correlations between the PSS and blood eosinophil (Eos) counts in AD patients. The green shaded area indicates normal eosinophil range (0.02 to 0.52 × 10^9/L), and the red gradient represents elevated levels. n = 42 AD patients. r = 0.439, P = 0.004 (two-tailed correlation test). (**J**) High psychological stress (PSS ≥ 43) increased the infiltration of MBP-marked eosinophils in the skin of AD patients. The dashed line represents the dermal-epidermal junction, and arrows indicate significant eosinophilic infiltration in the upper dermis. n = 3 AD patients per group. t_4 = 2.883, P = 0.045 (two-tailed unpaired Student's t test). Results in (H) and (J) are represented as means ± SEM from three independent experiments. Each data point represents one AD patient. Scale bars in (H) and (J), 100 μm.

Mice under stress

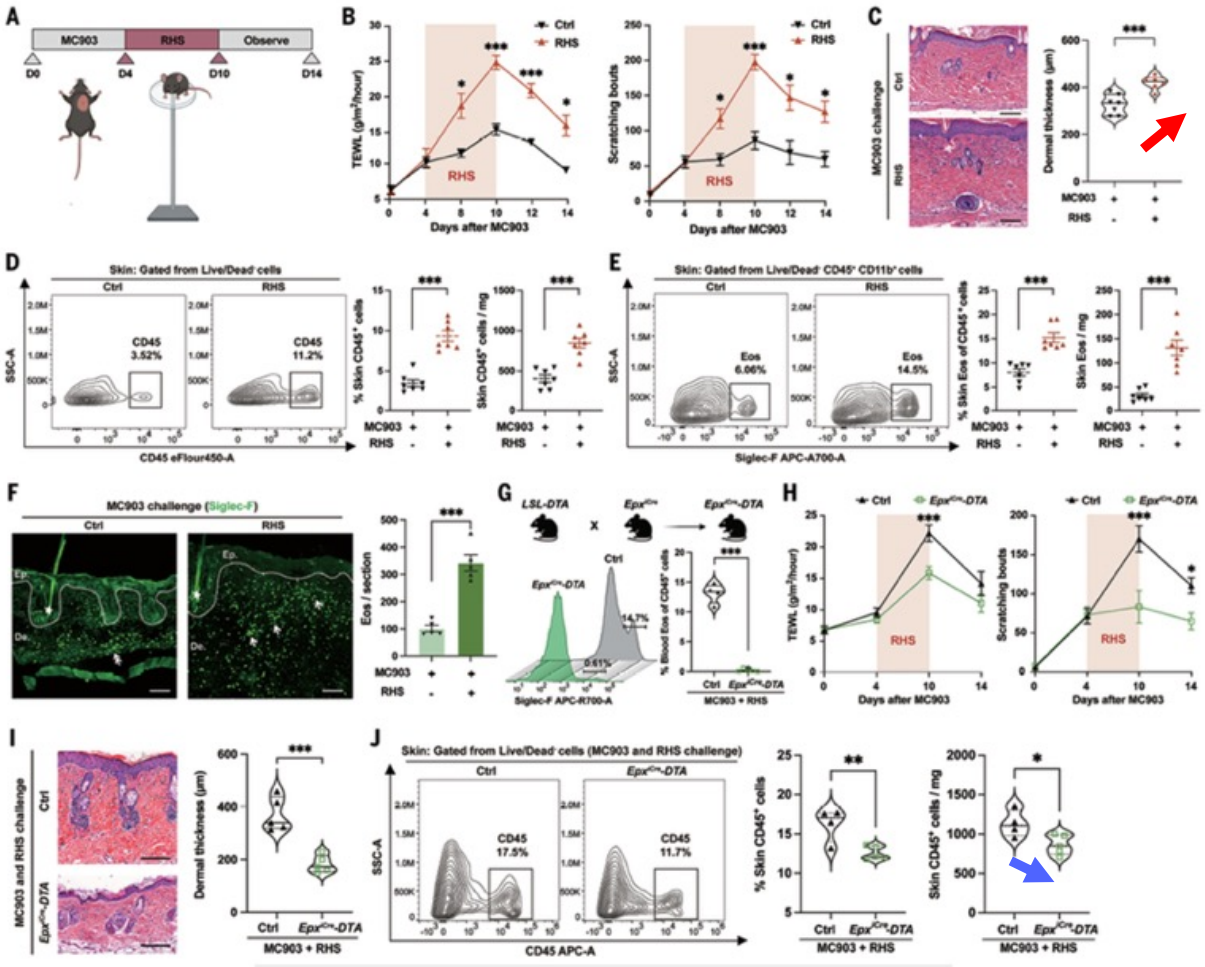

Genetic ablation of eosinophils (in *Epx*^{iCre}*-DTA* mice)

Fig. 2. Eosinophils play a crucial role in stress-evoked exacerbation of dermatitis. (**A**) Experimental schedule to examine the effect of RHS on MC903-induced AD-like mice. (**B**) RHS increased TEWL (left) and spontaneous scratching bouts (right) in MC903-challenged mice. $n = 7$ mice per group. Left: $F_{5,60} = 9.058$, •••$P < 0.001$; day 8: $P = 0.045$, day 10: •••$P < 0.001$, day 12: •••$P < 0.001$, day 14: $P = 0.026$ (two-way ANOVA followed by Šídák's multiple comparisons test). Right: $F_{5,60} = 8.887$, •••$P < 0.001$; day 8: $P = 0.032$, day 10: •••$P < 0.001$, day 12: $P = 0.047$, day 14: $P = 0.026$ (two-way ANOVA followed by Šídák's multiple comparisons test). (**C**) RHS increased dermal thickening in the lesional skin of MC903-challenged mice. $n = 6$ to 7 mice per group. $t_{11} = 4.576$, •••$P < 0.001$ (two-tailed unpaired Student's t test). (**D**) RHS promoted CD45$^+$ leukocyte infiltration in the inflamed skin of MC903-challenged mice. $n = 7$ mice per group. Left: $t_{12} = 7.363$, •••$P < 0.001$ (two-tailed unpaired Student's t test). Right: $t_{12} = 5.844$, •••$P < 0.001$ (two-tailed unpaired Student's t test). (**E**) RHS augmented eosinophil (Eos, CD45$^+$ CD11b+ Siglec-F+) accumulation in the inflamed skin of MC903-challenged mice. $n = 7$ mice per group. Left: $t_{12} = 5.765$, •••$P < 0.001$ (two-tailed unpaired Student's t test). Right: $t_{7.131} = 5.986$, •••$P < 0.001$ (two-tailed unpaired Student's t test with Welch's correction). (**F**) RHS induced pronounced eosinophilia within the upper dermis of lesional skin in MC903-challenged mice. The dashed line represents the dermalepidermal junction. Asterisks indicate hair follicles. The double-headed arrow (Ctrl) highlights Siglec-F–marked eosinophil accumulation in the deep dermis, whereas single arrows (RHS) indicate significant eosinophil infiltration throughout the superficial dermis. $n = 5$ mice per group. $t_8 = 7.52$, •••$P < 0.001$ (two-tailed unpaired Student's t test). (**G**) The *Epx*^{iCre}*-DTA* mouse model was generated by crossing mice harboring a Cre-dependent DTA expression allele (*LSL-DTA*) with strains expressing iCre recombinase under the control of eosinophil-specific *Epx* promoter (*Epx*^{iCre}). This genetic strategy enables selective eosinophil ablation. *Epx*^{iCre}*-DTA* mice exhibited a significant reduction in blood eosinophil counts compared with control animals after treatment with RHS and MC903. $n = 4$ to 5 mice per group. $t_{3.132} = 16.54$, •••$P < 0.001$ (two-tailed unpaired Student's t test with Welch's correction). (**H**) Lesional TEWL (left) and spontaneous scratching bouts (right) were significantly reduced in RHS-treated AD-like *Epx*^{iCre}*-DTA* mice. $n = 7$ mice per group. Left: $F_{3,36} = 3.015$, $P = 0.043$; day 10: •••$P < 0.001$ (two-way ANOVA followed by Šídák's multiple comparisons test). Right: $F_{3,36} = 7.571$, •••$P < 0.001$; day 10: •••$P < 0.001$, day 14: $P = 0.038$ (two-way ANOVA followed by Šídák's multiple comparisons test). (**I**) Compared with control mice, the dermal thickness of lesional skin was reduced in the AD-like *Epx*^{iCre}*-DTA* mice after RHS treatment. $n = 5$ mice per group. $t_8 = 5.875$, •••$P < 0.001$ (two-tailed unpaired Student's t test). (**J**) A reduction in cutaneous CD45$^+$ leukocyte infiltration was observed in RHS-treated AD-like *Epx*^{iCre}*-DTA* mice. $n = 4$ to 5 mice per group. Left: $t_7 = 3.599$, $P = 0.009$ (two-tailed unpaired Student's t test). Right: $t_7 = 2.724$, $P = 0.03$ (two-tailed unpaired Student's t test). Results in [(B) and (H)] are represented as means ± SEM from two independent experiments. Individual data points in (C) to (G) represent single animals, and bars show means ± SEM from two independent experiments. Individual data points in the remaining panels represent single animals and are shown as means ± SEM from one representative of two independent experiments with consistent results. Scale bars in (C), (F), and (I), 100 µm.

In mice, genetic ablation of eosinophils (in *Epx*^{iCre}*-DTA* mice) conferred protection against stress-exacerbated dermatitis. Through chemical sympathectomy with 6-hydroxydopamine and surgical removal of the adrenal glands, we determined that peripheral sympathetic nerves, rather than the hypothalamus-pituitary-adrenal axis, mediates the stress-induced worsening of skin inflammation. Using single-nucleus RNA sequencing and intersectional genetic approaches, we further identified two major populations of noradrenergic sympathetic neurons in mice, defined by prodynorphin (Pdyn) and neuropeptide Y (Npy) expression, that were activated by psychological stress. Our functional studies suggested that skininnervating Pdyn^{+} sympathetic neurons, but not their Npy^{+} counterparts, were both necessary and sufficient for driving stress-induced dermatitis and eosinophilia. Optogenetic activation of Pdyn^{+} neurons promoted eosinophil recruitment and exacerbated inflammation, effects that were abolished upon eosinophil depletion. These Pdyn^{+} neurons were found to release the chemokine C-C motif ligand 11 (CCL11), which acts on its receptor, C-C chemokine receptor type 3 (CCR3), to mediate eosinophil chemotaxis. Finally, adrenergic signaling through adrenergic receptor beta2 (Adrb2) on eosinophils was critical, because eosinophil-specific *Adrb2* knockout mitigated stress-induced exacerbation of dermatitis.

CONCLUSION: Our findings suggest that psychological stress exacerbates AD-like inflammation through a specialized subset of skin-innervating Pdyn+ noradrenergic sympathetic neurons that engage eosinophils through the CCL11-CCR3 chemotactic axis and Adrb2-mediated activation. These results indicate that stressinduced eosinophilia could be a potential biomarker of AD severity and suggest that targeting the Pdyn+ sympathetic neuron-eosinophil interface may offer therapeutic benefit in mitigating the inflammatory sequelae of psychological stress.

Der **β2 Adrenozeptor (ADRB2)** ist ein G-Protein-gekoppelter Rezeptor, der durch Adrenalin aktiviert wird und primär für die Entspannung der glatten Muskulatur (Bronchodilatation) sowie Herzfrequenzregulation verantwortlich ist. Er ist ein wichtiges therapeutisches Ziel bei Asthma und COPD. Das ADRB2-Gen befindet sich beim Menschen auf Chromosom 5.

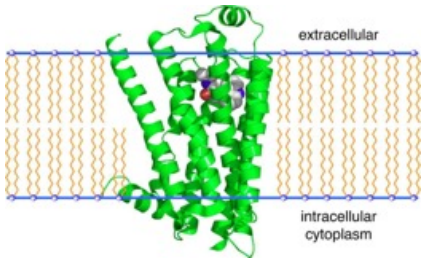

Thousands have swooned over this MAGA dream girl. She's made with AI.

The beautiful Army blonde Jessica Foster has posed with an F-22 Raptor fighter jet, donned camouflage in the desert and walked a tarmac with President Donald Trump on the first day of the strikes on Iran.

The slew of photos and videos depicting the patriotic life of the MAGA dream girl have led her Instagram account to explode, gaining more than a million followers since she began posting four months ago.

But Foster is an illusion — a fake woman who experts say was probably created by an artificial intelligence image generator. There's no public record of Foster's military service and the account, despite not being labeled AI, is packed with indicators that she is fake. Between many of her pro-Trump posts, Foster also prominently displays her feet.

Was bedeutet „swoon" im Slang? [intransitiv] in Ohnmacht fallen (über jemanden) sich sehr aufgeregt, emotional usw. fühlen über jemanden, den man sexuell attraktiv findet, so dass man fast ohnmächtig wird Er ist es gewohnt, dass Frauen für ihn in Ohnmacht fallen.

•**E-6 (Staff Sergeant):** Three chevrons, one rocker.

Feldwebel (OR-6) übersetzt.

Would FDR have supported the NAZIs in 1932?

Inside the Trump administration's campaign to expand 'free speech' in Europe

In early 2025, aides to Vice President JD Vance ordered a small office at the State Department to document how European regulators were censoring online speech.

Staffers launched an investigation focusing on the European Union's Digital Services Act, a sweeping 2022 social media law requiring large tech companies to limit the spread of harmful or illegal speech on the continent.

The weeks-long investigation, details of which have not previously been reported, uncovered no records indicating censorship, according to two people familiar with the matter, who spoke on the condition of anonymity for fear of retribution.

"There is no evidence that Member States of the European Union are overreaching the DSA to censor and criminalize online content," they wrote in conclusion.

Despite the finding, the Trump administration has pressed ahead with a wide-ranging State Department effort to crack down on what it alleges is widespread censorship in the E.U., according to documents reviewed by The Post and nine people involved or aware of the campaign, many of whom spoke on the condition of anonymity to protect their livelihoods.

It has banned some European researchers from entering the United States and dismantled federal programs intended to fight foreign disinformation campaigns. Behind the scenes, the administration has crafted a plan to allow American tech companies to skirt European rules, using the federal government's powers to control exports, according to two of the people and documents.

The department is preparing to launch a website to host banned content. A teaser for the site, freedom.gov, includes a mounted Paul Revere-type figure galloping over the words "Freedom is coming."

The push has refocused the State Department's agenda — which traditionally emphasized global free expression, particularly in authoritarian states — to prioritize fighting censorship by European governments.

The State Department said in a statement that it has been consistent in raising concerns about the Digital Services Act and a similar British law and had "never 'concluded' anything to the contrary."

Der Digital Services Act (DSA) ist eine EU-Verordnung, die seit Februar 2024 (bzw. August 2023 für große Plattformen) ein sichereres digitales Umfeld schafft. Er verpflichtet Online-Plattformen zu mehr Transparenz, strengerem Vorgehen gegen illegale Inhalte, Desinformation und Schutz von Minderjährigen. Die Regeln umfassen Meldemechanismen, Haftungsregeln und Risikomanagement.